

**Long-term Growth Arrest and Regrowth of Human Dermal
Fibroblasts after 8-MOP plus UVA Treatment – Implications
for Stress-Induced Premature Senescence and Replicative
Cellular Senescence**

Inaugural – Dissertation
zur
Erlangung des Doktorgrades
der Mathematisch-Naturwissenschaftlichen Fakultät
der Universität zu Köln

Vorgelegt von

Wenjian Ma
aus Shandong, China

2003

Berichtersteller:

PD. Dr. Roswita Nischt
Prof. Dr. Thomas Langer
Prof. Dr. Reinhard Krämer

Tag der mündlichen Prüfung: 21.05.2003

In my mother's memory
who passed away during my stay in Germany

CONTENTS

| | |
|--|-----------|
| 1. INTRODUCTION | 1 |
| 1.1. CELLULAR SENESCENCE | 1 |
| 1.1.1. Cellular lifespan: the Hayflick limit | 1 |
| 1.1.2. Replicative senescence and telomeres | 1 |
| 1.1.2.1. <i>Telomeres and their function</i> | 2 |
| 1.1.2.2. <i>The end replication problem</i> | 3 |
| 1.1.2.3. <i>Short telomeres cause replicative senescence</i> | 4 |
| 1.1.2.4. <i>Telomerase</i> | 5 |
| 1.1.3. Stress-induced premature senescence | 5 |
| 1.1.3.1. <i>DNA damage and genomic instability</i> | 5 |
| 1.1.3.2. <i>Oncogene activation</i> | 6 |
| 1.1.3.3. <i>Oxidative stress</i> | 7 |
| 1.1.4. Senescent phenotypes and molecular pathways | 7 |
| 1.1.5. Role of cellular senescence in cancer and aging | 9 |
| 1.1.5.1. <i>Implications for cancer</i> | 9 |
| 1.1.5.2. <i>Implications for aging</i> | 10 |
| 1.2. PUVA-TREATED FIBROBLASTS AS A MODEL FOR STRESS-INDUCED PREMATURE CELLULAR SENESCENCE | 11 |
| 1.2.1. Psoralen phototherapy | 11 |
| 1.2.2. 8-MOP photochemistry and photobiology | 12 |
| 1.2.3. PUVA-induced senescent-like growth arrest of fibroblasts | 13 |
| 1.3. AIM OF THE STUDY | 14 |
| | |
| 2 MATERIALS AND METHODS | 15 |
| 2.1. MATERIALS | 15 |
| 2.1.1. <i>Chemicals</i> | 15 |
| 2.1.2. <i>Cell culture material</i> | 15 |
| 2.1.3. <i>Cell strains, bacteria, vectors and plasmids</i> | 15 |
| 2.1.4. <i>Buffers</i> | 16 |
| 2.2. METHODS | 17 |
| 2.2.1. <i>Methods of cell biology</i> | 17 |
| 2.2.1.1. <i>Cell culture</i> | 17 |
| 2.2.1.2. <i>Freezing and thawing of fibroblasts</i> | 17 |
| 2.2.1.3. <i>Rho0 fibroblasts</i> | 17 |

| | |
|---|-----------|
| 2.2.1.4. Generation of stably transfected cell line..... | 18 |
| 2.2.1.5. Cell morphology..... | 18 |
| 2.2.1.6. MTT assay..... | 18 |
| 2.2.1.7. Trypan blue dye exclusion assay..... | 19 |
| 2.2.1.8. PUVA treatment..... | 19 |
| 2.2.1.9. β -galactosidase (β -Gal) Staining..... | 19 |
| 2.2.1.10. Soft agar assay..... | 20 |
| 2.2.1.11. BrdU immunostaining | 20 |
| 2.2.1.12. Cell enucleation and fusion..... | 20 |
| 2.2.2. Methods of molecular biology | 23 |
| 2.2.2.1. Isolation of genomic DNA..... | 23 |
| 2.2.2.2. Telomere repeat analysis..... | 24 |
| 2.2.2.3. Single strand telomere DNA length determination..... | 24 |
| 2.2.2.4. TRAP assay | 25 |
| 2.2.2.5. Immunoblot..... | 25 |
| 2.2.2.6. ELISA for MMP-1 expression | 26 |
| 2.2.2.7. ELISA for p53 and p21 ^{Cip1} expression..... | 27 |
| 2.2.2.8. PCR Amplification | 27 |
| 2.2.2.9. PCR products purification and sequence analysis..... | 31 |
| 2.2.3. Additional methods..... | 32 |
| 2.2.3.1. ROS measurements | 32 |
| 2.2.3.2. Supplementation of fibroblast culture with N-acetyl cystein and subsequent determination of intracellular ROS Levels | 32 |
| 2.2.3.3. Measurement of the mitochondrial membrane potential..... | 32 |
| 2.2.3.4. Measurement of mitochondrial biogenesis..... | 33 |
| 2.2.3.5. ATP measurements | 33 |
| 2.2.3.6. Densitometry measurement..... | 33 |
| 2.2.3.7. Statistics..... | 34 |
| 3 RESULTS | 35 |
| 3.1. HUMAN DERMAL FIBROBLASTS ESCAPE FROM PUVA-INDUCED LONG-TERM SENESENCE-LIKE GROWTH ARREST | 35 |
| 3.1.1. Regrowth of fibroblasts from PUVA-induced long-term senescence-like growth arrest..... | 35 |
| 3.1.2. Regrowth is not due to immortalization or transformation..... | 38 |
| 3.1.2.1. Regrowing fibroblasts post PUVA treatment do not show any telomerase activity, but a reduction in telomere length with increasing CPD..... | 38 |

| | |
|--|-----------|
| 3.1.2.2. <i>Regrowth of fibroblasts post PUVA treatment is anchorage dependent</i> | 40 |
| 3.1.2.3. <i>Regrowing fibroblasts post PUVA treatment reveal a decline in growth rates with increasing CPD</i> | 40 |
| 3.1.2.4. <i>Senescence control genes, p53, p21Cip1 and p16INK4a do not reveal mutations in regrowing fibroblasts</i> | 43 |
| 3.2. PUVA-INDUCED PREMATURE SENESCENCE DOES NOT FULLY REFLECT REPLICATIVE CELLULAR SENESCENCE | 46 |
| 3.2.1. <i>Reversibility of senescence-associated markers in regrowing fibroblasts post PUVA treatment</i> | 46 |
| 3.2.2. <i>Activation of the senescence control pathways p21/p53 and p16/Rb in PUVA-induced growth arrest</i> | 51 |
| 3.2.3. <i>PUVA treatment of fibroblasts with a null mutation in cell cycle controlling genes results in a similar growth arrest as in wild type human dermal fibroblasts</i> | 52 |
| 3.3. PUVA TREATMENT OF HUMAN DERMAL FIBROBLASTS INCREASES THE GENERATION OF INTRACELLULAR REACTIVE OXYGEN SPECIES | 56 |
| 3.3.1. <i>Increase in the number of mitochondria and decrease in the relative mitochondrial transmembrane potential in PUVA-treated fibroblasts</i> | 57 |
| 3.3.2. <i>Changes in ATP content in PUVA-treated fibroblasts</i> | 61 |
| 3.3.3. <i>PUVA-treated Rho0 fibroblasts still have a high ROS level</i> | 63 |
| 3.3.4. <i>Inhibition of NADPH Oxidase does not abrogate the ROS increase in PUVA-treated mitochondria-competent fibroblasts, whereas ROS production is suppressed in PUVA-treated Rho0 fibroblasts</i> | 65 |
| 3.3.5. <i>ROS contribute to the PUVA-induced senescence-like morphology</i> | 66 |
| 3.4. MOLECULAR MECHANISMS OF THE DECLINE IN THE OVERALL LIFE SPAN IN REGROWING FIBROBLASTS POST PUVA TREATMENT | 70 |
| 3.4.1. <i>Fibroblasts regrowing post PUVA treatment reveal a decline in the overall life-span</i> | 70 |
| 3.4.2. <i>Fibroblasts regrowing post PUVA treatment reveal enhanced reduction in telomere lengths</i> | 71 |
| 3.4.3. <i>Accumulation of single strand breaks in telomere regions</i> | 73 |
| 3.4.4. <i>Scavenging of reactive oxygen species by N-acetyl cystein rescues telomere length</i> | 76 |
| 3.4.5. <i>Partial restoration of the total life-span of PUVA-treated fibroblasts in the presence of N-acetyl cystein</i> | 76 |
| 3.4.6. <i>Up-regulated expression of p16^{INK4a} is maintained in regrowing fibroblasts post PUVA treatment</i> | 78 |
| 3.5. CHARACTERIZATION OF MOLECULAR MECHANISMS INVOLVED IN THE INDUCTION OF GROWTH ARREST IN PUVA-TREATED FIBROBLASTS | 79 |
| 3.5.1. <i>Short-term incubation with 8-MOP during UVA-irradiation does result in growth arrest while long-term preincubation with 8-MOP does not</i> | 79 |

| | |
|--|------------|
| 3.5.2. The number of DNA interstrand crosslinks is not related to growth arrest..... | 80 |
| 3.5.3. Characterization of the contribution of changes in the karyoplast and the cytoplast post PUVA treatment to PUVA-induced growth arrest..... | 82 |
| 3.5.3.1. Rationale for fusion of cytoplasts and karyoplasts..... | 82 |
| 3.5.3.2. Experimental design for the identification of fused fibroblasts..... | 83 |
| 3.5.3.3. Fusions of cytoplast/karyoplasts of fibroblasts immediately or at an early stage post PUVA with mock-treated karyoplasts/cytoplasts..... | 85 |
| 3.5.3.4. Fusions of cytoplast/karyoplasts of fibroblasts 2 weeks or 4 weeks post PUVA treatment with mock-treated karyoplasts/cytoplasts..... | 86 |
| 4 DISCUSSION..... | 92 |
| 4.1. THE ESCAPE OF HUMAN DERMAL FIBROBLASTS FROM PUVA-INDUCED SENESCENCE-LIKE GROWTH ARREST IS NOT DUE TO IMMORTALIZATION OR TRANSFORMATION..... | 92 |
| 4.2. PUVA-INDUCED GROWTH ARREST REPRESENTS A PHENOCOPY OF SENESCENCE WITH ROS CONTRIBUTING TO SENESCENCE-LIKE PHENOTYPE CHANGES..... | 94 |
| 4.2.1. Senescence features in PUVA-induced long-term growth arrest are reversible..... | 95 |
| 4.2.2. Senescence controlling genes are up-regulated in PUVA-treated fibroblasts in a sequential and interrelated manner..... | 96 |
| 4.2.3. PUVA treatment leads to elevated ROS production which is related to mitochondria and NADPH oxidase..... | 98 |
| 4.2.4. Enhanced ROS concentration of reactive oxygen species is responsible for the enlarged morphology of fibroblasts but not for the enhanced expression of SA- β -galactosidase after PUVA treatment..... | 102 |
| 4.3. PUVA TREATMENT OF HUMAN DERMAL FIBROBLASTS LEADS TO AN EARLY ONSET OF REPLICATIVE SENESCENCE RELATED TO OXIDATIVE TELOMERE SHORTENING..... | 103 |
| 4.4. INITIATION OF THE LONG-TERM GROWTH ARREST..... | 111 |
| 5 PERSPECTIVES..... | 115 |
| 6 REFERENCES..... | 118 |
| ABBREVIATIONS..... | 132 |
| SUMMARY..... | 133 |
| ZUSAMMENFASSUNG..... | 135 |
| ACKNOWLEDGEMENT..... | 136 |

1. Introduction

1.1. Cellular senescence

Cellular senescence is defined as an irreversible arrest of cell proliferation accompanied by changes in cell function and morphology. Senescent cells are viable and metabolically active for long periods of time, but are incapable of further division (Campisi *et al.* 1996). Historically, the senescent state has been associated with an intrinsically defined number of cell divisions *in vitro*. However, recently it has been shown that many extrinsic factors can prematurely induce a virtually indistinguishable senescent phenotype.

1.1.1. Cellular lifespan: the Hayflick limit

It had been generally believed that cells could proliferate indefinitely and that the maintenance of a cell culture was just a question of finding the right conditions (Hayflick 1998). This idea was radically changed in the early 1960s by Leonard Hayflick, who first described the finite life span in cultures of human diploid fibroblasts (HDFs) (Hayflick 1965; Hayflick and Moorhead 1961). Despite optimized culture conditions, HDFs can undergo 60-80 population doublings and thereafter every cell has stopped dividing. Since then, many types of normal somatic cells from humans, rodents, birds and several other species have been shown to have finite capacity for cell division (Campisi *et al.* 1996). This phenomenon, known as 'Hayflick limit', is termed 'replicative senescence'. When this limit is reached, cells stop dividing and undergo an array of biochemical and morphological changes. Senescent cells may remain metabolically active for a long period of time, even though they have permanently ceased to proliferate (Campisi 1996; Goldstein 1990).

1.1.2. Replicative senescence and telomeres

Replicative senescence depends on the overall number of cell divisions and not on the time in culture. The molecular mechanisms that determine this intrinsic replicative senescence appear to be mainly controlled by the shortening of telomeres (Mathon and Lloyd 2001).

1.1.2.1. Telomeres and their function

Telomeres are DNA-protein structures at the ends of linear chromosomes (Figure 1). In every organism studied, telomere DNA consists of long head-to-tail arrays of repeated DNA sequences. Mammalian telomeres, like all vertebrate telomeres, are tandem repeats of the sequence TTAGGG which is repeated many hundreds to thousands of times. The length varies greatly among species. While telomeres are 15 to 20 kb in the human germ line, they are ranging 30-50 kb in laboratory mice (Campisi *et al.* 2001). Most of the telomeric tract is double stranded DNA, but there are also short (50-200 base pairs) single stranded 3' overhangs at both chromosome ends (Campisi *et al.* 2001; Makarov *et al.* 1997). The telomere end folds back on itself, forming a protective structure called "T-loop" to hide the vulnerable 3' overhang (Mathon and Lloyd 2001). The T-loop is formed in association with or bound by proteins, such as TRF1, TRF2 and Ku (Broccoli *et al.* 1997; Chong *et al.* 1995; Hsu *et al.* 1999; Song *et al.* 2000). Besides maintaining the telomeric structure, many of these proteins were found to be involved in DNA repair processes (Campisi *et al.* 2001).

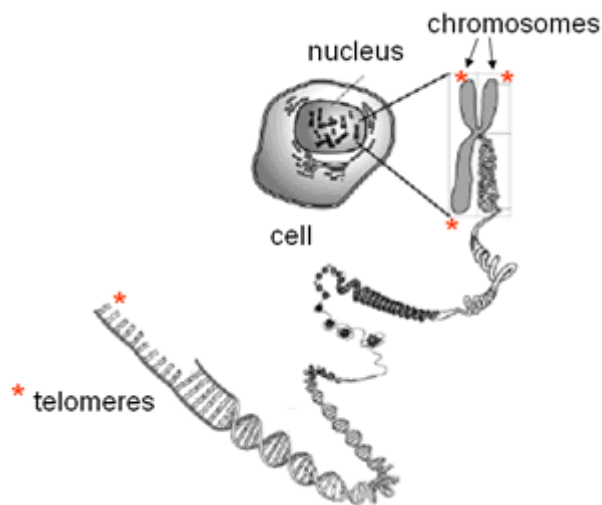


Figure 1. Structure of the telomeres. Each of the 46 linear human chromosomes has 2 telomeres. Telomeres are complex structures comprising the underlying DNA and associated proteins.

Telomeres share some basic functions and characteristics in all organisms. First, they enable cells to distinguish a chromosome end from a double strand break

(DSB) in the genomic DNA. DSBs can activate the checkpoints in the cell cycle, which cause that cell to stop dividing until the DNA strand break is rejoined. Thus, without a distinctive telomere structure, chromosome ends are at risk for degradation, recombination or random fusion by cellular DNA repair systems (Campisi *et al.* 2001; van Steensel *et al.* 1998). Second, telomeres provide a way to replicate the chromosome completely including restoration of a simple terminal repeat of characteristic length. This replication is achieved by the unique reverse-transcriptase-like enzyme telomerase or alternatively through recombination (Dubrana *et al.* 2001; Kass-Eisler and Greider 2000). Finally, telomeres control the positions of chromosomes within the nucleus (Dubrana *et al.* 2001).

1.1.2.2. The end replication problem

Eukaryotic organisms have much larger genomes compared to bacteria and viruses. Their DNA is divided into multiple linear chromosomes to keep the molecules at a manageable size. However, there is a major problem with the replication of the very ends of linear DNA during cell division known as 'end-replication problem' (Blackburn 1991; Klapper *et al.* 2001; Zakian 1995). It is a consequence of two properties of the semiconservative DNA replication machinery: the ability of DNA polymerases to work only in the 5' to 3' direction, and their requirement for a nucleic acid primer. DNA replication starts at many different sites (origins of replication) along each chromosome and is carried out by DNA polymerases. DNA polymerases initiate DNA replication only at a primer molecule, which is a short piece of RNA. The RNA primer will be degraded when DNA synthesis is complete. While replication is bidirectional where replication proceeds in both the 3' and 5' direction from an origin of replication, DNA polymerases work unidirectional and polymerize exclusively in 5' – 3' direction (Figure 2). Therefore, replication of the 'lagging strand' will form short gaps between Okazaki fragments after RNA primer degradation. Gaps are filled by DNA polymerase except for the one at the very end of the chromosome. This results in the loss of 50-200 bp in the new synthesized DNA strand at the 5' end, and forms 3' overhangs in the mother strand. Interestingly, there is a 3' overhang at both ends of mammalian chromosomes (Makarov *et al.* 1997). This finding suggests that a 5' – 3' exonuclease specifically trims back the completely synthesized telomere (Campisi *et al.* 2001).

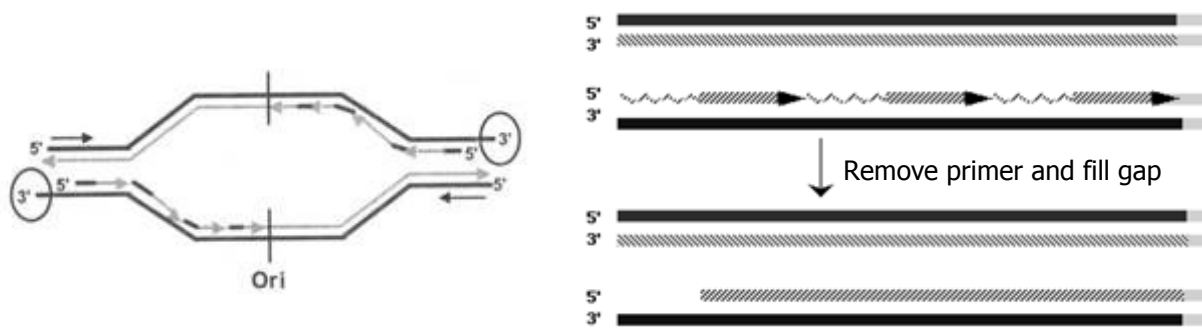


Figure 2. The end replication problem (Modified from Campisi *et al.* 2001; Greider and Blackburn 1985).

1.1.2.3. Short telomeres cause replicative senescence

The link between the Hayflick limit and the end-replication problem was first proposed by Alexey Olovnikov, a Russian theoretical biologist (Shay and Wright 2000). During successive cellular divisions the telomeres shorten progressively in normal human cells. When the telomeres erode from their maximum size of 10-15 kb (in the germ line) to an average size of 4-6 kb, replicative senescence is reached with an irreversible growth arrest. The underlying mechanisms are incompletely understood (Campisi 2001a; Mathon and Lloyd 2001). In human fibroblasts, senescent cells can be induced to bypass replicative senescence by functional inactivation of the tumor suppressor proteins p53 and pRb (Shay *et al.* 1991c). Continued proliferation of cells beyond the Hayflick limit leads to further shortening of telomeres, and cells eventually reach a second proliferative block, which is characterized by genomic instability associated with telomere dysfunction and massive cell death, termed “crisis” (Maser and DePinho 2002; Wright and Shay 1992). The hypothesis that telomere shortening is responsible for a limit in the proliferation lifespan has been generally accepted. Stable expression of telomerase is sufficient to bypass both senescence and crisis, and to confer immortality (Bodnar *et al.* 1998; Ramirez *et al.* 2001; Vaziri and Benchimol 1998). Thus, telomere shortening in normal human cells acts as a “mitotic clock” that ultimately limits the proliferative capacity of cells (Harley *et al.* 1992; Wright and Shay 1992).

1.1.2.4. Telomerase

Continuously growing cells, such as germline and tumor cells, have to circumvent the end-replication problem. This is solved by the enzyme telomerase that adds telomeric sequences onto the chromosome ends (Greider and Blackburn 1985). Telomerase is a RNA-dependent DNA polymerase that adds single-stranded telomeric repeats to the end of the telomeric DNA. It consists of two essential components: one is a RNA subunit which serves as a template for the synthesis of telomeric DNA, the encoding gene in human is referred to as hTR (Feng *et al.* 1995). The other is the catalytic protein (hTERT) with reverse transcriptase activity (Harrington *et al.* 1997; Lingner *et al.* 1997). Although hTR is highly expressed in all tissues regardless of telomerase activity, hTERT is – apart from some expression – repressed in somatic cells and upregulated in immortal cells suggesting that hTERT is the primary determinant for the enzyme activity (Ailion *et al.* 1996; Cong *et al.* 2002). Expression of telomerase is the major mechanism by which cancer cells stabilize their telomeres and, hence, avoid replicative senescence (Chiu and Harley 1997).

1.1.3. Stress-induced premature senescence

Recently, noxious stimuli with little or no impact on telomeres were shown to induce somatic cells to undergo growth arrest with a senescence phenotype. As these stimuli act before the replicative limit of a cell, this state of growth arrest has been termed premature senescence (Lloyd 2002). Stimuli that lead to premature senescence include DNA damage, genomic instability, oncogene upregulation and oxidative stress (Campisi 2001a).

1.1.3.1. DNA damage and genomic instability

The outcome of DNA damage is diverse. Acute effects from DNA damage trigger cell-cycle arrest or cell death. Long-term effects that resulted from mutations contribute to tumorigenesis (de Boer *et al.* 2002; Hoeijmakers 2001). Premature senescence can be induced by various types of DNA damage, with telomere dysfunction being the most efficient trigger. An early observation of DNA damage-induced senescence was the induction of a permanent and irreversible proliferation arrest in gamma irradiated human fibroblasts (Di Leonardo *et al.* 1994). Further evidence for the causal role of DNA damage and genomic

instability in senescence comes from human diseases featured by deficiencies in DNA damage repair pathways. Cells obtained from ataxia telangiectasia (ATM) patients or individuals suffering from Werner's and Bloom's syndromes undergo senescence earlier than age-matched healthy individuals (Schulz *et al.* 1996; Shiloh *et al.* 1985). Telomere damage seems to induce senescence as implied by the recent finding that the knockout of two DNA damage repair enzymes with similar function led to different outcome. DNA-dependent protein kinase (DNA-PK) and Ku86 are two proteins essential for the repair of DNA breaks through non-homologous end joining. Murine fibroblasts deficient in the DNA-PK catalytic subunit (DNA-PKCs) do not undergo premature senescence, whereas deficiency in Ku86 leads to premature senescence (Goytisolo *et al.* 2001; Samper *et al.* 2000). The dramatic differences in the induction of senescence between these two proteins with similar functions may be explained by the fact that Ku86 plays a specific role in the stabilization of telomeres (Serrano and Blasco 2001). In addition, disruption of TRF2 which is a critical protein involved in telomeric t-loop formation, causes immortal human tumor cells to die (Karlseder *et al.* 1999). Non-transformed cells, by contrast, undergo growth arrest with a senescent phenotype (van Steensel *et al.* 1998). Chromosomes that lack a protective telomeric structure are highly unstable, being subject to degradation, rearrangement and/or fusion, all of which could trigger the senescent program. Moreover, genomic instability, particularly in the absence of the senescence checkpoint and p53 function greatly increases the frequency of mutations (van Steensel *et al.* 1998). DNA damage and genomic instability might explain why mouse cells senesce after fewer doublings than human cells, despite having longer telomeres (Campisi 2001a). As has been reported, mouse and rat cells repair DNA damage far less efficiently than human cells and are much more sensitive to a variety of agents that produce oxidative stress (Hart and Setlow 1974; Kapahi *et al.* 1999).

1.1.3.2. *Oncogene activation*

Primary cells can not be transformed by a single oncogene *in vitro*, such as Ras or Myc (Weinberg 1989). Cells in response to these oncogenic activations often exit the cell cycle (Ras) or die (Myc) (Mathon and Lloyd 2001). Although Ras signaling pathways are constitutively activated in a large proportion of human

tumors (Hanahan and Weinberg 2000), the overexpression of the Ras oncogene in primary cells instead leads to a senescence-like state (Serrano *et al.* 1997). Ras-induced premature senescence shares similar features with replicative senescence not only phenotypically but also in cell cycle control pathways. In human fibroblasts, both Ras-induced premature senescence and replicative senescence reveal an upregulation of the tumor suppressor p16^{INK4a} which inactivates the D-type cyclins (Serrano and Blasco 2001).

1.1.3.3. Oxidative stress

Oxidative damage is another cellular stress that can induce senescence-like growth arrest. Culturing human fibroblasts in 2-3% oxygen results in 20-30% more population doublings compared to that under 20% oxygen (Balin *et al.* 1984; Chen *et al.* 1995b; Saito *et al.* 1995). Similarly, treatment of cultures of primary fibroblasts with non-lethal concentrations of hydrogen peroxide activates a rapid, senescence-like growth arrest (Chen and Ames 1994). The role of oxidants in cellular senescence was further underscored by the observation that Ras-induced senescence is also mediated by ROS and can be abrogated by culturing cells under low oxygen tension or in the presence of antioxidants (Lee *et al.* 1999). Oxidative stress is probably the most often used inducer of premature senescence and is likely to be the common denominator of the 'stress-induced premature senescence' (SIPS) (Toussaint *et al.* 2000c). Accumulation of cell damage as a result of oxidative damage to macromolecules is generally thought to play an important causal role in aging (Johnson *et al.* 1999).

1.1.4. Senescent phenotypes and molecular pathways

The universal characteristic of replicative senescence is a stable, irreversible loss of cell proliferative capacity (Campisi *et al.* 1996). Several phenotypic and biochemical changes are associated with replicative senescence and are used as markers to identify premature senescence. These changes include increased cell size which changes from a small, elongated or spindle-like shape in young cells to aged flattened cells with enlarged cytoplasm, expression of senescence associated β -galactosidase (SA- β -Gal), which is associated with an increased biogenesis of lysosomes. In addition, cellular senescence comprise an abrogated response to growth factors and other mitogens, a reduced membrane potential, a

decrease in respiration and energy metabolism, an increase in the duration of G1 phase of the cell cycle and the upregulation of certain growth inhibitory genes, such as p16 and p21. Furthermore, distinct changes were found in cellular functions such as the adaption of matrix-degrading phenotype by senescent fibroblasts as well as an altered secretion pattern of steroid hormones by senescent adrenal cortical epithelial cells (Campisi 1997, 1998, 2000, 2001b; Campisi *et al.* 1996; Campisi *et al.* 2001).

A number of regulatory proteins transduce senescence-inducing signals or mediate entrance of the cell into senescence, among which the most crucial are several tumor suppressors, such as p53 and p16^{INK4a} (Figure 3). Although p53 protein levels do not increase during replicative senescence, an increase in its activity in terms of DNA binding and transcriptional activity is observed (Atadja *et al.* 1995; Vaziri *et al.* 1997). p53 levels transiently increase in oxidative stress or oncogenic Ras-induced premature senescence (Chen *et al.* 1998; Dimri *et al.* 2000; Serrano *et al.* 1997). A major cause of p53 upregulation or activation is related to the increase in the expression of p14^{ARF} (p19^{ARF} in mouse), a tumor suppressor encoded by the INK4a locus (Campisi 2001a). p14^{ARF} could be induced by oncogenic Ras and DNA damage. p14^{ARF} directly binds and sequesters MDM2, a protein that facilitates p53 degradation. Loss of MDM2 function, in turn, results in the stabilization of p53 and activation of p53-mediated growth arrest (Bringold and Serrano 2000). Another cause for the increase in p53 activity might be the promyelocytic leukemia (PML) tumor suppressor which can be induced by oncogenic Ras (Ferbeyre *et al.* 2000; Pearson *et al.* 2000). Activation of PML acetylates p53 and thus stimulates its activity (Pearson *et al.* 2000). p53 induces the transcription of several genes responsible for the onset of senescence including the cyclin-dependent protein kinase (CDK) inhibitor p21, a well-recognized p53 target gene. Another pathway implicated in cellular senescence involves p16^{INK4a} and Rb. p16 is the second tumor suppressor encoded by the INK4a locus (Bringold and Serrano 2000; Lundberg *et al.* 2000). p16^{INK4a} is involved both in replicative senescence and stress-induced premature senescence (Serrano and Blasco 2001). Upregulation of p16 is in part due to Ets, a transcription factor that stimulates p16 expression and accumulates in senescent cells (Campisi 2001a). Ets activity is negatively regulated by the helix-

loop-helix protein Id1 (Ohtani *et al.* 2001). It is not known how other senescence inducers stimulate Ets activity, or how Id1 is repressed in response to senescence-inducing signals. Nonetheless, these findings have identified p16 expression as an important target for senescence-inducing signals (Campisi 2001a). In human cells, p16/Rb appear to be the major factors controlling the cell cycle checkpoint in response to inadequate culture conditions and other kinds of stresses, whereas p14^{ARF}/p53/p21 may initially have a more predominant role in human fibroblasts at their proliferative limits or in response to DNA damage. In each case, there are many overlapping roles for factors controlling these checkpoints of the cellular senescence (Wright and Shay 2001).

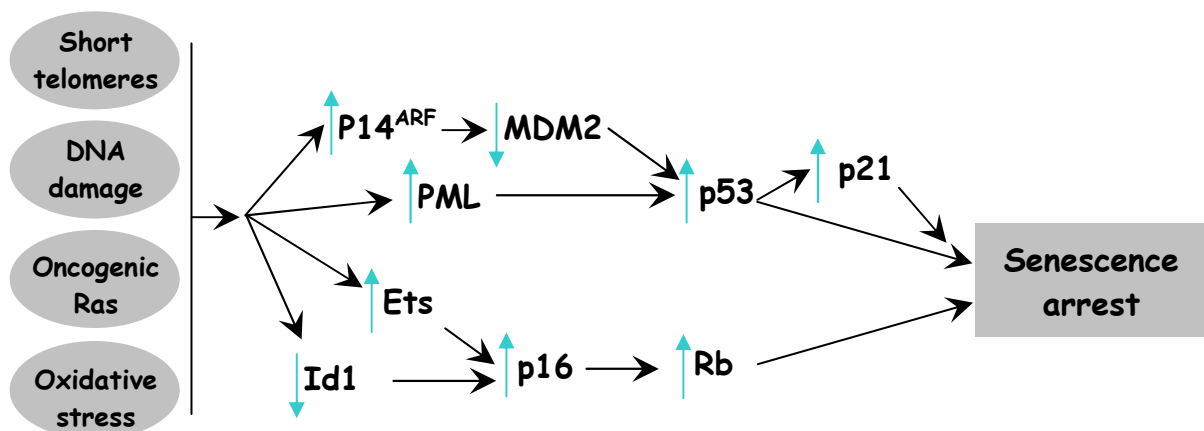


Figure 3. Cellular senescence pathways (Adapted from Campisi 2001a; Lundberg *et al.* 2000).

1.1.5. Role of cellular senescence in cancer and aging

1.1.5.1. Implications for cancer

One interpretation for the biological function of cellular senescence is that it serves as a mechanism for restricting cancer progression (Wright and Shay 2001). Cancer is a complex condition involving a multi-faceted evolutionary process which occurs at the cellular level within organs and organisms. One hallmark of tumor cells is that they can proliferate indefinitely. The extended growth potential of cancer cells is critically dependent on the maintenance of functional telomeres. Most human malignant tumors express telomerase. Tumor cells that do not express telomerase stabilize their telomeres by a different mechanism – alternative lengthening of telomeres (ALT) (Bryan *et al.* 1997; Kim

et al. 1994). The expression of telomerase in nearly all malignancies suggests that overcoming the proliferative limits imposed by telomere shortening represents a key step in oncogenesis (Kim *et al.* 1994). Apart from replicative senescence, it has been speculated that premature senescence can also serve as a tumor-suppressing mechanism. Another hallmark that distinguishes cancer cells from primary cells is the loss of growth control, resulting from both gain-of-function mutations in proto-oncogenes and loss-of-function mutations in tumor suppressors (Cong *et al.* 2002). The observation that many of the checkpoint control genes involved in premature senescence are oncogenes or tumor suppressors has been forwarded to argue that overcoming these proliferative checkpoints represents an important step in tumor development (Campisi 2001b; Mathon and Lloyd 2001).

1.1.5.2. Implications for aging

Aging is associated with a progressive decline in bodily functions, ultimately resulting in disease and death (Mathon and Lloyd 2001). The idea that cellular senescence reflects mechanisms also relevant for organismal aging is supported by several lines of evidence. First, limited inter-species comparisons showed an inverse correlation between species lifespan and the replicative life span of fibroblast cultures (Rohme 1981). Second, cells from patients with premature aging syndromes were observed to senesce after fewer doublings than age-matched healthy individuals (Martin 1970). Third, cells expressing SA- β -galactosidase are more prevalent in physiologically aged tissue than in young tissue (Campisi 2001b; Dimri *et al.* 1995). However, evidence for a role of replicative senescence in the aging process remains controversial, since the inverse correlation between donor age and the replicative ability of *in vitro* cell proliferation was not consistently observed in all studies (Cristofalo *et al.* 1998; Stanulis-Praeger 1987).

Cellular senescence drives some of the dysfunctions associated with aging. Senescent cells remain metabolically active but cannot proliferate, and may rather be disruptive and destructive in the tissues in some instances. Senescent cells show changes in gene expression and secrete a number of proteins that contribute to degeneration of connective tissues seen in aging (Shelton *et al.*

1999). This senescence-associated secretory proteolytic phenotype is particularly striking in fibroblasts. Senescence of fibroblasts is accompanied by increased expression of matrix-degrading enzymes like collagenase and stromelysin (Campisi 1996; Kim *et al.* 2002). These enzymes could be potentially detrimental to the adjacent environment of the cell and, thus, could affect all other adjacent nonsenescent cells. In skin, for example, this could lead to a loss of integrity resulting in wrinkles and loss of elasticity commonly observed in skin aging (Smith and Pereira-Smith 1996). Though the factors released from senescent cells are incompletely characterized, and little is known on mechanisms responsible for their overexpression (Campisi 2001a), senescent fibroblasts have been shown to accumulate with age in skin biopsies (Dimri *et al.* 1995).

1.2. PUVA-treated fibroblasts as a model for stress-induced premature cellular senescence

1.2.1. Psoralen phototherapy

PUVA is a combination of psoralen (P) and long-wave ultraviolet radiation (UVA) that is widely used for the treatment of various skin disorders. Even though topical exposure to extracts, seeds and parts of plants (e.g. Ammi majus, Psoralea corylifolia) that contain natural psoralens and subsequent irradiation with sunlight as a remedy for the treatment of vitiligo has been used for thousands of years by ancient Arab and Indian healers, the modern era of its use began in Egypt in the mid-1940s when the active components 8-methoxypsoralen (8-MOP), 5-methoxypsoralen (5-MOP) and isoamyleneoxypsoralen were isolated and chemically characterized (Lerner 1988). PUVA treatment for psoriasis, by far the most prevalent use of PUVA, was developed clinically in 1970s at Harvard Medical School (Honigsmann 1986; Lerner 1988). Ten years later, photopheresis using 8-MOP was introduced for the treatment of T-cell lymphoma (Edelson *et al.* 1987; Gasparro *et al.* 1998).

The combination of psoralen and UV irradiation results in beneficial therapeutic effects, which are not achieved by either of the single components alone. The

effectiveness of PUVA, as well as other kinds of phototherapy, provided treatment for a variety of different skin disorders besides psoriasis (Honig *et al.* 1994; Honigsmann 2001). However, PUVA treatment also raises the potential risk of the development of skin cancer and possibly premature skin aging (Jacobson-Kram *et al.* 1982). A study by Stern *et al.* (1994) of 1380 patients showed a statistically significant increase in the incidence of squamous cell carcinoma (SCC) in PUVA patients (Stern and Laird 1994). Although PUVA is the most widely employed photochemotherapy treatment in dermatology, many of the biochemical and molecular events induced by PUVA have not yet been intensively characterized.

1.2.2. 8-MOP photochemistry and photobiology

8-methoxypsoralen, the most widely used psoralen derivative for PUVA treatment, is a naturally occurring aromatic tricyclic molecule (Figure 4). Its planar and extended aromatic structure enables it to intercalate with nucleic acid base pairs. Upon photoactivation three different types of psoralen-DNA photoadducts were formed including two kinds of monoaddition products, 3,4-monoadducts and 4'5'-monoadducts, and one bi-adduct (psoralen-DNA interstrand crosslink (ICL)) (Gasparro 1988). Psoralens react with DNA in three steps. First the psoralen intercalates into the DNA double strand in the absence of UV radiation. Upon UV irradiation, cyclobutane monoadducts with a pyrimidine base are formed. If the initial photoreaction occurs at a 5'-TpA site, the 4'5'-monoadducts can absorb a second photon and undergo another cyclobutyl reaction with the adjacent thymine at the opposite strand resulting in the formation of a psoralen-DNA cross-link (Gasparro 1988; Gasparro *et al.* 1997). Because these DNA photoadducts are the most well-characterized psoralen photoadducts, most explanations of therapeutic efficacy have been based on the generation of DNA photoadducts, especially psoralen-DNA crosslink formation as the basis for the subsequent proliferation inhibitory or toxic effects (Schmitt *et al.* 1995). However, there is scant direct evidence supporting the biological impact of the photoadduct. Psoralens have also been shown to undergo photoaddition reactions with other cellular components, such as proteins and lipids (Schmitt *et al.* 1995). In addition to direct modification of nearby biomolecules, the excited 8-MOP can also react with molecular oxygen. The reactive oxygen species formed

by this reaction can directly lead to oxidative DNA damage or cause cell membrane damage by lipid peroxidation (Averbeck 1989; Gasparro *et al.* 1997).

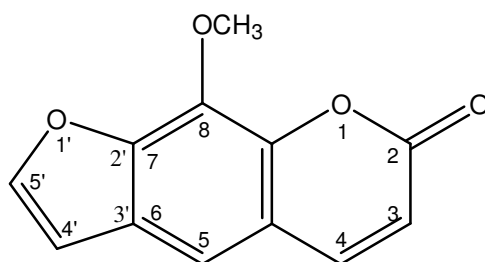


Figure 4. The chemical structure of 8-MOP.

1.2.3. PUVA-induced senescent-like growth arrest of fibroblasts

Previous work in our laboratory has shown that psoralen photoactivation promotes morphological and functional changes in fibroblasts *in vitro* reminiscent of replicative cellular senescence. A single non-toxic exposure of human dermal fibroblasts to PUVA with 50ng/ml 8-MOP and 90 kJ/m² UVA resulted in a long-term switch of mitotically active fibroblasts to growth-arrested fibroblasts without proliferative activity (Herrmann *et al.* 1998). In addition to arresting cell proliferation, PUVA treatment also induced a senescent-like phenotype with an enlarged phenotypic morphology, enhanced SA- β -Gal expression, and elevated expression of interstitial collagenase/matrix metalloproteinase-1 (MMP-1). Fibroblasts which had been subjected to PUVA treatment changed to a flattened and elongated phenotype at day 7 post treatment and revealed a substantial increase in size at day 14-21 after irradiation. Similarly, SA- β -Gal positive fibroblasts were detected from day 7 post PUVA and at day 28 essentially all fibroblasts revealed *de novo* expression of SA- β -Gal. Furthermore, MMP-1 was induced following PUVA treatment. The induction of MMP-1 was prolonged within the growth arrest phase, while TIMP-1, the major inhibitor of MMP-1, was only slightly induced. The imbalance between matrix-degrading metalloproteinases and their inhibitors may lead to connective tissue damage, a hallmark of skin aging (West *et al.* 1989). Interestingly, PUVA-treated fibroblasts could resume proliferation after a growth arrest period of about three months.

1.3. Aim of the study

The aim of this study is a more detailed characterization and understanding of the molecular mechanisms involved in the initiation, maintenance and release from the PUVA-induced long-term senescence-like growth arrest with particular focus on the development of the senescent phenotype and factors influencing replicative senescence. In detail, the following questions were addressed:

- i) What are the molecular mechanisms underlying the initiation and maintenance of the long-term growth arrest as well as what mechanisms are involved and contribute to the development of senescent-like biochemical and morphological changes?
- ii) What molecular mechanisms determine the re-proliferation of PUVA-treated fibroblasts after the long-term growth arrest? Is it due to immortalization or transformation as a result of loss-of-function of tumor-suppressor genes controlling cellular senescence? Or does PUVA-induced long-term growth arrest represents a phenocopy of senescence, activated to serve a damage-repairing function?

Answers to these questions are of general relevance and may shed light to other premature senescence models with the identification of similarities and differences and potential identification of therapeutic strategies to prevent or treat aging and neoplastic conditions.

2 Materials and methods

2.1. Materials

2.1.1. Chemicals

All analytical grade chemicals were purchased from Sigma-Aldrich (Deisenhofen), Molecular probes (MoBiTec, Goettingen), Merck (Darmstadt), USB (Amersham Life Sciences, Braunschweig), Merck (Darmstadt), Serva (Heidelberg), Bio-Rad (Munich), Pharmacia-Biotech (Freiburg); Radiochemicals were obtained from ICN (Eschwege).

Molecular weight markers for proteins (Broad Range) were purchased from Bio-Rad and DNA molecular weight standards from Roche (Mannheim) and New England Biolabs (Schwalbach). Antibodies were purchased from Santa-Cruz Biotechnology (Heidelberg).

Restriction enzymes used were from Boehringer (Mannheim), New England Biolabs.

Oligonucleotides were synthesized at MWG Biotech (Ebersberg).

2.1.2. Cell culture material

All plastic material for cell culture was from Greiner (Solingen). Cell culture medium and supplements were purchased from Gibco BRL (Eggenstein), and fetal calf serum (FCS) was from PAA Laboratories (Biochrom, Berlin).

2.1.3. Cell strains, bacteria, vectors and plasmids

The following cell strains had been used: two human dermal fibroblast strains, FF95 and FF-DA. The epithelial carcinoma cell line HeLa and the fibrosarcoma cell line HT1080. For transformation of plasmids the E. coli strain DH5 α (Gibco BRL, Eggestein) was used. The genotype is: F', supE44, Δ lacU169 (ϕ 80lacZ Δ M15), hsdR17, recA1, gyrA96, thi-1, relA1. The eukaryotic expression vector pEGFP-N1 was purchased from ClonTech Laboratories Inc. (Heidelberg).

2.1.4. Buffers

| | |
|------------------|---|
| PBS | 137 mM NaCl, 2.7 mM KCl, 8.4 mM Na ₂ HPO ₄ , 1.4 mM KH ₂ PO ₄ , pH7.4 |
| TBS | 20 mM Tris, 137 mM NaCl, pH7.6 |
| TBS-T | TBS, 0.1%(v/v) Tween 20 |
| 20× SSC | 3M NaCl, 0.3M Sodium citrate, pH7.0 |
| 100× Denhards | 2% ficoll, 2% polyvinylpyrrolidon, 2% BSA |
| TBE | 89 mM Tris base, 89 mM boric acid, 2 mM EDTA |
| TSE | 10 mM Tris, 150 mM NaCl, 10 mM EDTA |
| TAE (10×) | 2 M Tris, 5.7% (v/v) glacial acetic acid, 50 mM EDTA |

Protein extraction buffer

50 mM Hepes (pH 7.4), 1% (v/v) Triton X-100, 50 mM NaCl, 100 mM NaF, 10 mM EDTA, 10 mM Na₃VO₃, 0.1% (w/v) SDS; supplemented with a cocktail of protease inhibitors (Leupeptin 10 ng/ml, Aprotinin 10 µg/ml, Benzamidine and PMSF 2 mM).

RIPA buffer

50 mM Tris (pH 7.5), 5 mM NaCl, 1 mM EGTA, 1% Triton X-100, 50 mM NaF, 10 mM Na₃VO₄, 1 mg/ml aprotinin, 1 mg/ml leupeptin, 1 mg/ml pepstatin A, 0.1 mM phenylmethylsulfonyl fluoride and 1 mM DTT

Protein denaturing sample buffer (2×)

0.5 M Tris-HCl, pH6.8, 10% glycine, 10% SDS, 0.1% Bromophenol.

2.2. Methods

2.2.1. Methods of cell biology

2.2.1.1. Cell culture

Fibroblasts were established by outgrowth from foreskin of healthy human donors aged 3 to 6 years (Fleischmajer *et al.* 1981). Fibroblasts were maintained in Dulbecco's modified Eagle's medium (DMEM) supplemented with 10% fetal calf serum (FCS). Fibroblasts were incubated in a humidified 5% CO₂ - 95% air atmosphere at 37°C. For determination of growth rates and cumulative population doublings (CPDs), cells were counted at each transfer with a Fuchs-Rosenthal haemocytometer. CPD was calculated according to the following equation:

$$CPD_n = \sum_{i=1}^{i=n} (\ln(a_i / a_0) / \ln 2)$$

a_i = Cell number per dish at the end of each passage.

a_0 = cell number seeded per dish at the beginning of each passage.

2.2.1.2. Freezing and thawing of fibroblasts

Subconfluent fibroblasts were trypsinized, resuspended in FCS (GIBCO BRL) supplemented with 10% DMSO (Sigma-Aldrich). Aliquots were placed in a freezing container filled with isopropanol and remained for 1-2 days at -80°C before storage in liquid nitrogen. For thawing frozen fibroblasts were quickly transferred from liquid nitrogen into a 37°C water bath, thawed, seeded on a Petri-dish at a density of $2 \times 10^5 \sim 5 \times 10^5$ with subsequent change of medium one day later.

2.2.1.3. Rho0 fibroblasts

mtDNA depleted fibroblasts designated as Rho0 fibroblasts were prepared by treating human dermal fibroblasts with 0.1 µg/ml ethidium bromide at 37°C for 7-14 days in DMEM supplemented with 10% FCS, 110 µg/ml pyruvate, and 50 µg/ml uridine. During cell growth, because mtDNA replication is inhibited, the initial number of mtDNA molecules present in these cells is decreased by a factor of two each time the cells divide. The depletion of mtDNA was confirmed by the

mitochondria transcription factor, mtTFA, which has been shown to correlate with mtDNA copy number (Shen and Bogenhagen 2001). Afterwards, Rho0 fibroblasts were maintained in the same medium to ensure that mtDNA will not recover back.

2.2.1.4. Generation of stably transfected cell line

Fibroblasts (1×10^6) were seeded in a 10 cm diameter dishes 24 h before transfection. The plasmid (pEGFP-N1) containing GFP and neomycin resistant genes was transfected into skin fibroblasts using FuGENE 6 reagent according to the manufacturers's instructions (ClonTech Laboratories Inc, Heidelberg). pEGFP-N1 (4 μ g) and FuGENE reagent (24 μ l) prediluted in 372 μ l optimized MEM were mixed and incubated at room temperature for 45 min to allow the formation of DNA-lipid complexes. Fibroblasts were incubated with these complexes in serum free medium for 3-8 h at 37°C and 5% CO₂. Thereafter, FCS was added to the cells without removing the transfection mixture. 24 h after transfection, cells were cultured in fresh selective medium containing 200 μ g/ml geneticin (G418, Gibco BRL, Eggenstein, Germany). Selection was continued with changes of the medium every 3 days until colonies of cell become visible. Single clones were picked and expanded.

2.2.1.5. Cell morphology

In order to monitor fibroblast morphology at different time points after irradiation, fibroblasts were fixed using formaldehyde (3.7% in 1 \times PBS) for 10 min, washed briefly with 70% ethanol and stained with Coomassie Blue (0.05% in 20% methanol and 7.5% acetic acid) for at least 20-30 min (Bayreuther *et al.* 1988).

2.2.1.6. MTT assay

The cytotoxicity of reagents was determined by measurement of cell viability using MTT assay. This assay depends on the ability of mitochondrial dehydrogenases within viable cells to reduce MTT dye to a blue formazan product. The amount of the reduced dye is directly correlated to the number of viable cells. After treatment of fibroblasts with PUVA or chemicals, DMEM/10% FCS containing 0.5 mg/ml MTT (Sigma) was added to each dish. The cells were

incubated at 37°C for 1 h and then an equal amount of solubilization solution (0.04 N HCl in isopropyl alcohol) was added and mixed thoroughly to dissolve the crystals of MTT formazan. After all of the crystals were dissolved, the photoabsorption was measured at 540 nm was measure.

2.2.1.7. Trypan blue dye exclusion assay

Cell suspension in PBS was stained with 0.4% trypan blue (w/v, in PBS) for 5-15 min at room temperature. The cells excluding or stained with the dye were counted using a haemocytometer. Membrane integrity was expressed as the percentage of cells that excluded the dye.

2.2.1.8. PUVA treatment

Crystalline 8-methoxypsoralen (8-MOP) was dissolved in DMSO at a concentration of 1 mg/ml and stored in the dark. A working solution of 8-MOP was prepared in DMEM or phosphate-buffered saline (PBS) immediately prior to use. For PUVA treatment, fibroblasts were pre-incubated with 50 ng/ml of 8-MOP and cultured in DMEM for 16-18 h. Thereafter the medium was changed to pre-warmed PBS containing 8-MOP at a concentration of 50 ng/ml. Cells were irradiated at a dose of 90 kJ/m² using a high intensity UVA source (UVASUN 3000 equipped with the UVASUN safety filters, Mutzhas, Munich, Germany) emitting wavelengths in the 340-450 nm range. Fluencies were determined with a spectrum adapted UVA-ultraviolet meter (Dr. Hönle, Planegg, FRG). Under these non-toxic conditions of PUVA treatment > 85% of fibroblasts survived.

2.2.1.9. β -galactosidase (β -Gal) Staining

β -galactosidase staining was performed according to published method (Dimri *et al.* 1995). Cells were fixed in 2% formaldehyde/0.2% glutaraldehyde, rinsed with PBS, and stained in fresh senescence-associated β -galactosidase (SA- β -Gal) stain solution (1 mg/ml X-Gal, 40 mM citric acid/sodium phosphate/pH 6.0, 5 mM K₃Fe[CN]₆, 5 mM K₄Fe[CN]₆, 150 mM NaCl, 2 mM MgCl₂) overnight at 37°C. To detect lysosomal β -Gal, staining was performed with citric acid/sodium phosphate at pH 4.0.

2.2.1.10. *Soft agar assay*

Fibroblasts regrowing post PUVA treatment and mock-treated (under a same experiment procedure but without psoralen and UVA irradiation) control fibroblasts were tested for anchorage independent growth in soft agar (Saitoh *et al.* 1999). 5×10^3 cells were suspended in 1.5 ml DMEM medium of 0.4% agar supplemented with 10% FCS and overlaid on 1.5 ml of a similarly prepared 0.8% agar-medium basal layer in 35 mm plastic tissue culture dishes. The epithelial carcinoma cell line HeLa and the fibrosarcoma cell line HT1080 (Rasheed *et al.* 1974) served as positive controls. All cultures were incubated at 37°C in an humidified 5% CO₂ 95% air atmosphere. Thereafter colony formation was assessed and photographed at a magnification of x100. Three independent experiments were performed in triplicates. As no colony formation occurred in regrowing fibroblasts post PUVA treatment, numbers of single cells post PUVA treatment and the mock-treated control were calculated at different time points after seeding cells into soft agar. Data are expressed as the mean \pm standard deviation of 10 randomly selected high power fields (x100 magnification).

2.2.1.11. *BrdU immunostaining*

BrdU incorporation was performed using an in situ proliferation kit (FLUOS, Roche, Mannheim). After PUVA treatment, cells were cultured in 35 mm plastic tissue culture dishes, and BrdU incorporation was determined at different time points post PUVA treatment. Fibroblasts were incubated with BrdU at a concentration of 10 μ M for 10 to 14 hours, and subsequently stained with a fluorescence linked anti BrdU antibody. Microphotographs were taken with a CCD-camera attached to a fluorescence microscope (Nikon) at a magnification of $\times 100$. BrdU labelled nuclei as well as unlabelled and total nuclei were counted and calculated, repetitively, in 10 randomly selected high power fields (x100 magnification). The results were expressed as percent BrdU positive cells of total cell number.

2.2.1.12. *Cell enucleation and fusion*

Reagents and solutions: Cytochalasin B was prepared as a 1 mg/ml solution in 95 or 100% ethanol. Stored at -20°C, this solution is stable for more than 1 year.

Ficoll-400 is prepared as a 50% (w/w) solution in distilled water, dissolved by stirring overnight at room temperature and then sterilized by autoclaving. Fifty percent (w/v) solution of Polyethylene glycol 1000 (PEG) was prepared by first liquefying the PEG by briefly heating the Erlenmeyer flask in a microwave oven. The liquefied PEG is allowed to cool, and, before it solidifies, 8 ml DMEM and 2 ml DMSO were added. The pH of the final solution was adjusted to pH 7.4 with 10 N NaOH using the phenol red pH indicator dye (present in the DMEM) to visually estimate the pH of the solution. The exact pH of the solution has been found not to be critical for cell fusions. This PEG solution can be stored at 4°C up to 1 month. As the concentration of PEG is critical for successful cell fusions any evaporation that occurs during storage will adversely affect the results. Therefore, the PEG solution was kept in a tightly sealed container if not used immediately. If stored at 4°C, the PEG should be re-dissolved at 37°C prior to use.

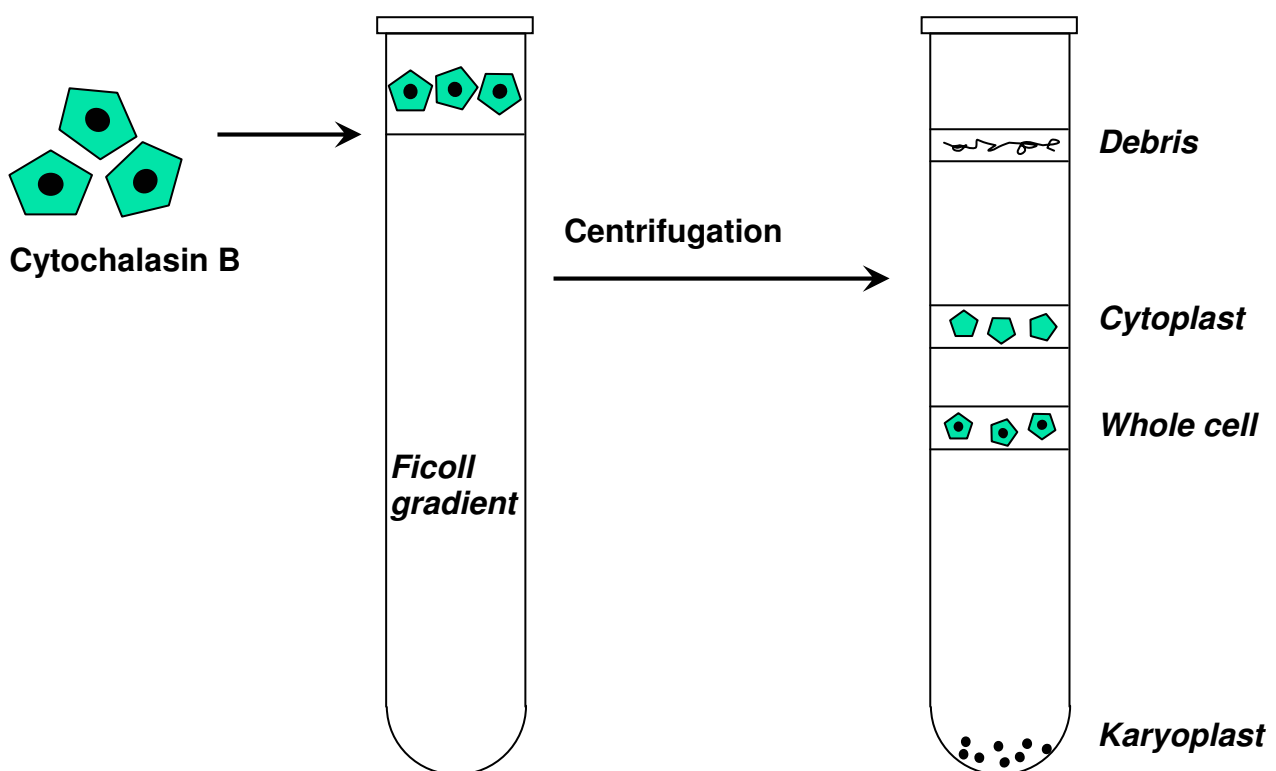
Ficoll gradient preparation: A discontinuous Ficoll gradient is prepared in a 14×89 mm polypropylene ultracentrifuge tube. Two ml 25%, 2 ml 17%, 0.5 ml 16%, 0.5ml 15% and 2 ml 12.5% Ficoll were prepared as shown in the following table and filled into tube in order.

| Final Ficoll Conc. (%) | 50% Ficoll Stock (ml) | FCS free DMEM (ml) | Cytochalasin B [1 mg/ml] (μl) |
|------------------------|-----------------------|--------------------|-------------------------------|
| 25 | 5 | 4.9 | 100 |
| 17 | 3.4 | 6.5 | 100 |
| 16 | 3.2 | 6.7 | 100 |
| 15 | 3 | 6.9 | 100 |
| 12.5 | 5 | 14.8 | 200 |

Pipet exactly the stated volume of each concentration of Ficoll into polypropylene tube, mix thoroughly before pipetting since a gradient is formed in the stock. It is recommended that the interfaces of the Ficoll layers be marked on the outside of the centrifuge tube to facilitate their identification after centrifugation. The gradient is prepared at least 4 hr but less than 24 hr prior to use. The Ficoll

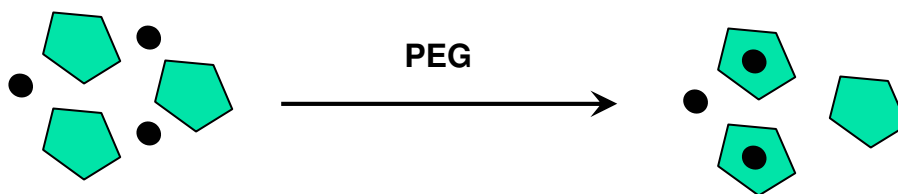
gradient was used 6-8 hours after preparation in the experiments. Keep at 37°C in CO₂ incubator to maintain the temperature and the pH.

Enucleation Procedure: Cells are trypsinized and collected by centrifugation. Resuspending in 3ml 12.5% ficoll with additional 30 µl cytochalasin B (final concentration is 20µg/ml). 1-3×10⁷ cells are required. The cell suspension is layered on the gradient, incubated with cytochalasin B at room temperature for 10 min before centrifugation. Centrifugation was performed with SW 41 swinging-bucket ultracentrifuge rotor (Beckman Instruments Inc.). The rotor and centrifuge are prewarmed by prior centrifugation at 10,000 rpm for 2 hr. Centrifugation of the gradients is performed at 26,000 rpm for 1 hr at 29°C (The highest temperature provided. The cytoplasts and fragments of cytoplasts are found through the 12.5, 15, and 16% ficoll solution, collecting by a transfer pipette and diluting with 10-20 volumes of DMEM. The karyoplasts are collected from the pellet in the tube bottom. Wash with DMEM before collecting.



Fusion of cytoplasts and karyoplasts: Mix the collected cytoplasts of normal cells and the karyoplasts of the PUVA-treated cells. For the fusion between the PUVA cytoplasts and mock-treated karyoplasts, treat cytoplasts with 20µg/ml Hoechst

33342 for 20-30 min in DMEM medium and wash once before mix. Centrifuge at 1000-1100g for 5 min to pellet the cytoplasts and karyoplasts. Remove as much medium as possible with a pasteur pipette and add 200µl-500µl of fusion solution for exactly 1 min at room temperature. Quickly add 10 ml of complete growth medium, and centrifuge at 800g for 5 min. Decant the supernatant, gently resuspend fusion product using a Pasteur pipette and plate out in culture dishes at low density. Twenty four hours later, the medium is changed to remove the dead cytoplasts and other fragments. For the fusions between mock-treated cytoplasts and PUVA karyoplasts, the medium was discarded and new medium supplemented with 200µg/ml G418 was used for selection.



2.2.2. Methods of molecular biology

2.2.2.1. Isolation of genomic DNA

Cell monolayers were trypsinized and washed with TSE. The pellets were thoroughly resuspended in 200-250 µl TSE. Two hundred-250 µl of TSE containing 0.4% SDS and 0.6-0.8 mg/ml proteinase K (final concentration 0.2% SDS and 0.3-0.4 mg/ml proteinase K) was added. Incubation was carried out subsequently at 55°C overnight (at least 5-6 hours) or until no cellular debris is visible. An equal volume of phenol/chloroform/isoamyl alcohol (24:24:1) was added to the lysate, mixed by inversion and centrifuged for 10 min with 12600 g at 16°C. The upper aqueous phase containing genomic DNA was removed and mixed with an equal volume of chloroform. A further extraction was performed to remove any remaining phenol. The upper aqueous layer was then collected. Two to 3-fold volumes of pre-cooled ethanol were added and the solution was well mixed by inversion. DNA precipitates should be visible. Recovering DNA precipitates was carried out using a drawn out Pasteur pipet and with subsequent lifting the DNA out of the alcohol (spinning out). DNA was dipped into 70% EtOH

and transferred to new Eppendorf tube. After briefly air drying the DNA was resuspended in TE. Isolated genomic DNA was stored at 4°C.

2.2.2.2. Telomere repeat analysis

Telomere length was analyzed using a commercially available assay (PharMingen, San Diego, USA). Isolated genomic DNA was digested with two frequently cutting restriction enzymes, RsaI and HinfI, which does not have a target sequence within the telomeric repeat (TTAGGG). The chromosomal DNA is therefore cut into small fragments except for the telomeres and subtelomeric regions (DNA adjacent to the telomere), which will be left intact and which together comprise the Terminal Restriction Fragments (TRF). Using multiple frequent cutters, it is assured that the chromosomal DNA is minimal in comparison to the DNA conferring the telomere length. The cleaved DNA is separated on a low percentage agarose gel and transferred for Southern blot analysis. Briefly, 1.5 µg of HinfI/RsaI-digested DNA of each sample was size-fractionated by electrophoresis on 0.6% agarose gels in TAE buffer (0.04M Tris-acetate, 0.001M EDTA, pH 8.0). After electrophoresis, blotting was carried out by alkaline transfer to a positively charged nylon membrane (Amersham Hybond-N⁺). Hybridization was carried out using a 51-mer biotinylated telomeric probe (TTAGGG)₈-TTA, which was boiled for 5 min before being added to the hybridization buffer. Prehybridization was performed for 2 hours with subsequent hybridization overnight at 60°C. After washing and blocking unspecific binding, the membrane was probed with streptavidin-HRP (1:300) for 15 min at RT. The membranes were then washed with TBS-T again, incubated with North2South Luminol/Peroxide solution (PERBIO Science Deutschland, Bonn, Germany) for 5-10 min and exposed to X-ray film. The TRF (terminal restriction fragments) length was estimated by comparing the position of the signal smear or calculated by positions relative to the molecular weight markers.

2.2.2.3. Single strand telomere DNA length determination

Genomic DNA isolated from growth-arrested fibroblasts at different time points post PUVA treatment as well as mock-treated control and regrowing fibroblasts were digested first with RsaI/HinfI (1U/µl) overnight at 37°C. After digestion, half

of the sample (20µl, 5µg DNA) was treated with alkaline buffer (0.4M NaOH, 4 mM EDTA) for 5-10 min to separate DNA double strands, then subjected to electrophoresis and Southern blot as described above. The other half of the samples was used without denaturing as control for double-stranded telomere length determination.

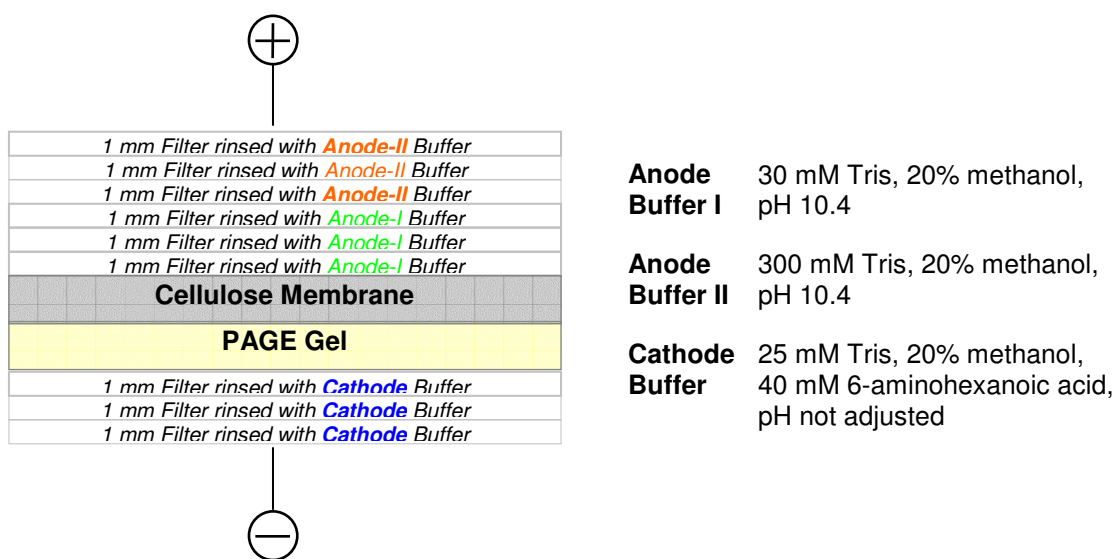
2.2.2.4. *TRAP assay*

The TRAP assay was carried out according to published protocols (Blackburn 1991; Greider and Blackburn 1985). Frozen samples or cell pellets from cell lines were homogenized in cold CHAPS lysis buffer. After a 30 min incubation period on ice, the homogenized lysates were centrifuged at 12,000 g for 30 min at 4 °C and the supernatants were aliquoted and stored frozen at -80 °C until use. The telomerase activity was determined by PCR. Briefly, 50 µl of TRAP reactions including cell extract, 0.1 µg TS forward primer (5'-AATCCGTCGAGCAGAGTT-3'), 0.1 µg reverse primer (5'-GCGCGG(CTTACC)₃CTAACC-3'), and 2.5 unit of Taq DNA polymerase were mixed. After 20 min incubation at 30 °C for telomerase-mediated extension of the TS primer, the mixture was subjected to PCR amplification (94 °C/30 sec, 58 °C/30 sec, 72 °C/15 sec for 35 cycles). The resulting PCR products were electrophoresed on a 14% polyacrylamide gel, and stained with SYBRTM green. Three independent experiments were carried out with similar results.

2.2.2.5. *Immunoblot*

Cells were treated with 0.4-0.6ml Ripa buffer and harvested by scraping. The cell pellet was sonicated and kept immediately on ice. Cell debris was clarified by centrifugation at 12000-14000g for 10-15 min and protein samples were stored at -80 °C. Tween µg of total cell proteins were mixed with an equal volume of 2× protein denaturing sample buffer, boiled for 5 min and subsequently resolved by electrophoresis with 10%-20% (depends on protein molecular weight) polyacrylamide gels at 40mA for 40-60 min. The proteins were electro-blotted on nitrocellulose membrane as follows. Electro-transfer was preformed at 2.5 mA/cm² for 1 hour, using the transfer assembly as shown below. The membranes were blocked (RT, 1 hour) in TBS containing 0.05% Tween 20, 1% casein and 1% PVP. The membranes were then incubated in TBS containing

0.05% Tween 20, 0.5% casein, 0.5% PVP and 0.1% PEG-6000 with specific primary antibodies (at the appropriate dilution) overnight at 4°C. Thereafter membranes were washed two times with TBS containing 1% Tween-20 (TBS-T) and probed with HRP-conjugated secondary antibodies (1:2000) and HRP conjugated anti-biotin antibodies (1:3000) for 1 hour at RT. After incubation, the membranes were washed again with TBS-T and incubated with LumiGLO (New England Biolabs, Inc.) for 1 min at RT, wrapped in transparency foil and exposed to X-ray film.



2.2.2.6. ELISA for MMP-1 expression

A specific "sandwich" ELISA for MMP-1 was performed according to the manufacturer's recommendations, (MMP-1 human ELISA system, Amersham Pharmacia Biotech, Freiburg) using precoated 96-well immunoplates, rabbit anti-human MMP-1 antibodies and anti-rabbit horse-radish peroxidase substrate. 3,3',5,5'-tetramethylbensidine (TMB) was used as peroxidase substrate. Fibroblast monolayer cultures were incubated in FCS-free medium for 16 h, thereafter the supernatants were collected and MMP-1 concentrations were determined. Optical densities were read at 450 nm using a microtiter plate reader LP 400 (Sanofi Diagnostics Pasteur, Freiburg). Concentrations of MMP-1 were determined against standard curves using Graph Pad™ Software (San Diego, CA).

2.2.2.7. ELISA for p53 and p21^{Cip1} expression

p53 and p21^{Cip1} concentration were measured by sandwich ELISA immunoassays with p53 pan ELISA (Roche, Mannheim) and p21^{Cip1} ELISA (Oncogene, Cambridge, MA). Cell extracts were prepared by detergent lysis using Ripa buffer. The isolated proteins react first with biotin-labeled capture antibody which was pre-bound to the streptavidin-coated microtiter plate. The subsequent reaction with a peroxidase-labeled detection antibody forms a stable immuno-complex. After washing and peroxidase developing, p53/p21^{Cip1} expression was determined by photometry at 450 nm.

2.2.2.8. PCR Amplification

The typical setup for 25µl reaction mixtures contains 100 ng genomic DNA, 200 µM dNTPs, 1 µM primers (0.5 µM sense primer and 0.5 µM antisense primer), 2.5 µl of 10× Taq DNA polymerase buffer (Amersham Biosciences Europe, Freiburg), Mg²⁺ concentrations ranging from 1.0 to 2.5 mM, and 2.5 units of Taq DNA polymerase (Perkin-Elmer, Heidelberg, Germany). Amplifications were performed in a thermal cycler under the following conditions: 94°C/3 min, 94°C/0.5 min, 55 °C/1 min (subject to changes for different amplifications, ranging from 53-62°C), 72 °C/1 min, 30-35 cycles, 72 °C 10 min and then stored at 4°C. Hot start was utilized throughout all PCR reactions. Amplifications of PCR mixtures without template DNA served as negative controls. The PCR products (4 µl) were separated in an 1.5-2.0% agarose gel (80-120V for 1-2 hours), and then stained with ethidium bromide. PCR primers were designed based on the human DNA sequence. The following primer sets were used for PCR amplifications.

- Human p53 (TP53) gene: It has 11 exons, as shown in table 1. The entire sequence was from NCBI GenBank with the accession number U94788. The numbering scheme of the NCBI GenBank was used. Due to the difficulty in sequencing DNA samples with a length longer than 1 kb, we subdivided the exon 11 into 2 regions, from nucleotides 500 to 1210 and 1200 to 1600. The products were designated as Exon 11-1 and Exon 11-2.

Table 1. Human p53 (TP53) gene exons and PCR products

| Exon | Length and Location | PCR product length and location |
|------|-----------------------|---------------------------------|
| 1 | 107 bp, 843 - 949 | 220 bp, 801-1020 |
| 2 | 102 bp, 11689 - 11790 | 229 bp, 11668-11896 |
| 3 | 22 bp, 11906 - 11927 | 248 bp, 11774-12021 |
| 4 | 279 bp, 12021 - 12299 | 402 bp, 11998-12399 |
| 5 | 184 bp, 13055 - 13238 | 392 bp, 12922-13313 |
| 6 | 213 bp, 13320 - 13432 | 186 bp, 13296-13481 |
| 7 | 110 bp, 14000 - 14109 | 211bp, 13939-14149 |
| 8 | 137 bp, 14452 - 14588 | 252 bp, 14360-14611 |
| 9 | 74 bp, 14681 - 14754 | 254 bp, 14594-14847 |
| 10 | 107 bp, 17572 - 17678 | 272 bp, 17540-17811 |
| 11 | 1278bp, 18599 - 19876 | 1461 bp, 18523-19983 |
| 11-1 | 617 bp, 18599-19215 | 752bp, 18481-19232 |
| 11-2 | 690 bp, 19187-19876 | 800bp, 19187-19986 |

Exon 1 Sense, 5'-ATG TGC TCA AGA CTG GCG-3'
 Antisense, 5'-CGA GCT GAA AAT ACA CGG-3'
 Condition: AT, 52°C, 1.5mM Mg²⁺

Exon 2 Sense, 5'-TCC CCA CTT TTC CTC TTG-3'
 Antisense, 5'-AAG AGC AGA AAG TCA GTC CC-3'
 Condition: AT, 60°C, 1.5mM Mg²⁺

Exon 3 Sense, 5'-TCA GAC CTA TGG AAA CTG TGA G-3'
 Antisense, 5'-CTG TAG ATG GGT GAA AAG AGC-3'
 Condition: AT, 58°C, 1.5mM Mg²⁺

Exon 4 Sense, 5'-CTG CTC TTT TCA CCC ATC-3'
 Antisense, 5'-AAG GGT GAA GAG GAA TCC-3'
 Condition: AT, 52°C, 2.5mM Mg²⁺

- Exon 5 Sense, 5'-CAA CTC TCT CTA GCT CGC-3'
 Antisense, 5'-GCA ATC AGT GAG GAA TCA-3'
 Condition: AT, 55°C, 1.5mM Mg²⁺
- Exon 6 Sense, 5'-TGA TTC CTC ACT GAT TGC-3'
 Antisense, 5'-ACA ACC ACC CTT AAC CCC-3'
 Condition: AT, 55°C, 1.5mM Mg²⁺
- Exon 7 Sense, 5'-TGC TTG CCA CAG GTC TCC-3'
 Antisense, 5'-CAC AGC AGG CCA GTG TGC-3'
 Condition: AT, 60°C, 1.0mM Mg²⁺
- Exon 8 Sense, 5'-GTT GGG AGT AGA TGG AGC-3'
 Antisense, 5'-CGC TTC TTG TCC TGC TTG-3'
 Condition: AT, 55°C, 1.5mM Mg²⁺
- Exon 9 Sense, 5'-CAA GCA GGA CAA GAA GCG-3'
 Antisense, 5'-CCC AAT TGC AGG TAA AAC-3'
 Condition: AT, 52°C, 1.5mM Mg²⁺
- Exon 10 Sense, 5'-ATA CTT ACT TCT CCC CCT-3'
 Antisense, 5'-CAA TGA GAT GGG GTC AGC-3'
 Condition: AT, 60°C, 1.5mM Mg²⁺
- Exon 11 Sense, 5'-ATT GGT CAG GGA AAA GGG-3'
 Antisense, 5'-CAC ACT CAT TGC AGA CTC-3'
 Condition: AT, 49°C, 1.5mM Mg²⁺, 400nM dNTP, extension time
 (72°C) increases to 2 min.
- Exon 11-1 Sense, 5'-TGA TTT GAA TTC CCG TTG TCC-3'
 Antisense, 5'-AAC CCA CCA GCC AAC AGG-3'
 Condition: AT, 60°C, 1.5mM Mg²⁺

Exon 11-2 Sense, 5'-TTG AGG GTG CCT GTT CCC-3'
 Antisense, 5'-GTC CAC ACT CAT TGC AGA CTC AG-3'
 Condition: AT, 60°C, 1.5mM Mg²⁺

- Human p21^{cip1} gene: It has 4 exons, as shown in table 2. [the entire sequence was from GenBank, accession number Z85996, and the numbering scheme was adopted]

Table 2. Human p21^{cip1} gene exons and PCR products

| Exon | Length and Location | PCR product length and location |
|------|----------------------|---------------------------------|
| 1 | 73bp, 3226- 3298 | 159bp, 3171- 3328 |
| 2 | 452bp, 8594- 9045 | 631bp, 8549- 9179 |
| 3 | 196bp, 10247- 10442 | 290bp, 10221- 10510 |
| 4 | 1370bp, 10456- 11825 | 1705bp, 10348- 12206 |

Exon 1 Sense, 5'-GCG GGG CGG TTG TAT ATC-3'
 Antisense, 5'-GGT CCC CTG TTG TCT GCC-3'
 Condition: AT, 58°C, 1.5mM Mg²⁺

Exon 2 Sense, 5'-GTC TAA TCT CCG CCG TGA C-3'
 Antisense, 5'-GGT TGC TTC CCC TCT CTG-3'
 Condition: AT, 58°C, 1.5mM Mg²⁺

Exon 3 Sense, 5'-CCT GGC TGA CTT CTG CTG-3'
 Antisense, 5'-GAA CCT CTC ATT CAA CCG C-3'
 Condition: AT, 58°C, 1.0mM Mg²⁺

Exon 4 Sense, 5'-CCC GCT CTA CAT CTT CTG CC-3'
 Antisense, 5'-CCA GTT GCT CCA TAA CCT TGC -3'
 Condition: AT, 62°C, 1.5mM Mg²⁺

- Human p16^{INK4a} gene: It has 3 exons, as shown in table 3. [Sequence was from GenBank accession numbers U12818, U12819 and U12820. The entire sequence was the composite and the numbering scheme was adopted as U12818-U12819-U12820 (1-340)-(341-925)-(926-1347)]

Table 3. Human p16^{INK4a} gene exons and PCR products

| Exon | Length and Location | PCR product length and location |
|------|---------------------|---------------------------------|
| 1 | 126bp, 129 - 254 | 272 bp, 66 - 338 |
| 2 | 307bp, 491 - 797 | 453 bp, 414 - 866 |
| 3 | 14bp, 1199 - 1212 | 172 bp, 1071 - 1243 |

Exon 1 Sense, 5'-GGA GAG GGG GAG AGC AGG-3'

Antisense, 5'-GCT ACC TGA TTC CAA TTC CCC-3'

Condition: AT, 60°C, 1.0mM Mg²⁺

Exon 2 Sense, 5'-AGG GGG CTC TAC ACA AGC TTC-3'

Antisense, 5'-GTG CTG GAA AAT GAA TGC TCT G-3'

Condition: AT, 60°C, 1.5mM Mg²⁺

Exon 3 Sense, 5'-AGC CAT TGC GAG AAC TTT ATC C-3'

Antisense, 5'-CCC GAG GTT TCT CAG AGC C-3'

Condition: AT, 62°C, 1.5mM Mg²⁺

2.2.2.9. PCR products purification and sequence analysis

PCR products were purified using the QIAquick PCR purification kit (QIAGEN, Hilden), and then sequenced on both DNA strands using the same primers for PCR. The sequence data were compared to the human genome sequence from GenBank. Sensitivity of the method was evaluated by employing 2 positive controls: a) a fibroblast cell line derived from Li-Fraumeni patients which contains a single base pair deletion in its p53 gene at exon 5 (codon 184, from GATA to GAA); b) a lung fibroblast cell line which reveals a deletion and insertion of neomycin and hygromycin in its p21^{cip1} gene.

2.2.3. Additional methods

2.2.3.1. ROS measurements

Levels of intracellular ROS were assessed by loading cells with 10 µg/ml of fluorescent ROS indicator 2',7'-dichlorodihydrofluorescein diacetate (H₂DCF-DA) (Molecular Probes, MoBiTec, Goettingen) for 20 min and with subsequent detection using a Zeiss laser scanning confocal microscope. H₂DCF-DA is a nonpolar compound that is converted into a nonfluorescent polar derivative by cellular esterases after incorporation into cells. H₂DCF is membrane impermeable and is rapidly oxidized to the highly fluorescent 2',7'-dichlorofluorescein (DCF) in the presence of intracellular ROS (Frenkel and Gleichauf 1991). The excitation wavelength is 488 nm and emission wavelength is 521 nm. The resulting image is an artificial colour made by the computer program based on intensity of the emitted photons. To determine the involvement of NADPH oxidase, two NADPH oxidase inhibitors, diphenylene iodonium (DPI, Sigma, 10µM) or 4-(2-aminoethyl)-benzenesulfonyl fluoride (AEBSF, Sigma, 100µM) were added to control or PUVA-treated fibroblasts for 2 hours before ROS detection.

2.2.3.2. Supplementation of fibroblast culture with N-acetyl cystein and subsequent determination of intracellular ROS Levels

Immediately after PUVA treatment, fibroblasts were maintained in DMEM/10% FCS containing 5 mM NAC. The medium was changed every three days to ensure an efficient antioxidant capacity. PUVA-treated fibroblasts were fed with NAC until they started to proliferate. ROS levels in these NAC supplemented fibroblasts were determined by DCF staining at different time points post PUVA treatment.

2.2.3.3. Measurement of the mitochondrial membrane potential

To measure $\Delta\Psi_m$, cells (1×10^6 cells/ml) were resuspended in 5 mg/ml solution of JC-9 (Molecular Probes, MoBiTec, Goettingen) in phosphate buffered saline at different time points post PUVA treatment (Salvioli *et al.* 1997). The dye exists as a monomer at low concentrations (emission, 530 nm, green fluorescence) but at higher concentrations forms J-aggregates (emission, 590 nm, red fluorescence).

Because accumulation of the JC-9 dye is reversible, cells were maintained in a stable concentration of the dye throughout the time of measurement. After a 20 min incubation period at 37 °C, cells were immediately analyzed by flow cytometry. Dead cells were excluded by forward and side scatter gating. Data were collected by analyzing an average population of 20,000 cells. JC-9 aggregates were detectable in the propidium iodide channel (red fluorescence, emission at 590 nm), and JC-9 monomers were detectable in the fluorescein isothiocyanate channel (green fluorescence, emission at 527 nm) (Reers *et al.* 1995).

2.2.3.4. Measurement of mitochondrial biogenesis

To stain mitochondria, cells were incubated in DMEM medium containing 25nM MitoTracker Red CMXRos (Molecular Probes, MoBiTec, Goettingen) for 30 min at 37°C. Cells were photographed using a 568-nm line of fluorescence excitation using a Zeiss laser scanning confocal microscope.

2.2.3.5. ATP measurements

ATP was measured by a bioluminescence assay (Kricka 1988) using an ATP determination kit (Merck Biosciences, Schwalbach). The assay is based on the requirement of luciferase for ATP to produce light (emission maximum ~560 nm at pH 7.8). Briefly, after PUVA treatment cells ($\sim 5 \times 10^5$) were resuspended in reaction buffer containing 1 mM DTT, 0.5 mM luciferin, and 12.5 µg/ml luciferase, gently mixed, and light production was monitored using a luminometer (Lumicount, Packard Instrument Co. Meriden, USA). ATP standard curves were run with different concentrations of ATP, and calculations were made against these curve. Cellular ATP levels were expressed both per cell and per total protein.

2.2.3.6. Densitometry measurement

The bands from Southern or Western blots were quantified with densitometry analysis using a computerized digital imaging system, Scanpac software (Alpha Innotech, San Leandro, CA). The intensity of each band or the distribution of DNA fragments was obtained by integrating the pixel values after subtracting the background.

2.2.3.7. Statistics

Mean values standard errors was determined using the Microsoft Excel program. Student-t test was used to compare the differences between two groups and ANOVA test for comparing three or more groups. In all cases, the statistical significance of differences between the two variants was determined at the level of $p < 0.05$. All the data presented were from the average of at least three independent experiments.

3 Results

3.1. Human dermal fibroblasts escape from PUVA-induced long-term senescence-like growth arrest

As observed in our laboratory, a single PUVA treatment promotes morphological and functional changes in fibroblasts in vitro reminiscent of cellular senescence (Herrmann *et al.* 1998). In addition to long-term growth arrest, PUVA-treated fibroblasts showed an enlarged morphology, increased SA- β -Gal and MMP-1 expression, markers which are often up-regulated in replicative-senescent cells (Bayreuther *et al.* 1988; Dimri *et al.* 1995; West *et al.* 1989). In contrast to the permanent growth arrest in replicative senescence PUVA-treated fibroblasts start to regrow after a three-month growth arrest post PUVA treatment. As growth arrest in replicative or premature senescence has earlier been claimed to be irreversible (Chen 2000; Dumont *et al.* 2000), it was the aim to further characterize the underlying mechanisms responsible for the escape of PUVA-treated fibroblasts from the senescence-like state.

3.1.1. Regrowth of fibroblasts from PUVA-induced long-term senescence-like growth arrest

After a single PUVA treatment, the growth-arrested fibroblasts gradually gained an enlarged phenotype. Figure 5A shows enlarged fibroblasts 28 days post PUVA treatment. At 90 to 110 days after PUVA treatment and the subsequent long-term growth arrest, multiple foci of small proliferating fibroblasts were observed in 4 independent experiments. Note the small spindle shaped, regrowing fibroblasts among the enlarged growth-arrested fibroblasts (Figure 5B). Figure 5C reveals the high magnification of the smaller regrowing fibroblasts adjacent to growth-arrested large fibroblasts. Concomitantly occurring foci were distributed throughout the dish. To further determine the time point of regrowth and to answer the question whether regrowing fibroblasts may result from rare fibroblasts which have never been growth-arrested instead of from concomitantly regrowing fibroblasts in multiple foci, BrdU incorporation was performed to monitor proliferation of PUVA-treated fibroblasts at different time points post

treatment. As shown in Figure 6, no positively stained nuclei were observed even at the

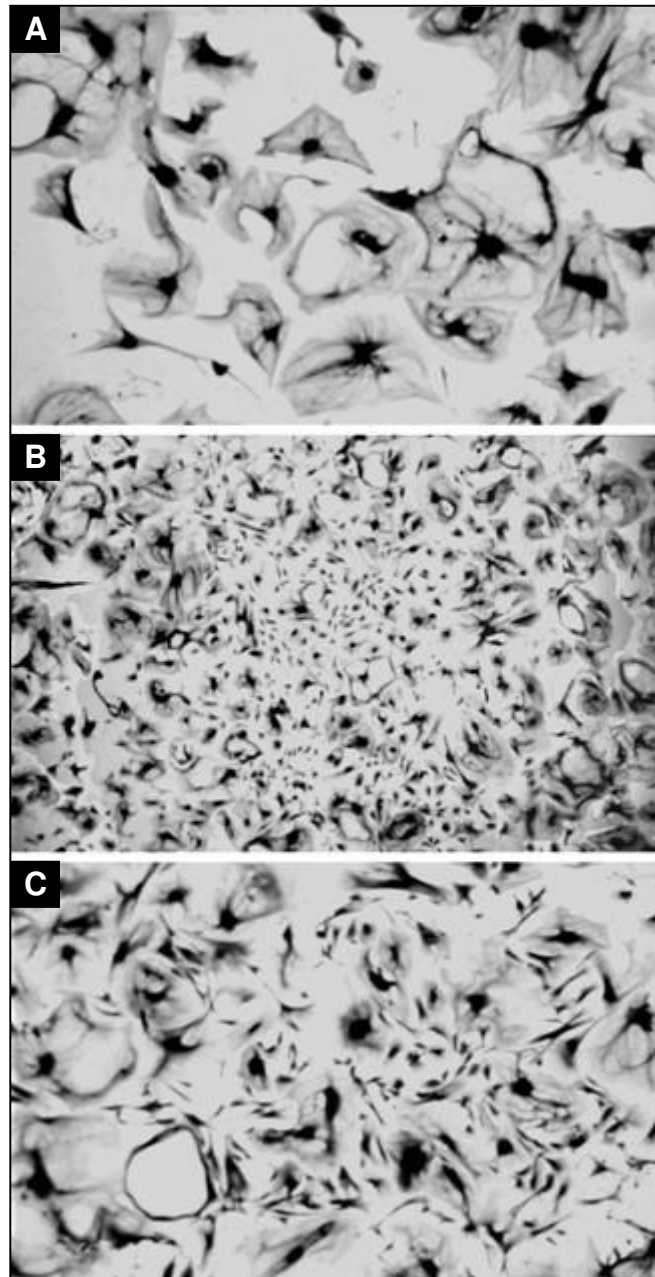


Figure 5 Regrowth of fibroblasts post PUVA treatment. (A) Growth-arrested fibroblasts showed a senescent-like morphology at day 28 after a combined treatment with 50ng/ml psoralen and 90 kJ/m² UVA (magnification $\times 50$). (B) and (C) Two independent foci of regrowing small fibroblasts occurred concomitantly between cells with enlarged cytoplasm at 90 to 110 days post PUVA treatment in the same dish (B, magnification $\times 20$; C, magnification $\times 50$).

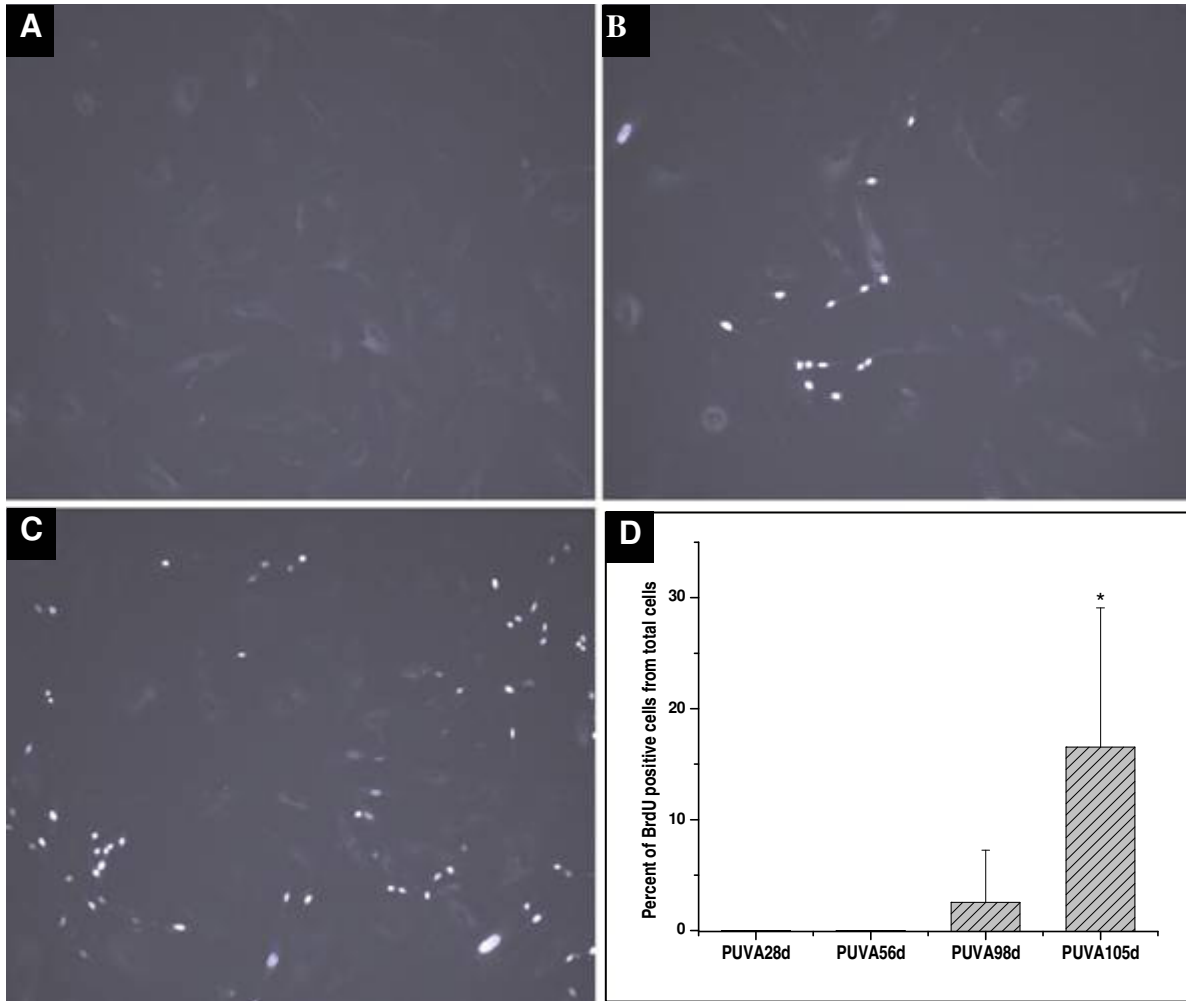


Figure 6. BrdU incorporation at different time-points post PUVA treatment. BrdU incorporation was performed using the “in situ proliferation kit FLUOS” as described in detail in Materials and Methods. BrdU labeled nuclei as well as unlabelled and total nuclei were counted and calculated, respectively, in 10 randomly selected high power fields ($\times 100$ magnification). After PUVA treatment, cells were seeded in 35 mm plastic dishes with a total cell number of 3×10^4 cells/dish. (A) At 56 days post PUVA treatment no BrdU incorporation into nuclei was detected. (B) At 98 days post PUVA treatment many concomitantly occurring BrdU labeled nuclei were detected. (C) One week later at day 105 post PUVA treatment even more cells revealed BrdU incorporation in nuclei. (D) The results are summarized in the graph and BrdU incorporation at different time points post PUVA treatment were expressed as percent of BrdU positive cells of total cell number/high power field. Cells in ten power fields were counted and the data are shown as mean \pm standard deviation. * $p < 0.006$ compared with cells 98 days post PUVA treatment (students t-test).

end of 8 weeks post treatment (Figure 6A). Fourteen weeks post treatment scattered foci-like cell proliferation could be observed (Figure 6B). These data indicate that regrowth occurred around day 100 post PUVA treatment. After initial appearance of re-proliferating fibroblasts at multiple regions of the dish, it took only 8 days until the dish revealed predominantly small re-proliferating fibroblasts (Figure 6C, D). Confluence was reached at day 10-12 after the appearance of re-proliferating cell foci.

3.1.2. Regrowth is not due to immortalization or transformation

As cellular senescence has been proposed to be activated as a barrier against tumorigenesis, and senescence induced growth arrest is controlled by tumor suppressor genes such as p53 and p16^{INK4a} (Campisi 2001a), we studied whether the regrowth of fibroblasts after PUVA treatment was due to loss-of-function of these tumor suppressors and other related cellular senescence controlling genes. In this case, it was expected that the regrowing fibroblasts were most likely either immortalized or transformed.

3.1.2.1. Regrowing fibroblasts post PUVA treatment do not show any telomerase activity, but a reduction in telomere length with increasing CPD

Immortalization and the overall proliferation capacity of human cells depend on the maintenance of telomere length (Blackburn 1991). Since expression of telomerase is the most common mechanism for immortalized or cancer cells to stabilize their telomeres, we determined the telomerase activity in regrowing fibroblasts post PUVA treatment. Figure 7 shows that no telomerase activity was determined either in fibroblasts regrowing post PUVA treatment or in mock-treated (under a same experiment procedure but without psoralen and UVA irradiation) control fibroblasts. The epidermal cell line HaCaT (Figure 7 lane 2 and 3) and the fibrosarcoma cell line HT1080 (Figure 7 lane 6 and 7) with a high telomerase activity served as positive controls. In line with this, a decrease in telomere length occurred in fibroblasts regrowing post PUVA treatment with increasing CPD. As shown in Figure 29 (see page 79), the terminal restriction fragments (TRF), as an indication of telomere length, was determined in regrowing fibroblasts post PUVA treatment and mock-treated control fibroblasts. Lane 3, 5, 7, 9 showed telomere length of regrowing fibroblasts at different CPDs.

It can be seen that with increasing CPD, the telomere length in regrowing fibroblasts decreased. Interestingly, a significantly shorter telomere length was observed in regrowing fibroblasts post PUVA treatment compared to mock-treated control fibroblasts at exactly the same CPD. The underlying mechanism will be discussed later. Taken together, regrowing fibroblasts did not reveal any telomerase activity and their telomere lengths, in fact, erode with increasing CPD.

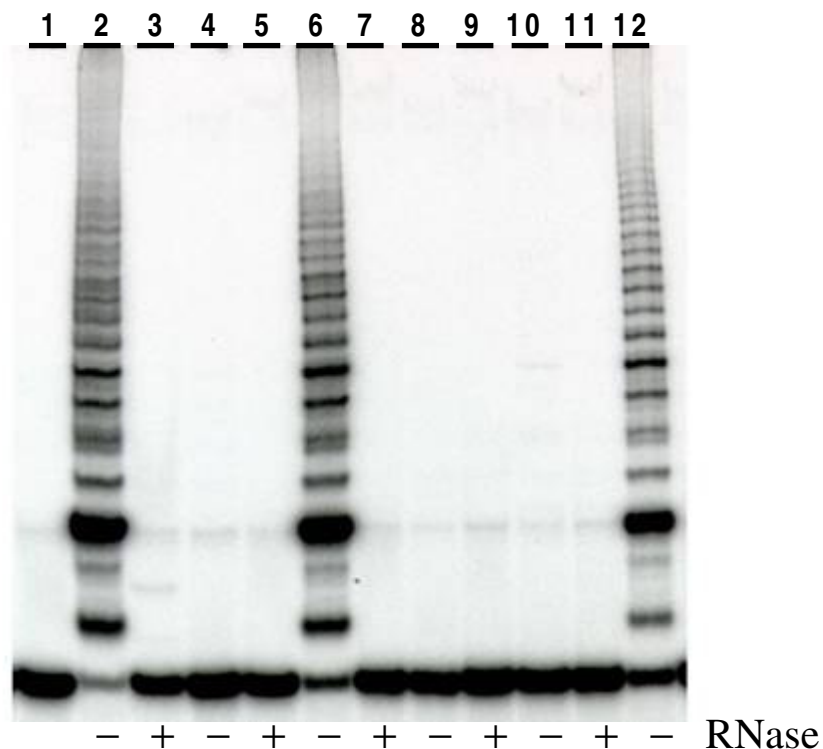


Figure 7. Telomerase activity does not differ in mock-treated control fibroblasts and in PUVA-treated fibroblasts during growth arrest and their regrowing phase. Telomerase activity was measured by the standard TRAP assay. Cell lysates and telomerase assay were performed using the TRAPeze kit. Fifty ng of total protein extract were used for each assay, each with or without RNase-inactivation. Products were separated in non-denaturing 10% polyacrylamide gels, visualized by autoradiography and photoimage scanning. Lane 1: Lyses buffer; Lane 2-11 represent the analysis of different cell lines without and with RNase-inactivation; lane 2, 3: HaCaT cells; lane 4,5: Mock-treated control fibroblasts; lane 6,7: HT1080 (Fibrosarcoma cell line); lane 8,9: fibroblasts of the same strain as in lane 6,7 in their regrowing phase post PUVA treatment; lane 10,11: PUVA-treated growth-arrested fibroblasts at 4 weeks post PUVA treatment; lane 12: 5 ng of total protein extract of HaCaT cells were used.

3.1.2.2. Regrowth of fibroblasts post PUVA treatment is anchorage dependent

In a first attempt to study whether regrowing fibroblasts are transformed - a state which is characterized by anchorage independent growth (Saitoh *et al.* 1999) - fibroblast proliferation and colony formation were studied by means of the soft agar assay. For this purpose regrowing fibroblasts post PUVA treatment, mock-treated control fibroblasts of the same strain at the same CPD and, as positive controls, two tumor cell lines (fibrosarcoma cell line HT1080, HeLa cell line) were placed into soft agar and cultured for 10 to 14 days. While the HeLa cell line and the fibrosarcoma cell line HT1080 formed numerous colonies confirming anchorage independent growth (Figure 8A, B), neither control fibroblasts nor fibroblasts with resumed growth post PUVA treatment formed any colony in the soft agar (Figure 8C, D). Following an extended observation period of 35 days, mock-treated control and regrowing fibroblasts did not form colonies, instead the number of cells gradually decreased and eventually disappeared (data not shown). Thus, the growth of regrowing fibroblasts was anchorage dependent. These data indicate that the regrowth of fibroblasts observed at days 100 to 130 after a single PUVA treatment is not due to transformation.

3.1.2.3. Regrowing fibroblasts post PUVA treatment reveal a decline in growth rates with increasing CPD

To further confirm that regrowth of fibroblasts after PUVA treatment is not due to transformation and immortalization – as both states would show unlimited proliferation – the CPD was determined in regrowing fibroblasts and in mock-treated fibroblasts of the same strain. Immortalized or transformed continuously dividing cells should show a constant and sustained linear increase in their CPD, while primary fibroblasts – due to the replicative senescence – are rather expected to reveal a saturation curve with increasing CPD. Fibroblasts in the regrowing phase post PUVA treatment and mock-treated fibroblasts with comparable CPD (~ 48) were passaged over a period of 5 months until the regrowing fibroblasts reached replicative senescence with no increase in cell numbers. Figure 9 reveals the CPD in regrowing fibroblasts and mock-treated control fibroblasts. The proliferation rate of regrowing fibroblasts decreased with time and reached a stationary phase (replicative senescence) after 90 day at a CPD of 62. By contrast, mock-treated control fibroblasts were still proliferating

even at 120 days at a CPD of 70. The observed CPD kinetics strongly indicates that regrowing fibroblasts post PUVA treatment were neither immortalized nor transformed.

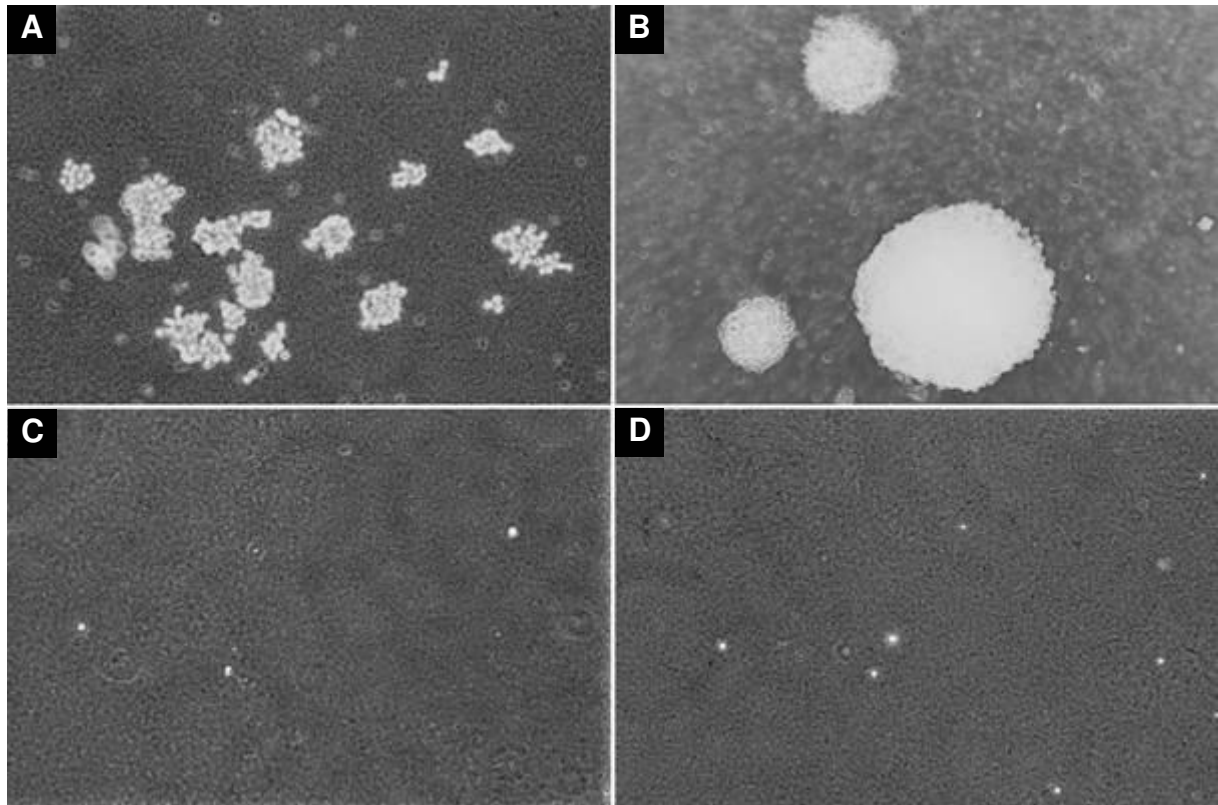


Figure 8. Fibroblasts regrowing post PUVA treatment do not show any anchorage independent growth in the soft agar assay. The epithelial carcinoma cell line Hela (A) and the fibrosarcoma cell line HT1080 (B) which served as positive controls, mock-treated fibroblasts (C) and fibroblasts of the same strain in their regrowing phase post PUVA treatment (D) were tested for anchorage independent growth in soft agar as detailed in Material and Methods. Briefly, 5×10^3 cells were suspended in 1.5 ml of 0.4% agar supplemented with 10% FCS and overlaid on 1.5 ml of a 0.8% agar-medium basal layer in 35 mm plastic tissue culture dishes. All cultures were incubated at 37°C in a humidified 5% CO₂ - 95% air atmosphere without further feeding for 10 to 14 days. Thereafter, colony formation was assessed and photographed at x100 magnification. Three independent experiments were performed in triplicates.

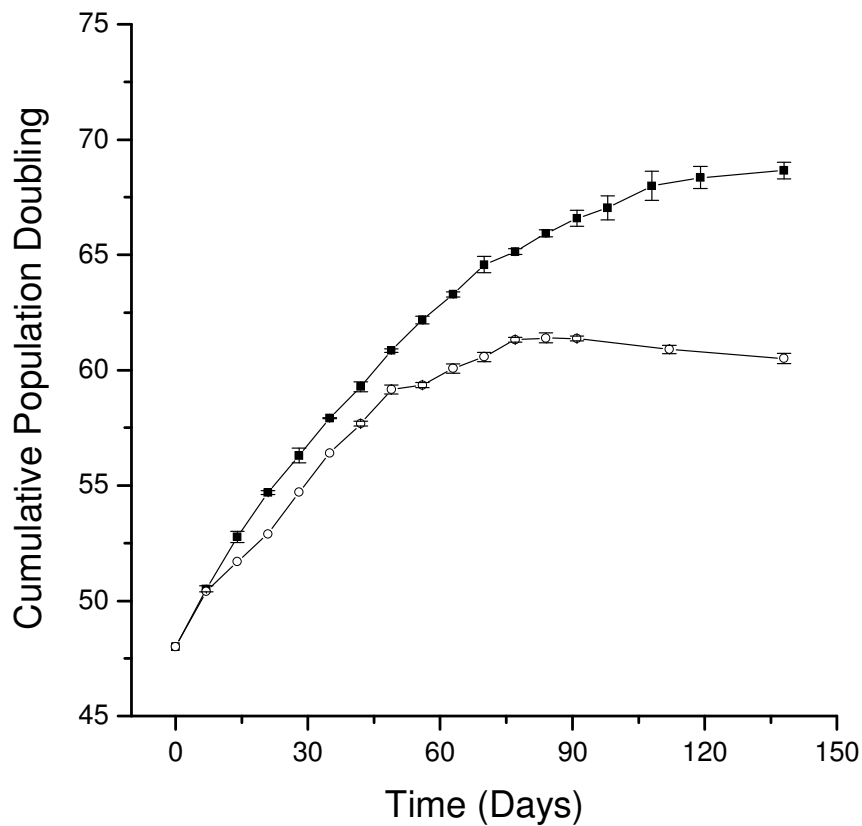


Figure 9. Fibroblasts regrowing post PUVA do not show constant proliferation rates. Comparable cumulative population doublings (CPD) of mock-treated fibroblasts (CPD = 47.9) and fibroblasts of the same strain in their regrowing phase post PUVA treatment (CPD = 48.4) were chosen for comparison. At different time points thereafter, cell numbers were determined in triplicates for each experimental group and equal cell numbers (2×10^5) were transferred to a new tissue plate for further observation. The data represent cumulative population doublings (CPDs) determined in a secondary human dermal fibroblast cell line and are representative for two additional fibroblast cell lines from independent donors. Each data point represents the mean \pm standard deviation of three independent counting. Experimental groups: (■) mock-treated control fibroblasts; (○) fibroblasts of the same strain in their initial regrowing phase post PUVA treatment.

3.1.2.4. Senescence control genes, p53, p21^{Cip1} and p16^{INK4a} do not reveal mutations in regrowing fibroblasts

Cellular senescence is mainly controlled by two major senescence controlling pathways, namely the p53/p21^{Cip1} and/or pRb/p16^{INK4a} pathway (Lundberg *et al.* 2000). Among the tumor suppressors genes, a p53 and p16^{INK4a} loss-of-function occurs most commonly in mammalian cancers. To answer whether the escape of regrowing fibroblasts from PUVA-induced growth arrest is due to disruption of these important check-point genes, their integrity in nucleotide sequence was determined in regrowing fibroblasts post PUVA treatment, in growth-arrested fibroblasts and in mock-treated control fibroblasts. For this purpose, all exons of p53, p21^{Cip1} and p16^{INK4a} genes from the three experimental groups of fibroblasts were amplified by PCR. The sequence of each exon was then analyzed and compared with the genomic DNA sequence from the gene bank of NCBI. No major mutation, deletion or modifications were found, neither in growth-arrested fibroblasts nor regrowing fibroblasts post PUVA in the 11 exons of p53, 4 exons of p21^{Cip1} and 3 exons of p16^{INK4a} (data not shown). In order to evaluate the PCR amplification protocol for detection of major deletions and single point mutations, 2 positive controls were employed. As shown in Figure 10-A and B, both a single point mutation in exon 5 of p53 from Li-Fraumeni (a disease related to loss of p53 function) cells and an 18-base deletion in exon 2 of p16^{INK4a} from p16^{INK4a}-deficient fibroblasts could be detected.

In summary, the data indicate that PUVA-induced senescence-like growth arrest is reversible in a large proportion of cells between days 90 and 120 post PUVA treatment. The finally returning growth capacity is not due to immortalization, transformation or loss of function of the senescence controlling genes p53, p21 and p16. This leads to important question as to whether the growth arrest triggered in PUVA-induced premature senescence is identical to replicative senescence or rather a phenocopy thereof.

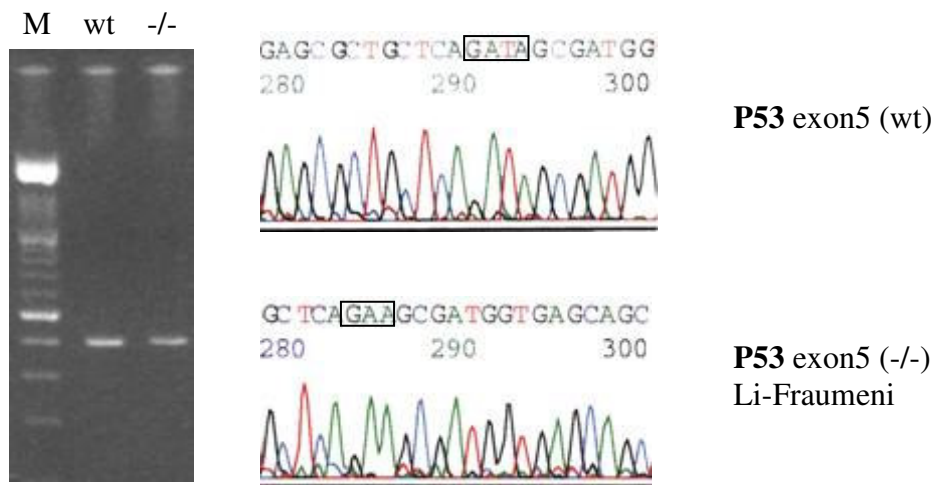
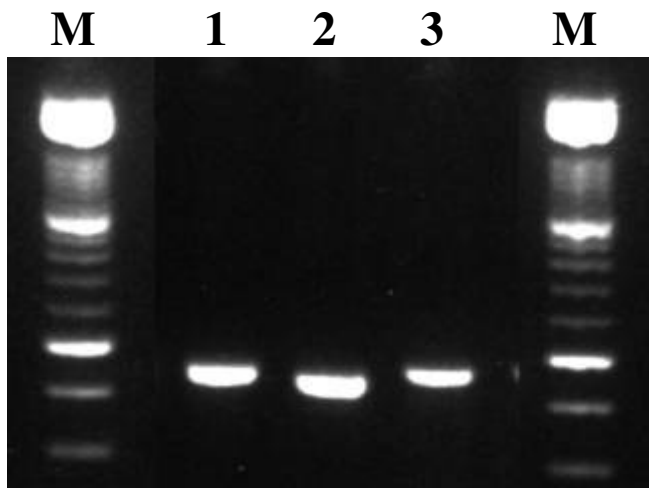
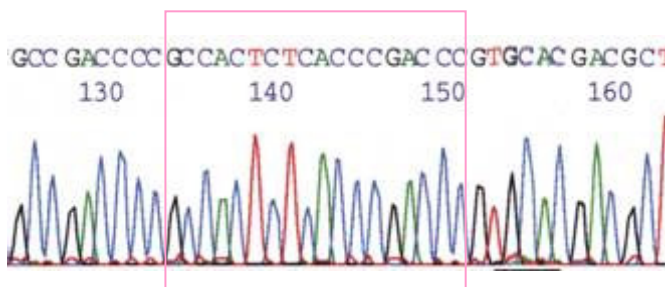


Figure 10-A. PCR amplification and sequence analysis can detect point mutations if they are present in all cells. Exon 5 of the p53 gene was amplified and sequenced using the genomic DNA template either from p53 deficient Li-Fraumeni cells or from wild type human dermal fibroblasts. The primer sequence and experimental conditions were used as described in Materials and Methods.

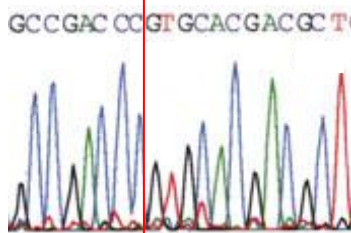


M. 100bp DNA length marker

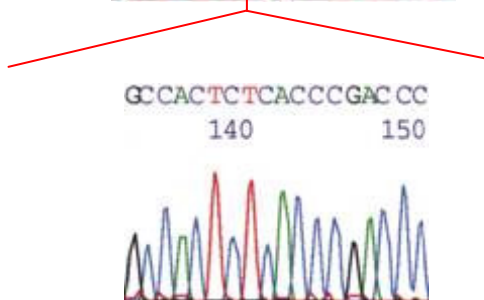
1. PCR product: exon 2 of normal human dermal fibroblasts.
2. PCR product: exon 2 of p16^{INK4a} deficient cells.
3. PCR product: exon 2 of regrowing fibroblasts post PIIVA



Exon 2 of p16^{INK4a} (WT)
(part of the sequence)



Exon 2 of p16^{INK4a} (+/-)
(part of the sequence)



Deleted part

Figure 10-B. PCR amplification and sequence analysis can detect a DNA deletion if it is present in all cells. The deletion in exon 2 of p16^{INK4a} deficient lung fibroblasts was detected after sequence analysis. The primer sequence and experimental conditions were used as described in Materials and Methods.

3.2. PUVA-induced premature senescence does not fully reflect replicative cellular senescence

Growth arrest in replicative and stress-induced premature senescence has been claimed to be irreversible (Chen 2000; Dumont *et al.* 2000). As PUVA-induced growth arrest shares many features similar to other stress-induced premature senescence models as occurring in response to oxidative stress, DNA damage or oncogenic Ras, the question was addressed whether stress-induced premature senescence is identical to replicative senescence or rather a phenotypic and functional mimic of replicative senescence. In fact, the results of the previous section already indicate that PUVA-induced premature senescence is different from replicative senescence in that PUVA-treated fibroblasts regain their proliferation capacity after 1-3 month of growth arrest post PUVA treatment. In order to further characterize different features between stress-induced premature senescence and replicative senescence, the following questions were experimentally addressed:

- Are established senescent phenotypic and biochemical markers of cellular senescence reversible in PUVA-induced premature senescence?
- Is the PUVA-induced senescence-like growth arrest controlled by the same molecular pathways as in replicative senescence?
- Which mechanisms are involved and contribute to the senescence-like features?

3.2.1. Reversibility of senescence-associated markers in regrowing fibroblasts post PUVA treatment

In a first attempt to address the question whether fibroblasts which escape from growth arrest also lose senescence markers such as morphology and senescence associated β -galactosidase expression, these parameters were studied in PUVA-arrested and regrowing fibroblasts at different time points post PUVA treatment. After PUVA treatment growth-arrested fibroblasts revealed a substantial increase in cell size compared to mock-treated control fibroblasts with time after PUVA treatment (Figure 11A to Figure 11D). At 14-16 weeks post PUVA treatment, small regrowing fibroblasts were visible among

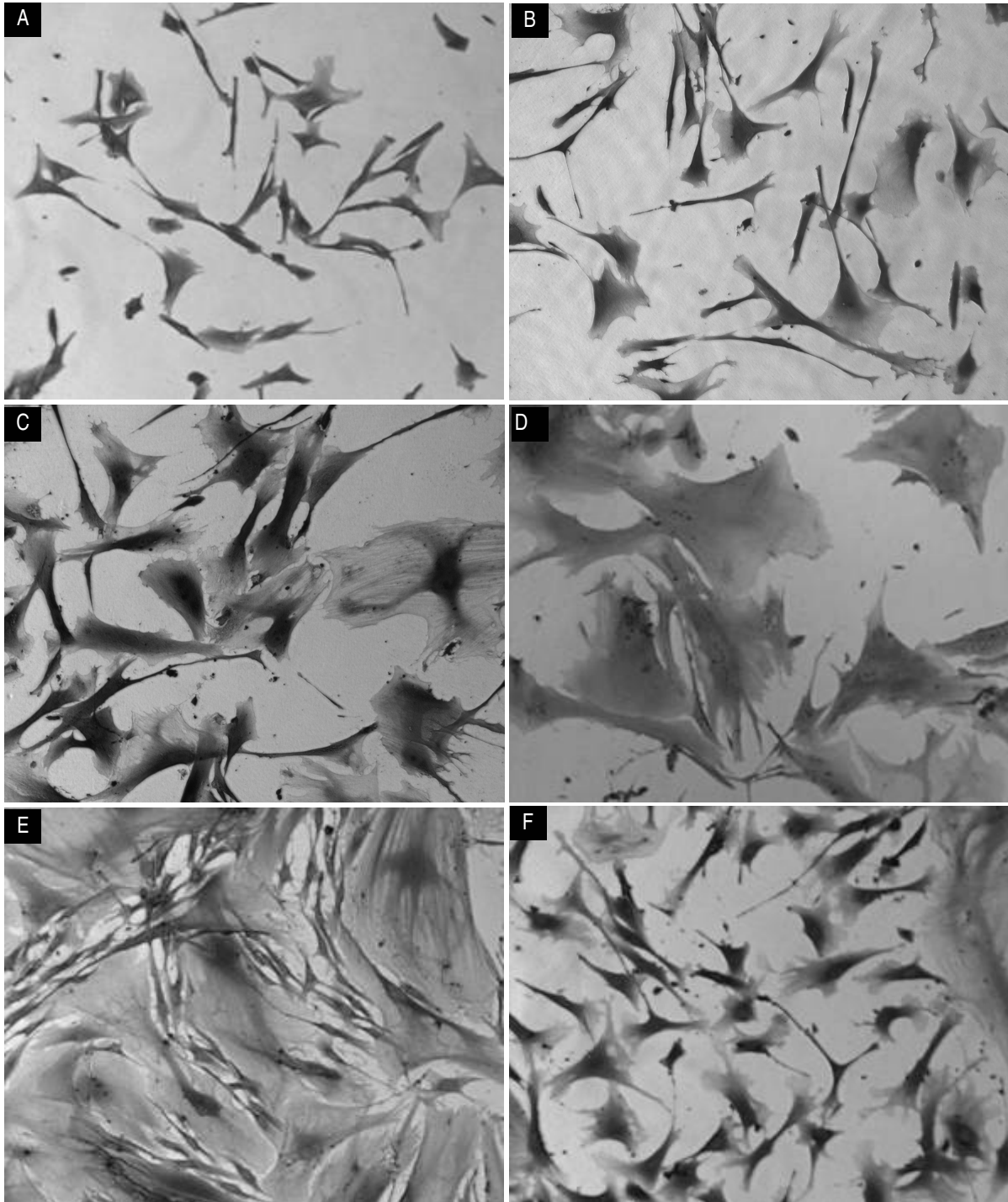


Figure 11. Cell morphology changes in growth-arrested fibroblasts at different time points post PUVA in regrowing fibroblasts and in mock-treated control fibroblasts. Fibroblasts were fixed and stained with Coomassie blue as detailed in Materials and Methods and photographed at $\times 100$ magnification. A, mock-treated control fibroblasts; B-D, fibroblasts at 1, 2, 4 weeks post PUVA treatment; E, 16 weeks post PUVA treatment; F, regrowing fibroblasts post PUVA treatment.

enlarged growth-arrested fibroblasts (Figure 11E). Regrowing fibroblasts did not show any difference in cell size compared to mock-treated control fibroblasts (Figure 11F).

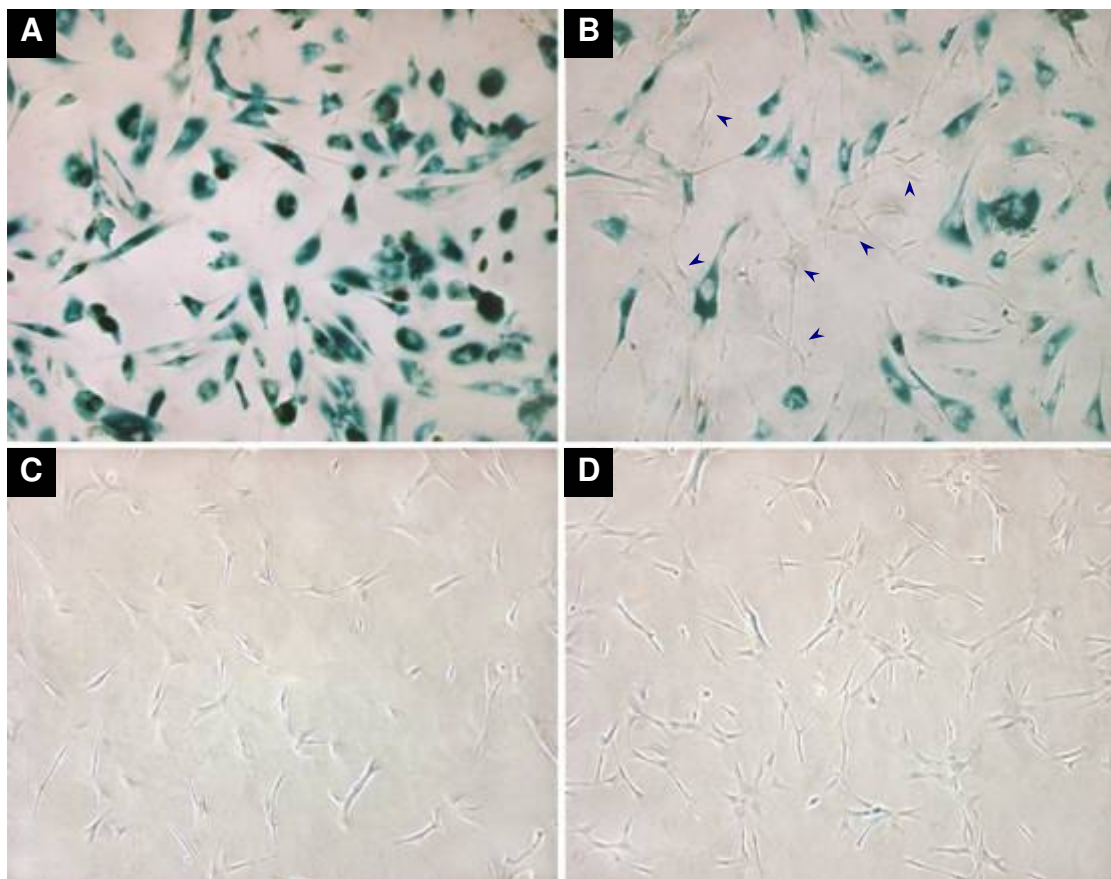


Figure 12. The induced expression of senescence-associated β -galactosidase (SA- β -Gal) in PUVA-treated fibroblasts is lost in regrowing fibroblasts post PUVA. (A) Fibroblasts 21 days post PUVA; (B) At 98 days post PUVA, SA- β -Gal staining was lost in some cells (arrows) which morphologically represent the smaller regrowing cells, while still maintained in those enlarged growth-arrested cells. (C) No staining was observed in fully regrowing fibroblasts post PUVA treatment or (D) in mock-treated fibroblasts. Fibroblasts were stained for SA- β -Gal and photographed at $\times 100$ magnification. Three independent experiments have been performed with similar results.

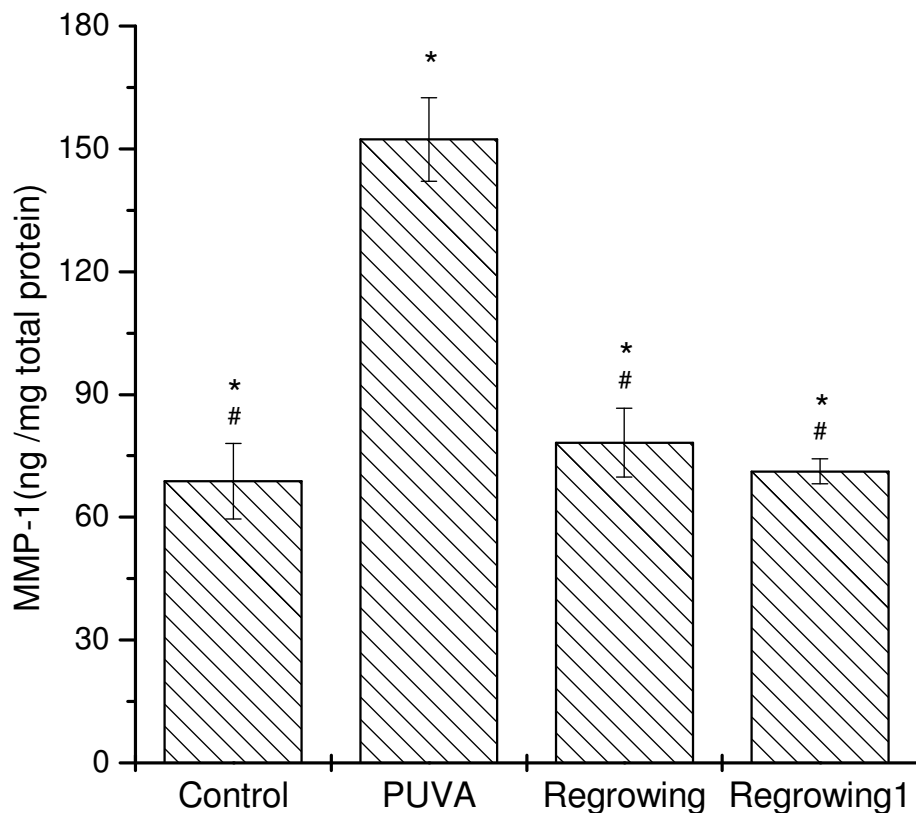


Figure 13. The increased release of MMP-1 from human dermal fibroblasts upon a single PUVA treatment is no longer detectable in fibroblasts in their regrowing phase post PUVA treatment. Confluent fibroblasts were PUVA-treated (50 ng/ml 8-MOP / 90 kJ/m² UVA) or mock-treated. Supernatants were collected from mock-treated fibroblasts (Control), at 14 days post PUVA treatment (PUVA), at 130 days post PUVA treatment in the regrowing phase of the same fibroblast strain (Regrowing) and at 110 days post PUVA treatment in the regrowing phase of another fibroblast strain (Regrowing 1). All supernatants were subjected to ELISA detection of MMP-1, as detailed in Materials and Methods. Three independent experiments were performed to determine specific MMP-1 protein concentrations. **p* ≤ 0.0001 compared with PUVA-treated cells; #*p* = 0.32 compared with mock-treated cells (One way ANOVA).

Reversal of changes in the enlarged cell morphology and growth arrest post PUVA treatment was also accompanied by the loss of biochemical markers of senescence. While all fibroblasts revealed SA-β-Gal expression at 4 weeks post PUVA treatment (Figure 12A) and SA-β-gal expression was sustained during > 2 months of growth arrest, SA-β-Gal staining was lost at 98 days post PUVA treatment in some cells, which morphologically represent regrowing cells (Figure

12B). No SA- β -Gal expression was observed in regrowing fibroblasts post PUVA treatment (Figure 12C) and in mock-treated fibroblasts (Figure 12D).

Besides morphological changes and SA- β -gal expression, another senescence-associated marker, matrix-metalloprotease-1 (MMP-1) which was up-regulated after PUVA treatment, completely returned back in regrowing fibroblasts to levels of mock-treated control fibroblasts (Figure 13).

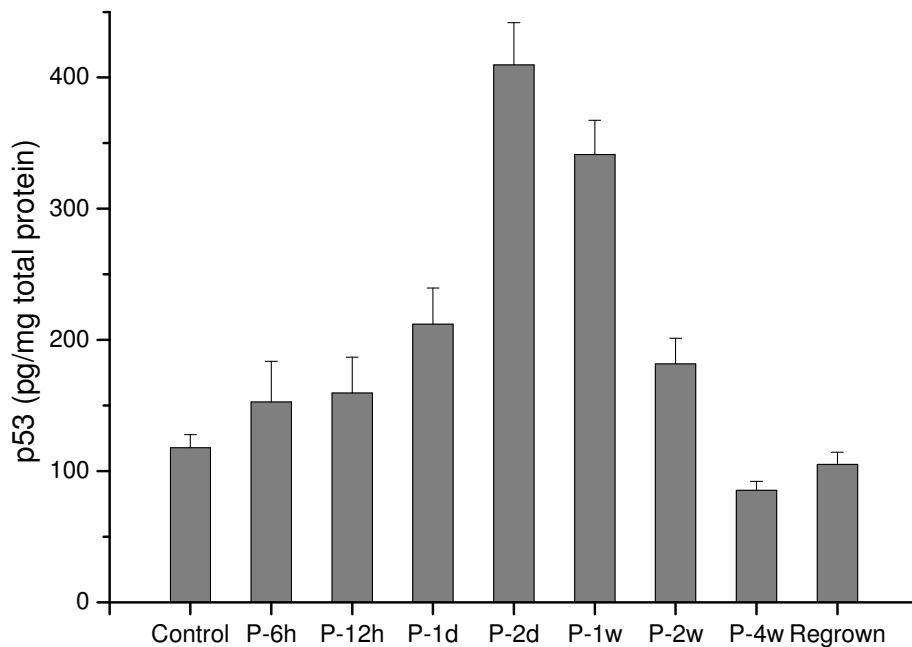


Figure 14. Expression of p53 at different time points after PUVA treatment. p53 expression of fibroblasts at different time post PUVA treatment as well as mock-treated and regrowing fibroblasts was determined by an ELISA specific for p53, as described in Materials and Methods. The results were expressed as the mean of triplicates, three experiments were performed with similar results. Control represents values of p53 concentration in mock-treated fibroblasts. P-6h, P-12h represent values of p53 concentration at 6 hour and 12 hour post PUVA treatment. P-1d, P-2d represent values of p53 concentration at 1 day and 2 day post PUVA treatment. P-1w, P-2w and P-4w represent values of p53 concentration at 1, 2 and 4 weeks post PUVA treatment.

3.2.2. Activation of the senescence control pathways p21/p53 and p16/Rb in PUVA-induced growth arrest

As PUVA-induced growth arrest showed many senescence-like features, and it has earlier been shown that the terminal replicative growth arrest is controlled either by the p53/p21^{Cip1} or the pRb/p16^{INK4a} pathway, the time-dependent expression of these important cell cycle control proteins was determined in PUVA-treated fibroblasts. p53 and p21^{Cip1} protein levels increased concomitantly at day 1 after PUVA treatment, and reached their maximum 2 days later (Figure 14, Figure 15). Thereafter, both p53 and p21^{Cip1} protein amounts decreased with time and are almost back to levels of mock-treated control fibroblasts at 4 weeks post PUVA treatment.

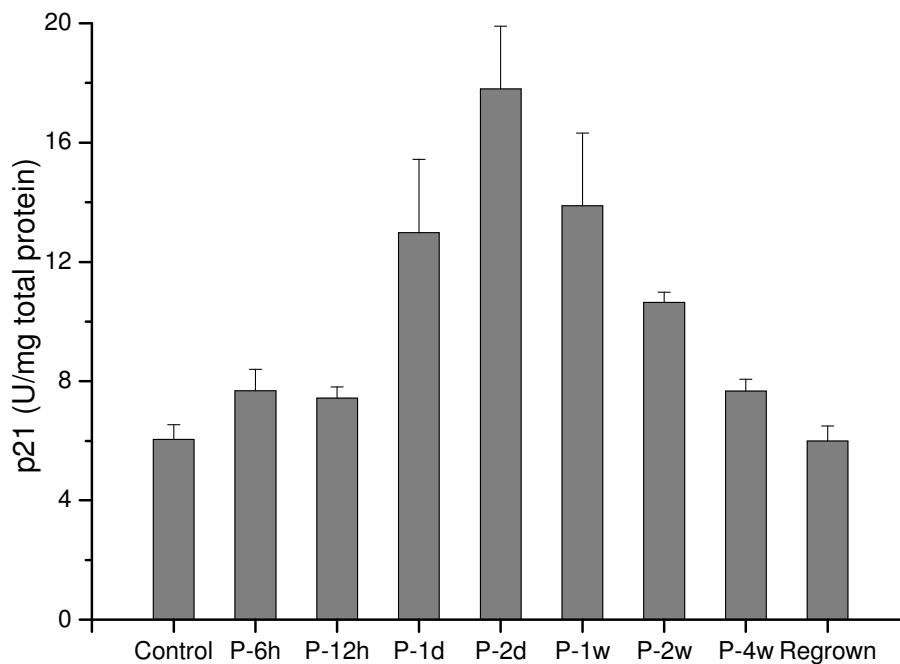


Figure 15. Expression of p21^{Cip1} at different time points after PUVA treatment. p21^{Cip1} expression of fibroblasts at different time post PUVA treatment as well as mock-treated and regrowing fibroblasts was determined by ELISA specific for p21^{Cip1}, as described in Materials and Methods. The results were expressed as the mean of triplicates, three experiments were performed with similar results. Control represents values of p53 concentration in mock-treated fibroblasts. P-6h, P-12h represent values of p21^{Cip1} concentration at 6 hour and 12 hour post PUVA treatment. P-1d, P-2d represent values of p21^{Cip1} concentration at 1 day and 2 day post PUVA treatment. P-1w, P-2w and P-4w represent values of p21^{Cip1} concentration at 1, 2 and 4 weeks post PUVA treatment.

However, as fibroblasts did not re-proliferate at the end of 4 weeks post PUVA treatment, and continued to be arrested for another 2 months, there must be other mechanisms controlling the prolonged growth arrest stage. Similar to the decrease in p53 and p21^{Cip1}, p16^{INK4a} concentrations started to increase 1 week after PUVA treatment and remained elevated for up to 10 weeks post PUVA treatment (Figure 16). These data provide correlative evidence that p16^{INK4a} might be involved in maintaining fibroblasts in this long-term growth arrest stage.

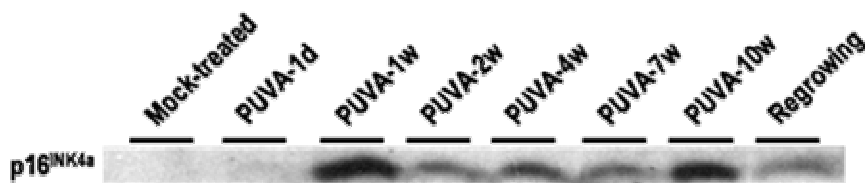


Figure 16. Expression of p16^{INK4a} at different time points after PUVA treatment. Lysates derived from PUVA-treated fibroblasts at different time points post PUVA treatment, mock-treated fibroblasts and regrowing fibroblasts post PUVA treatment were subjected to Western blot analysis for expression of the p16^{INK4a}. Western blot was performed as described in Materials and Methods. P-1d represents values of p16^{INK4a} at 1 day post PUVA treatment. P-1w, P-2w, P-4w, P-7w, P-11w represent values of p16^{INK4a} at 1, 2, 4, 7, 10 weeks post PUVA treatment.

3.2.3. PUVA treatment of fibroblasts with a null mutation in cell cycle controlling genes results in a similar growth arrest as in wild type human dermal fibroblasts

To further address the question whether p16^{INK4a}, p21^{Cip1} and p53 are causally involved in the growth arrest following PUVA treatment, the effect of PUVA treatment on human fibroblasts with homozygous deficiencies in these genes was studied in terms of their proliferation rate and cell phenotype. Following selection of non-cytotoxic conditions fibroblasts were incubated with 50 ng/ml 8-MOP and irradiated with 10 - 90 kJ/m² UVA. Growth rate and cell morphology were monitored over 28 days in p16^{INK4a}, p21^{Cip1} and p53 deficient cells. Unexpectedly, p16^{INK4a}, p21^{Cip1} and p53 deficient cells ceased proliferation and arrested with similar features compared to PUVA-treated wild type fibroblasts with functional p16^{INK4a}, p21^{Cip1} and p53 genes (Figure 17). The lack in mitotic

activity was accompanied by prominent alterations in cell morphology similar to wild type fibroblasts. p16^{INK4a}, p21^{Cip1} and p53 deficient fibroblasts, which had been subjected to combined 8-MOP/UVA treatment changed to an elongated and flattened phenotype at day 7 post PUVA treatment and revealed a substantial increase in size at day 28 (Figure 18). However, it was also obvious that p16^{INK4a}, p21^{Cip1} and p53 deficient fibroblasts are more sensitive to PUVA-induced toxic effects. When the same dose of PUVA (50ng/ml 8-MOP and 90kJ/m² UVA) is applied on fibroblasts deficient for cell cycle control genes as on wild type fibroblasts, a large proportion of deficient fibroblasts died after PUVA treatment, especially p53 deficient fibroblasts. The PUVA treatment that results in growth arrest without cytotoxic effect on p53 deficient fibroblasts is 50ng/ml 8-MOP and 10kJ/m² UVA.

In summary, the data suggest that senescent markers of replicative senescence, such as cell enlargement and SA-β-gal expression, are reversible in PUVA-treated fibroblasts. The senescence controlling genes p53, p21 and p16 were all upregulated after PUVA treatment, but after regrowth returned, apart from p16, back to the level of mock-treated control fibroblasts. However, these senescence controlling genes are not exclusively required for the long-term growth arrest. These data indicated that stress-induced premature senescence after PUVA treatment definitely differs from the irreversible growth arrest and permanent expression of distinct senescence-associated phenotypic and biochemical features.

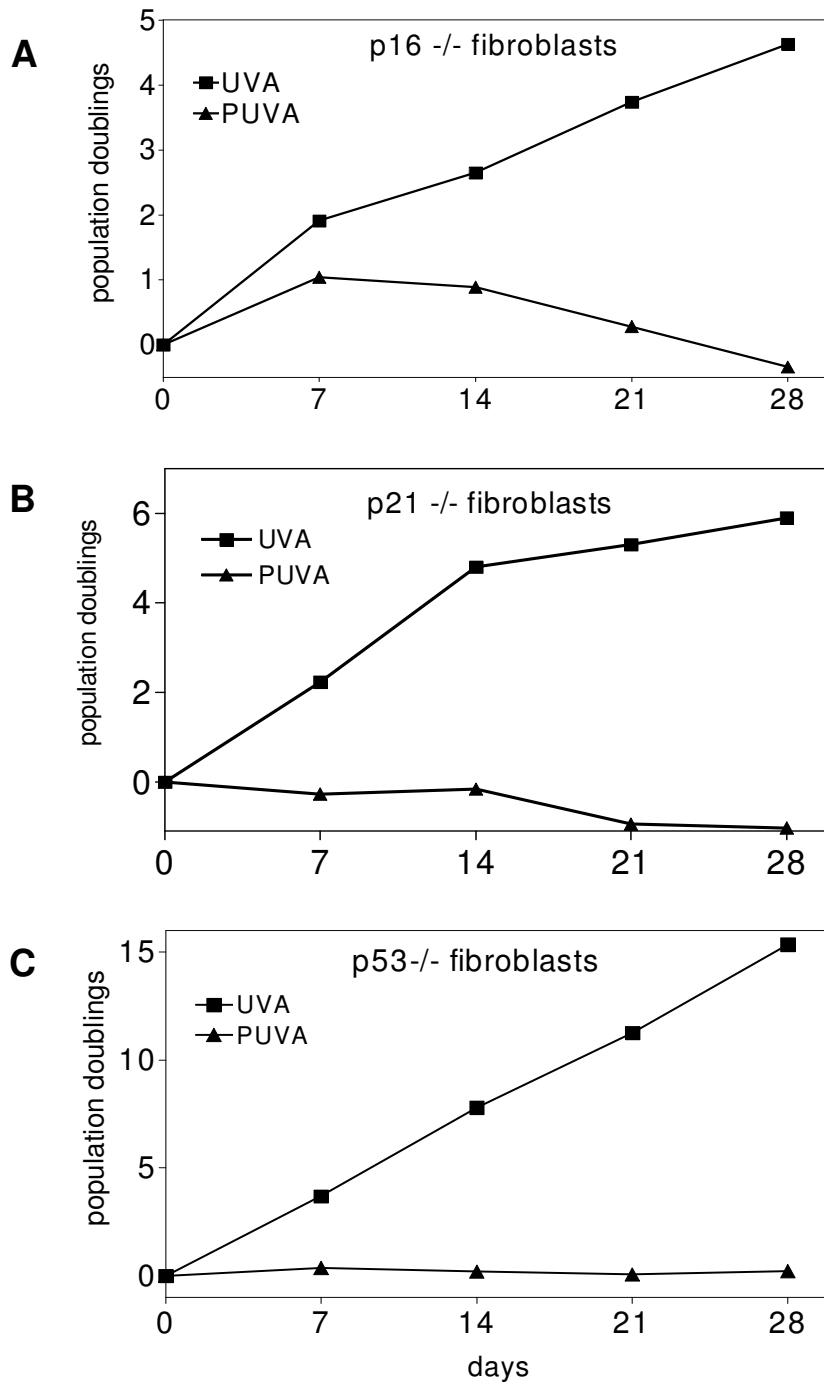


Figure 17. PUVA treatment of p16^{INK4a}, p21^{Cip1} or p53-deficient fibroblasts results in growth arrest. p16^{INK4a} and p21^{Cip1} Fibroblasts were PUVA-treated with 50 ng/ml 8-MOP plus 45 kJ/m² UVA, and p53-deficient fibroblasts were PUVA-treated with 50 ng/ml 8-MOP plus 10 kJ/m² UVA. At different time points thereafter, cell numbers were determined in triplicates for each experimental group and equal cell numbers were plated for further culture. The data represent growth curves expressed as the increase in cumulative population doublings. A: p16^{INK4a} deficient fibroblasts treated with PUVA or UVA irradiation only. B: p21^{Cip1} deficient fibroblasts treated with PUVA or UVA irradiation only. C: p53 deficient fibroblasts treated with PUVA or UVA irradiation only.

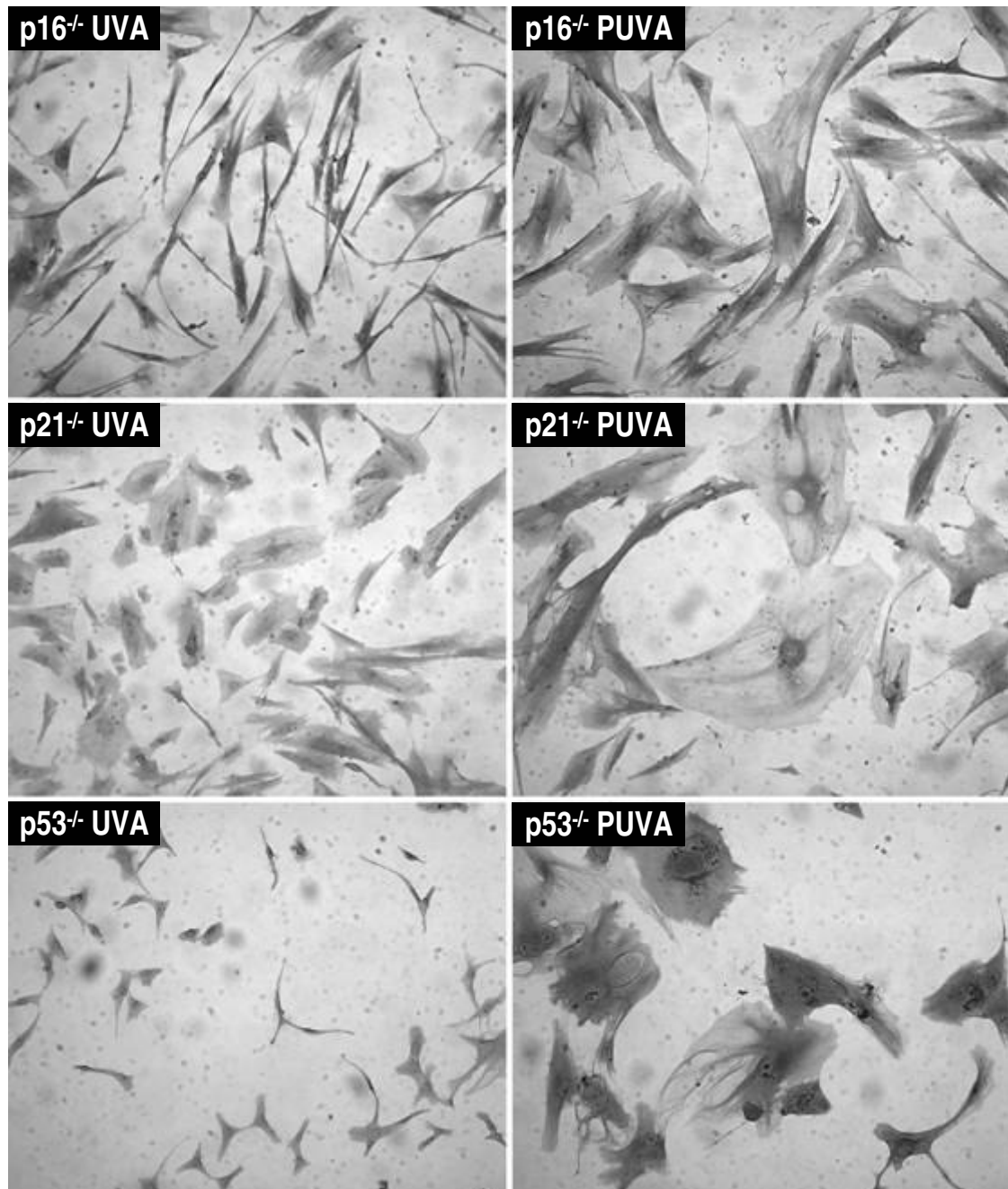


Figure 18. Combined 8-MOP/UVA treatment of $p16^{INK4a}$, $p21^{Cip1}$ or $p53$ deficient fibroblasts promotes the senescence-like phenotype. Fibroblasts were fixed and stained at day 28 after PUVA or UVA treatment, and photographed at 100X magnification. A,B: $p16^{INK4a}$ deficient fibroblasts irradiated with UVA (45 kJ/m^2) or PUVA (50 ng/ml 8-MOP plus 45 kJ/m^2 UVA). C, D: $p21^{Cip1}$ deficient fibroblasts irradiated with UVA (45 kJ/m^2) or PUVA (50 ng/ml 8-MOP plus 45 kJ/m^2 UVA). E,F: $p53$ deficient fibroblasts treated with UVA (10 kJ/m^2) or PUVA (50 ng/ml 8-MOP plus 10 kJ/m^2 UVA).

3.3. PUVA treatment of human dermal fibroblasts increases the generation of intracellular reactive oxygen species

In a first attempt to address the mechanisms by which PUVA-treated fibroblasts gained their senescence-like phenotypic and biochemical changes, it was studied whether reactive oxygen species (ROS) are produced at high concentrations and whether ROS play a role for the long-term senescence-like growth arrest. To determine ROS generation after PUVA treatment, fibroblasts were loaded with the peroxide-sensitive fluorophore 2'-7' dichlorodihydrofluorescein diacetate (H₂DCFDA). H₂DCFDA is cell membrane permeable and can be deesterified to H₂DCF by intracellular esterases located in the cell membrane (LeBel *et al.* 1992). The resulting H₂DCF is membrane impermeable and can

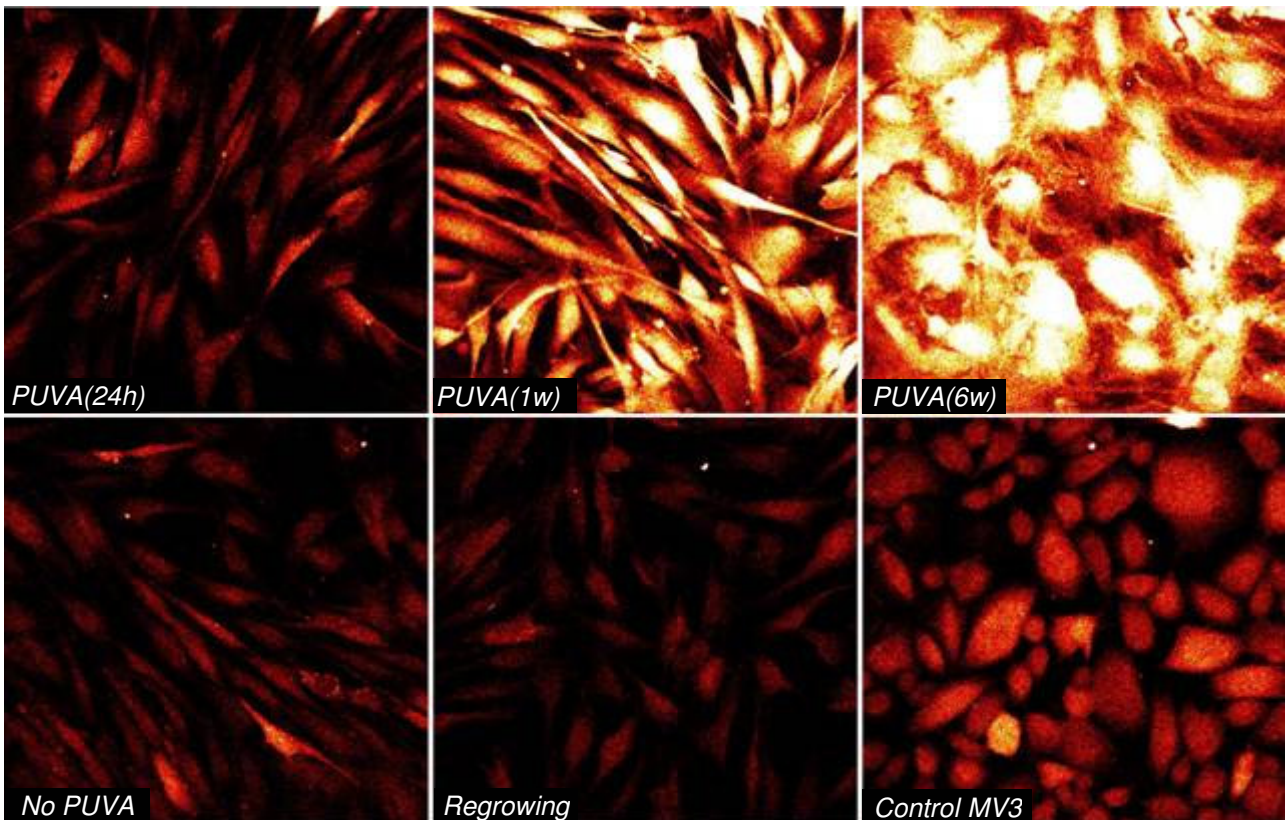


Figure 19. Increased ROS production in human dermal fibroblasts at different time points after PUVA treatment. ROS levels were determined by DCF staining in PUVA-treated fibroblasts, regrowing fibroblasts and mock-treated control fibroblasts, as described in Materials and Methods. A melanoma cell line (MV3) was included as positive control. Fluorescence intensity was recorded with a Zeiss laser scanning confocal microscope ($\times 100$ magnification).

be rapidly oxidized to the highly fluorescent 2',7'-dichlorofluorescein (DCF) in the presence of intracellular ROS and RNS (reactive nitrogen species), particularly H₂O₂ and Nitric oxide (NO). As shown in Figure 19, PUVA treatment resulted in a moderate 2-fold increase in DCF fluorescence intensity at 24h post PUVA treatment which time-dependently increased to 5-fold at 1 week and >20 fold 6 weeks post PUVA treatment compared to mock-treated and regrowing fibroblasts. The DCF fluorescence intensity was not related to NO, since inhibition of NO production by specific NO inhibitors was not able to decrease the fluorescence. These results derived from experiments with inducible NO synthesis (iNOS) inhibitors, which controls the intracellular level of NO (Amin *et al.* 1999). Culture medium was supplemented with the iNOS inhibitor 1400w for one day in PUVA-treated fibroblasts at different time points post treatment. Independent of all tested concentrations of the iNOS inhibitor 1400w, no decrease in DCF fluorescence was observed indicating that the increasing intensity of DCF fluorescence post PUVA treatment is not due to NO production, but rather to enhanced generation of ROS.

3.3.1. Increase in the number of mitochondria and decrease in the relative mitochondrial transmembrane potential in PUVA-treated fibroblasts

The mitochondrion is the main site of ROS production in mammalian cells. Both unbalanced mitochondria biogenesis and damages of the mitochondrial electron phosphorylation chain may lead to enhanced ROS generation. To study whether mitochondria are involved and contribute to the enhanced ROS production of PUVA-treated fibroblasts, mitochondrial proliferation and mitochondrial membrane integrity were determined after PUVA treatment. To measure changes in the number of mitochondria, fibroblasts were stained with the mitochondria-selective vital dye MitoTracker Red at different time points post PUVA treatment. MitoTracker probes are specifically sequestered in mitochondria where they react with thiols on proteins and peptides to form an aldehyde-fixable conjugate. As shown in Figure 20, PUVA-treated fibroblasts showed a progressive increase in mitochondria mass with time after PUVA treatment, Figure 20 B and C represent PUVA-treated cells at 16 days and 7 weeks post PUVA, respectively. Figure 20 A and D showed the number (mass) of mitochondria in mock-treated (A) and in regrowing fibroblasts (D).

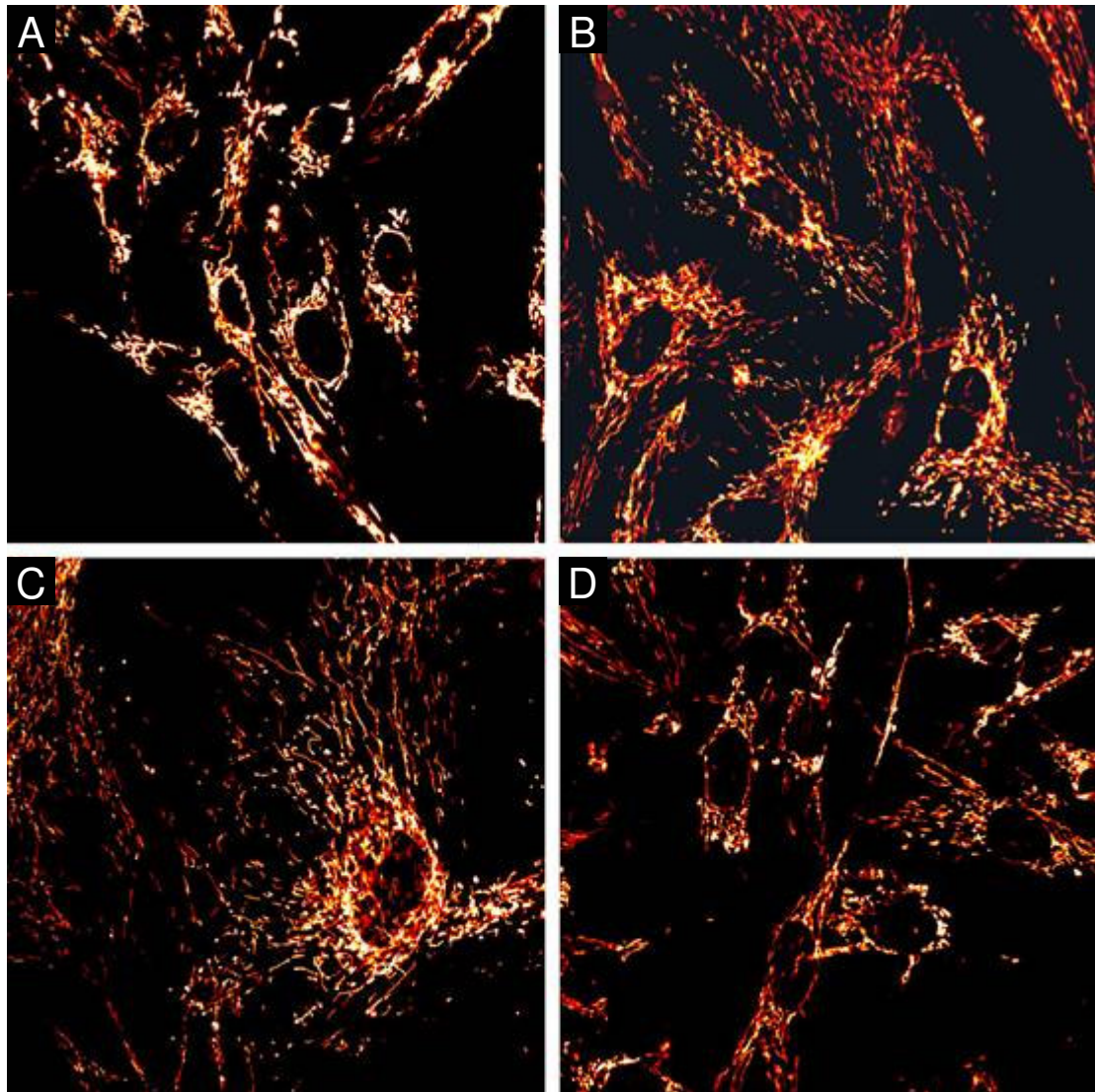


Figure 20. The number of mitochondria per cell increases at different time points after PUVA treatment. Fibroblasts at different time post PUVA treatment, mock-treated and regrowing fibroblasts were stained for mitochondria using MitoTrack Red as described in Material and Methods. A: mock-treated fibroblasts; B and C: PUVA-treated fibroblasts at 16 days and 7 weeks post PUVA; D, regrowing fibroblasts.

To monitor the integrity of the mitochondrial membrane as a means for the functional integrity of the oxidative phosphorylation chain, the mitochondrial membrane potential ($\Delta\Psi_m$) was measured using a polarization-sensitive dye JC-9. JC-9 is directed into mitochondria and exists in two interchangeable forms, either as a monomer (J-monomer) or as a dimer (J-aggregate). J-monomer leads to the emission of green fluorescence and J-aggregates to the emission of red fluorescence. In cells with intact mitochondrial membranes, JC-9 is driven into mitochondria due to a high $\Delta\Psi_m$. Accumulation of JC-9 in negatively charged mitochondria forms J-aggregate and results in red fluorescence. When $\Delta\Psi_m$ decreases, JC-9 subsequently diffuses out of the mitochondria and leads to decrease in the intensity of red fluorescence. Since the green fluorescence is relatively constant due to potential-independent interactions of JC-9 monomer with the mitochondrial membrane, which is only related to the mitochondria number, changes in the ratio between J-aggregate (red fluorescence) and J-monomer (green fluorescence) indicates $\Delta\Psi_m$ value changes (Reers *et al.* 1991; Smiley *et al.* 1991). In order to determine $\Delta\Psi_m$ changes, the same number of PUVA-treated fibroblasts at different time points post PUVA treatment was monitored for the intensity of green and red fluorescence by FACS analysis. As shown in Figure 21, JC-9 green fluorescence was greatly increased in PUVA-treated fibroblasts 2 weeks (PUVA-2w) and 11 weeks (PUVA-11w) post PUVA treatment. The majority of fibroblasts at 2 or 11 weeks post PUVA treatment revealed a fluorescent value around 1000 while the fluorescent value of mock-treated control fibroblasts was 30, indicating a 33-fold increase in the number of mitochondria. However, no similar increase in the red fluorescence was observed. The peak of the red fluorescence in fibroblasts at 2 weeks post PUVA treatment revealed a value of about 50, and in fibroblasts at 11 weeks post PUVA treatment the fluorescent value was 35. Compared to the value of 20 in mock-treated fibroblasts, there was only a 1.8-2.5 fold increase in the intensity of red fluorescence. Thus, the red/green fluorescence ratio, which represents the $\Delta\Psi_m$ value, revealed a 4-fold decrease in PUVA-treated fibroblasts as calculated in Figure 22. These data indicate that the $\Delta\Psi_m$ is significantly decreased in PUVA-treated fibroblasts.

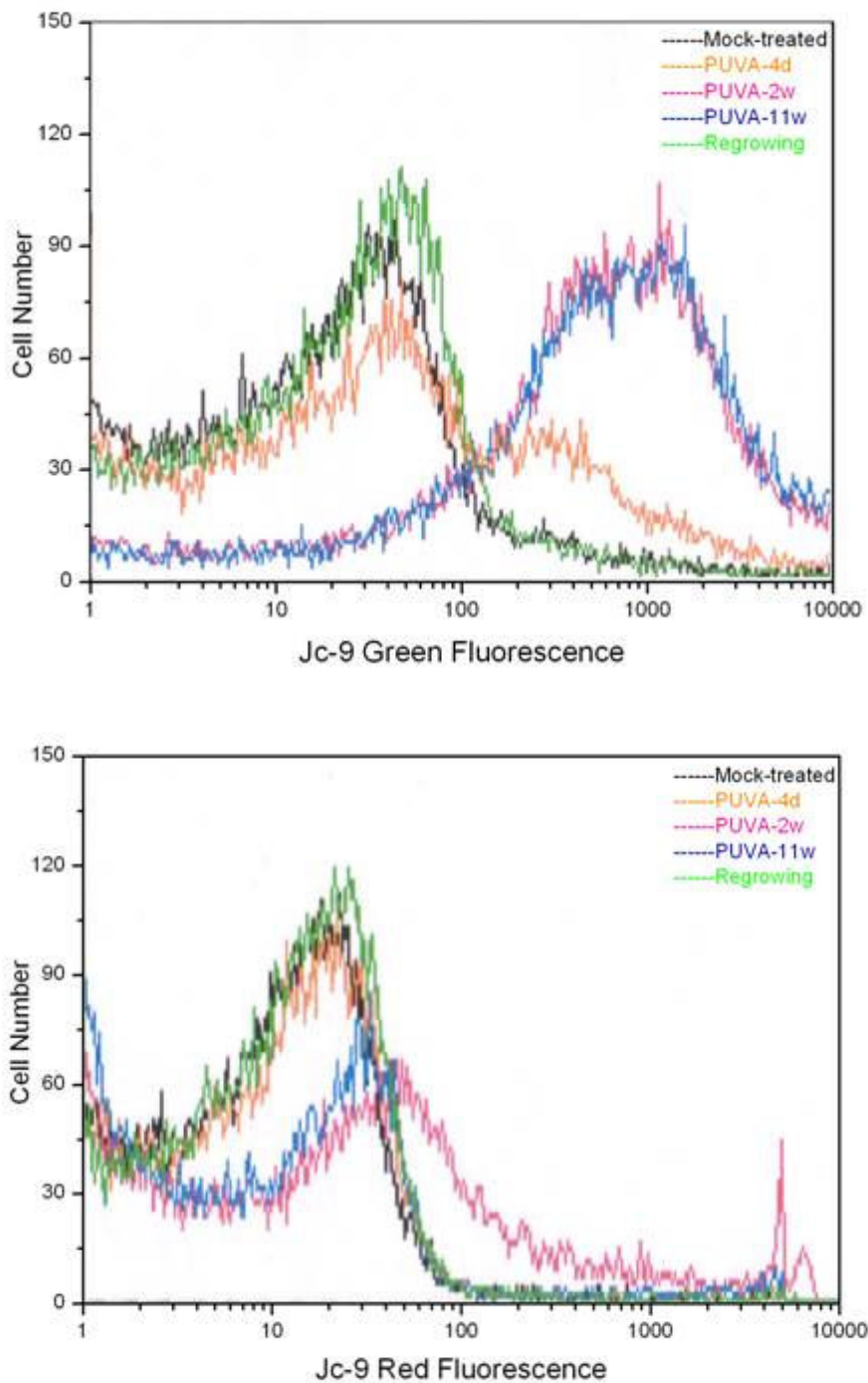


Figure 21. JC-9 fluorescent staining for PUVa-treated fibroblasts at different time post PUVa treatment. After incubation with JC-9, 1×10^6 cells/ml of PUVa-treated fibroblasts 4 days (PUVA-4d), 2 weeks (PUVA-2w) and 11 weeks (PUVA-11w) post PUVa treatment, regrowing fibroblasts post PUVa treatment and mock-treated control fibroblasts were determined for red and green fluorescence by FACS, as described in Materials and Methods.

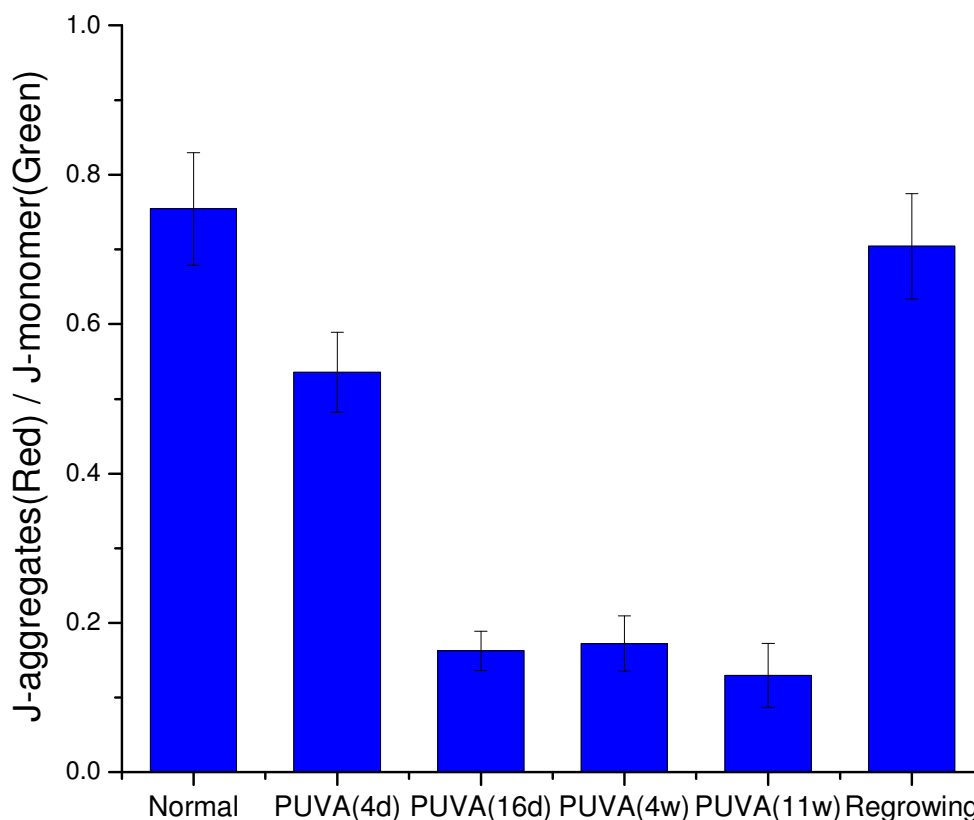


Figure 22. The ratio of J-aggregates/J-monomer decreases after PUVA treatment. After incubation with JC-9, 1×10^6 cells/ml of PUVA-treated fibroblasts 4 days, 16 days, 4 weeks and 11 weeks post PUVA treatment, regrowing fibroblasts post PUVA treatment and mock-treated control fibroblasts were determined for red and green fluorescence by FACS, as described in Materials and Methods. The data are measured in triplicates and shown as mean \pm standard deviation.

3.3.2. Changes in ATP content in PUVA-treated fibroblasts

Depolarization of mitochondrial membrane potential should lead to reduced ATP production. ATP concentrations were measured in PUVA-treated fibroblasts at different time points post treatment, in regrowing and mock-treated control fibroblasts. PUVA-treated fibroblasts showed a dramatic increase in total ATP content per cell resulting in a 3-fold increase in ATP concentrations at 2 weeks and a 4.2-fold increase at 4 weeks post PUVA treatment compared to much lower ATP concentrations in regrowing and mock-treated fibroblasts (Figure 23). However, considering that PUVA-treated fibroblasts reveal a great increase in

cell size and mitochondria mass, the average ATP concentration per unit total protein was constant (Figure 23).

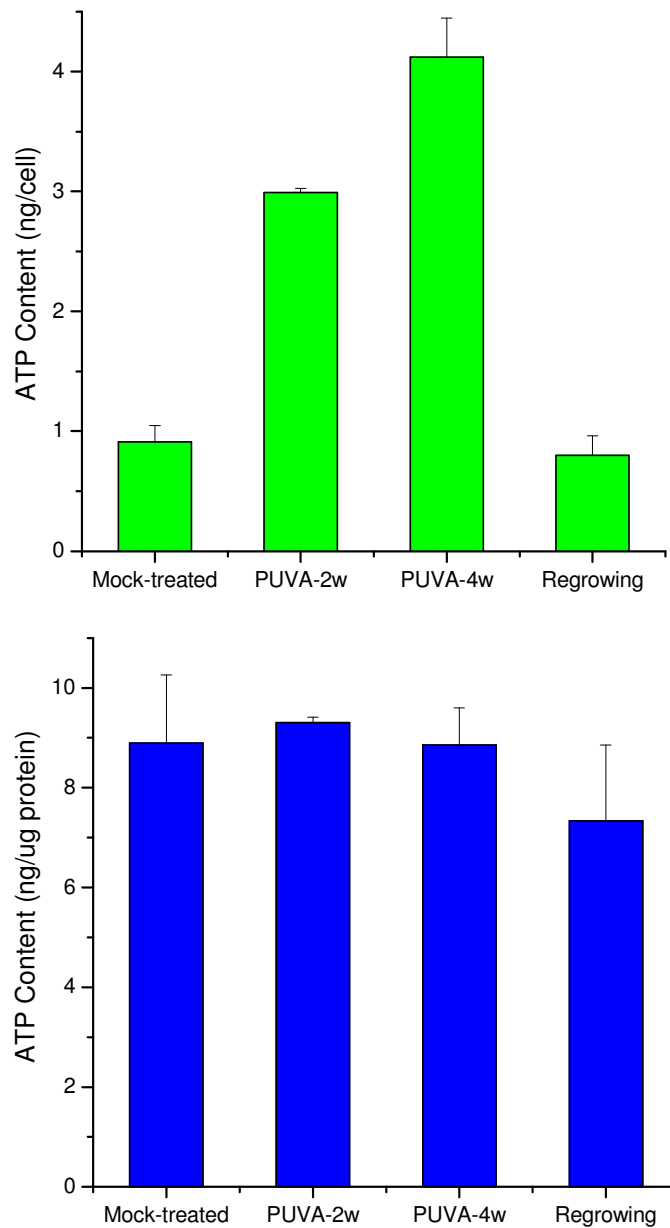


Figure 23. Changes in ATP concentrations at different time points post PUVA treatment. The ATP content was determined by a luminescent method as described in Materials and Methods. The upper panel showed ATP content per cell, the lower panel show ATP content as a ratio of total ATP per total protein content. Experiments were performed in triplicates and expressed as mean \pm standard deviation.

3.3.3. PUVA-treated Rho0 fibroblasts still have a high ROS level

To further investigate whether mitochondria are responsible for PUVA-induced ROS production, fibroblasts depleted in their mitochondrial DNA (mtDNA), designated as Rho0 fibroblasts, were generated using low concentrations of ethidium bromide. Low ethidium bromide concentrations lead to the depletion of the mtDNA resulting in the disruption of electron transport/oxidative phosphorylation (King and Attardi 1989). The number of mitochondria was decreased by a factor of two with each cell division since - due to lack of mtDNA - no new mitochondria were generated. The depletion of mtDNA was confirmed by the mitochondria transcription factor mtTFA, which plays a role in controlling mtDNA copy number and varies concomitantly with levels of mtDNA (Shen and Bogenhagen 2001). The mtTFA expression was completely suppressed 1 week after incubation of fibroblasts with ethidium bromide as shown by immunoblotting (Figure 24). To ensure that mtDNA would not recover, Rho0 fibroblasts were maintained in ethidium bromide-containing medium. Rho0 fibroblasts were then subjected to PUVA treatment and ROS levels were determined by DCF staining. As shown in Figure 25H and I, PUVA-treated Rho0 fibroblasts still revealed a high intensity of DCF fluorescence at 3 weeks and 6 weeks post treatment compared to mock-treated Rho0 fibroblasts (Figure 25G). The overall unchanged DCF intensity indicates that other factors may contribute alone or in conjunction with mitochondrial dysfunction to the enhanced ROS concentration in PUVA-treated fibroblasts.

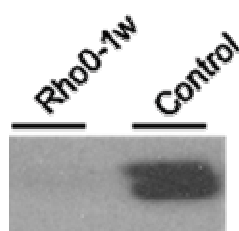


Figure 24. The expression of the mitochondrial transcription factor mtTFA is suppressed after incubation of human dermal fibroblasts with ethidium bromide. Human dermal fibroblasts were incubated with ethidium bromide at a concentration of 0.1 $\mu\text{g/ml}$ as described in Materials and Methods. One week after treatment, Rho0 fibroblasts as well as mock-treated control fibroblasts were studied for mtTFA expression by Western blot analysis.

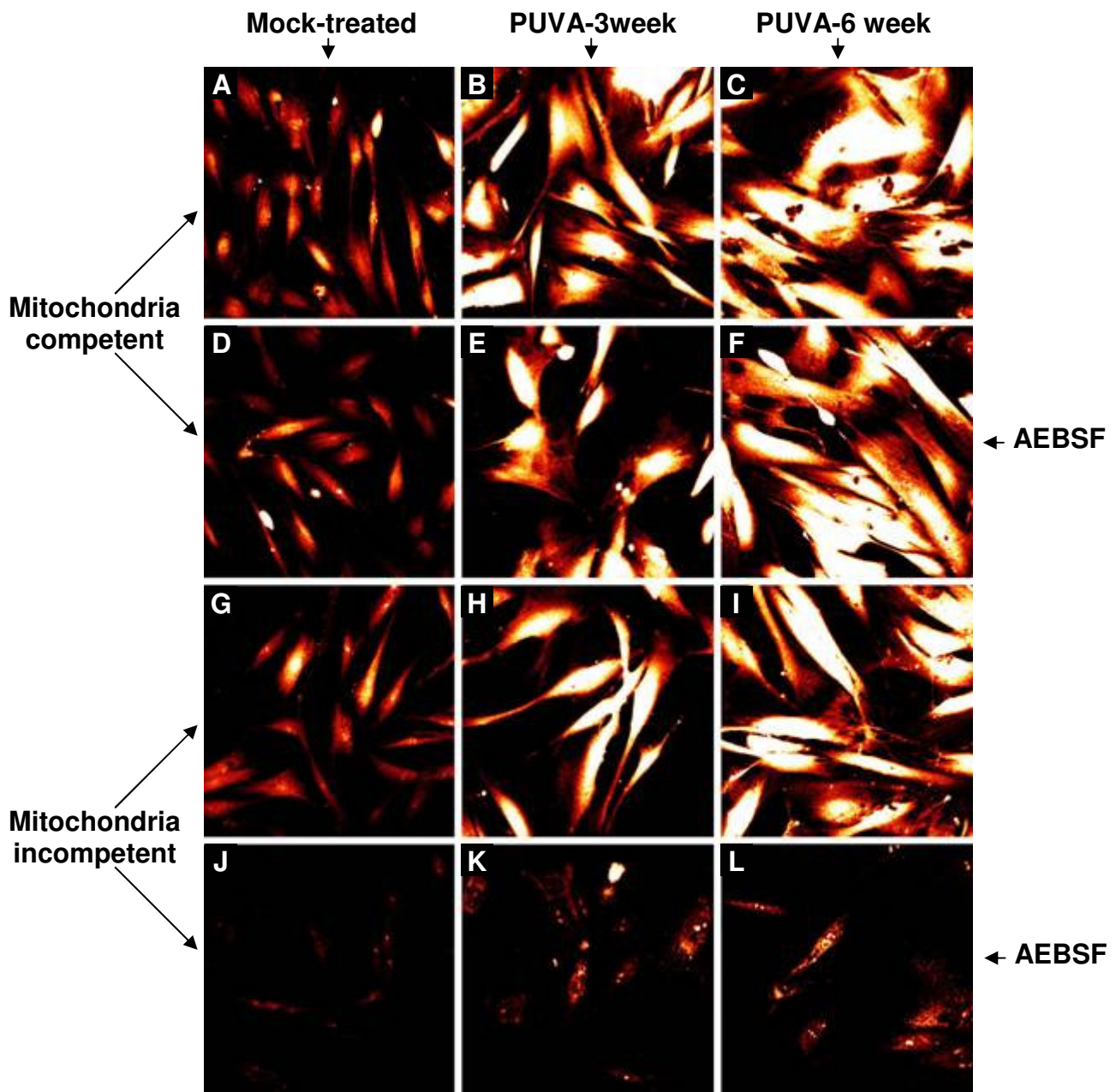


Figure 25 The generation of reactive oxygen species after PUVA treatment of human dermal fibroblasts is due to both mitochondria and NADPH oxidase. Human dermal mitochondria competent or mitochondria incompetent fibroblasts were subjected to PUVA treatment. ROS generation was monitored at 3 and 6 weeks post PUVA treatment in the presence and absence of the NADPH oxidase inhibitor AEBSF by loading fibroblasts of the differently treated experimental groups with 10 $\mu\text{g}/\text{ml}$ of the fluorescent ROS-indicator $\text{H}_2\text{DCF-DA}$ as described in Material and Methods. Depletion of mitochondrial function was achieved by treating human dermal fibroblasts with 0.1 $\mu\text{g}/\text{ml}$ ethidium bromide at 37°C for 7 to 14 days. The depletion of mitochondria DNA was confirmed by a complete suppression of the expression of the mitochondrial transcription factor which correlate with the mitochondria number. A-F: mitochondria competent fibroblasts showing in A: mock-treated, B: PUVA-treated 3 weeks after PUVA

treatment. C: PUVA-treated 6 weeks after PUVA treatment. D: mock-treated after incubation with the NADPH oxidase inhibitor AEBSF for 1 hour. E: PUVA-treated 3 weeks after PUVA treatment after incubation with the NADPH oxidase inhibitor AEBSF for 1 hour. F: PUVA-treated 6 weeks after PUVA treatment after incubation with the NADPH oxidase inhibitor AEBSF for 1 hour. G-L: mitochondria in competent fibroblasts showing in G: mock-treated. H: PUVA-treated 3 weeks after PUVA treatment. I: PUVA-treated 6 weeks after PUVA treatment. J: mock-treated after incubation with the NADPH oxidase inhibitor AEBSF for 1 hour. K: PUVA-treated 3 weeks after PUVA treatment after incubation with the NADPH oxidase inhibitor AEBSF for 1 hour. L: PUVA-treated 6 weeks after PUVA treatment after incubation with the NADPH oxidase inhibitor AEBSF for 1 hour.

3.3.4. Inhibition of NADPH Oxidase does not abrogate the ROS increase in PUVA-treated mitochondria-competent fibroblasts, whereas ROS production is suppressed in PUVA-treated Rho0 fibroblasts

Among other sources for ROS production, cyclooxygenase 2 (COX-2) and NADPH oxidase are involved. These two enzymes are not constitutively expressed in cells, but can be induced or activated under certain conditions (Finkel 1999). In the first attempt to study whether these enzymes are activated and may play a role in the high ROS production in PUVA-treated fibroblasts, specific inhibitors for each of the enzymes were employed. Although inhibition of COX-2 with the selective COX-2 inhibitor NS398 (Liu *et al.* 1998) post PUVA treatment did not reveal any decrease in ROS levels in fibroblasts at different time point post PUVA treatment (data not shown), inhibition of NADPH oxidase in PUVA-treated Rho0 fibroblasts almost completely blocked ROS production.

In detail, the human NADPH oxidase consists of two membrane components and several cytosolic components, and is activated in case these cytosolic components translocate into the plasma membrane. Activated NADPH oxidase catalyzes the reaction:



Two NADPH oxidase inhibitors, 4-(2-aminoethyl)-benzenesulfonyl fluoride) (AEBSF) and diphenylene iodonium (DPI), were employed in this study. As shown in Figure 25D, E and F, AEBSF did not result in a decrease of ROS production in PUVA-treated fibroblasts at different time post PUVA treatment compared to PUVA-treated fibroblasts in the absence of AEBSF treatment

(Figure 25A, B and C). However, the intensity of DCF fluorescence of PUVA-treated Rho0 fibroblasts at different time post treatment (as shown in Figure 25G, H and I) was almost completely abrogated in the presence of AEBSF in the culture (Figure 25J, K and L). The alternative inhibitor of the NADPH oxidase, DPI, showed similar results (data not shown). Trypan blue staining revealed a more than 85% exclusion rate after incubation with these inhibitors indicating that the used concentrations are not toxic to Rho0 fibroblasts. Moreover, PUVA-treated Rho0 fibroblasts were incubated with corresponding concentrations of these inhibitors for up to 1 week or longer with no detectable increase in cell death as compared to that of without inhibitors. These results exclude the possibility that the decrease in ROS levels is due to cytotoxicity related cell death.

3.3.5. ROS contribute to the PUVA-induced senescence-like morphology

Under PUVA-induced long-term growth arrest fibroblasts showed senescence-like features. To determine whether the increase in ROS levels after PUVA treatment was simply correlative or alternatively whether ROS may play a causal role in the initiation and maintenance of these senescence-like features, the role of enhanced ROS levels in the increase in SA- β -gal-positive cells and phenotypic changes was tested under conditions with reduced ROS levels. For this purpose, PUVA-treated fibroblasts were exposed to the antioxidant N-acetyl cysteine (NAC). NAC is a reduced glutathione (GSH) provider and a direct and efficient scavenger of hydroxyl, H₂O₂ and possibly other kinds of ROS (Staal *et al.* 1990). As shown in Figure 26, ROS levels of PUVA-treated fibroblasts incubated with NAC were substantially decreased compared to PUVA-treated fibroblasts without NAC. At different time points post PUVA treatment, NAC-supplemented (NAC(+)) and non-supplemented fibroblasts (NAC(-)) were examined for phenotypic changes and for SA- β -Gal expression. As shown in Figure 27, NAC(+) and NAC(-) fibroblasts showed a similar morphology at 2 days after PUVA treatment. At 1 week after PUVA treatment, NAC(-) fibroblasts changed to an elongated phenotype and revealed – as expected – a substantial increase in cytoplasmic size at 2 weeks after PUVA treatment, while phenotypic changes in NAC(+) fibroblasts were not apparent. Although a moderate enlargement could be seen in some NAC(+) fibroblasts at 4 weeks after PUVA treatment, overall these changes were neglectable when compared to the greatly enlarged NAC(-)

fibroblasts at the same time points suggesting that the high ROS production after PUVA treatment is involved and contributes to the phenotypic changes. SA- β -gal positive fibroblast numbers of NAC(+) dishes, on the contrary, did not show any difference compared to that of NAC(-) dishes at the same time points after PUVA treatment. As shown in Figure 28, at 1 week after PUVA treatment, the percentage of SA- β -gal positive fibroblasts increased with time and over 90% of fibroblasts were positive at the end of 4 weeks post PUVA treatment. This suggests that SA- β -gal expression represents a marker which is either not downstream of ROS or that the low levels of ROS maintained in NAC(+) fibroblasts are already sufficient to up-regulate SA- β -gal expression.

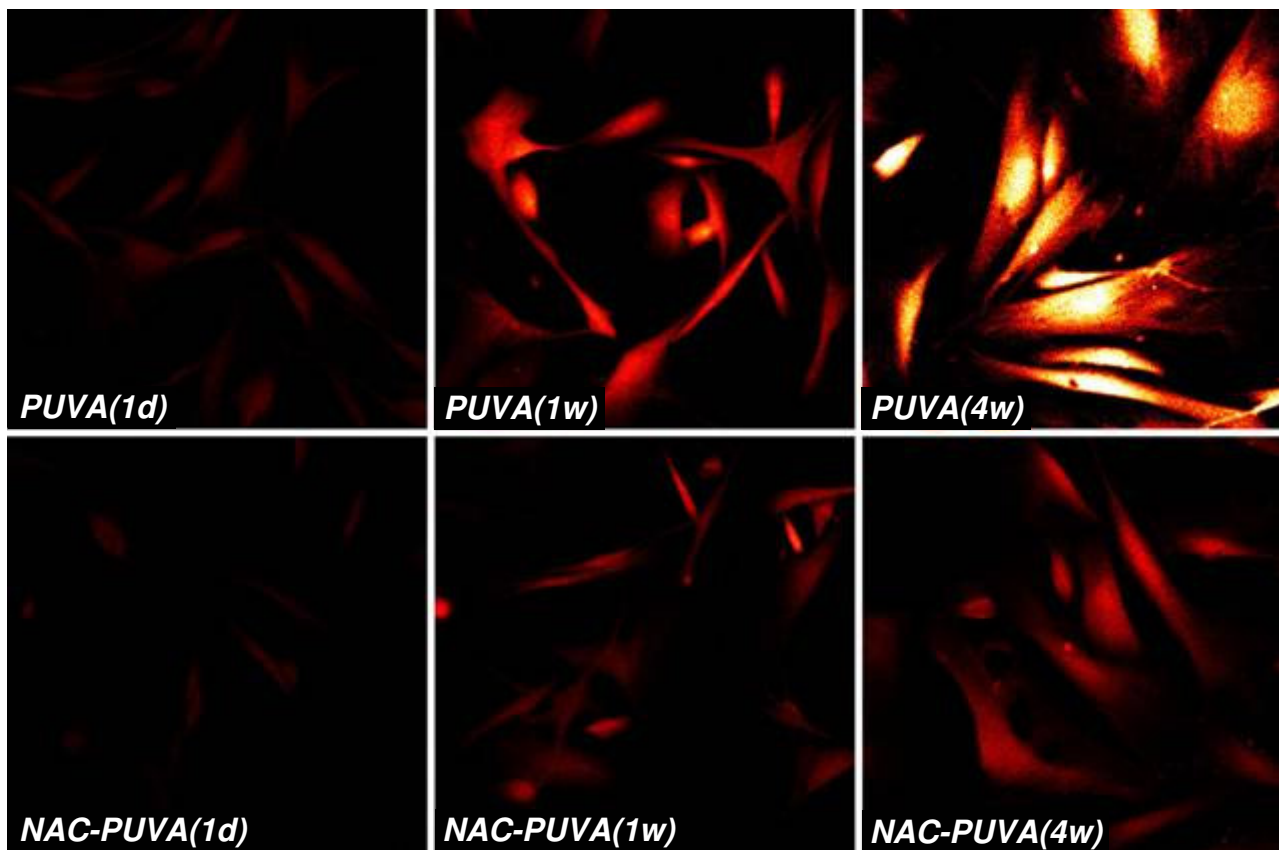


Figure 26. Supplementation of human dermal fibroblasts with N-acetyl cystein (NAC) during the growth arrest stage post PUVA treatment leads to a decrease in ROS levels. Immediately after PUVA treatment, fibroblasts were maintained in culture medium containing 5 mM NAC. The medium was changed every three days to ensure an efficient antioxidant capacity. ROS levels in fibroblasts at different time points post PUVA treatment were determined by DCF at day 2 after NAC treatment. PUVA (1d) (1w) (4w) represents PUVA-treated fibroblasts at 1 day, 1 week and 4 weeks after PUVA treatment; NAC-PUVA (1d) (1w) (4w) represents PUVA-treated fibroblasts at 1 day, 1 week and 4 weeks after PUVA treatment which had been cultured in the presence of NAC.

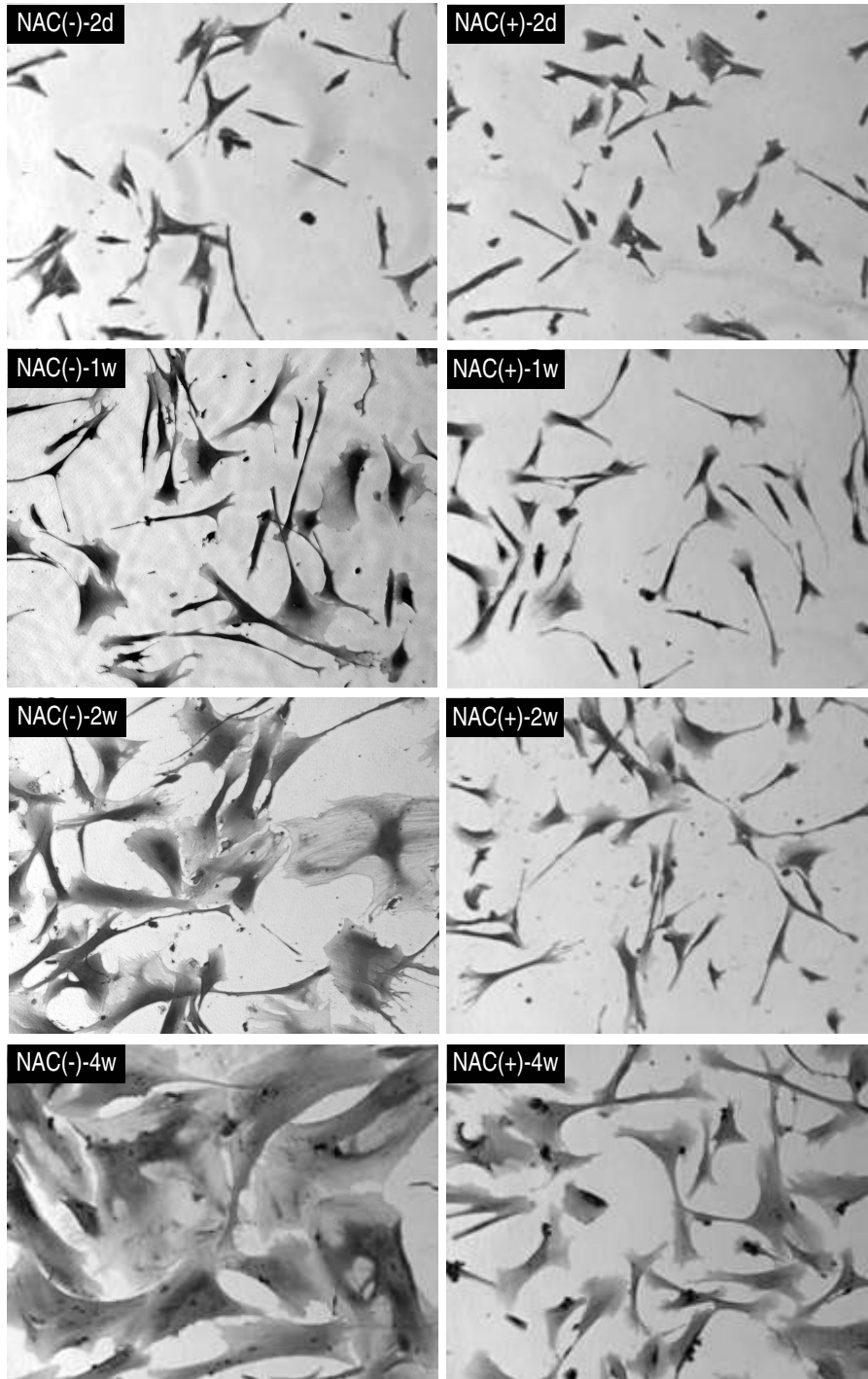


Figure 27. Incubation with N-acetyl cystein prevented PUVA-treated fibroblasts from enlargement. After PUVA treatment fibroblasts were cultured in the presence (NAC(+)) or absence (NAC(-)) of NAC at a concentration of 5 mM. The medium was changed every 3 days to ensure an efficient antioxidant capacity. Fibroblasts were fixed at 1 week (1w), 2 weeks (2w) and 4 weeks (4w) with Comassie blue. Photographs were taken at $\times 100$ magnification.

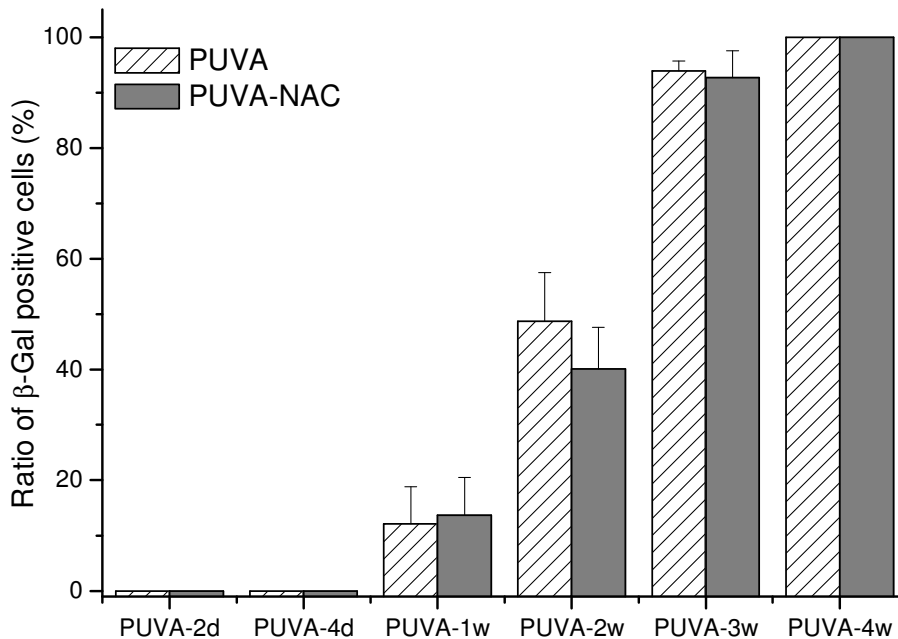


Figure 28. Senescence-associated β -galactosidase expression in PUVA-treated fibroblasts with or without N-acetyl cystein. After PUVA treatment fibroblasts were seeded in 35 mm plastic dishes at a density of 3×10^4 cells per dish in the presence (PUVA-NAC) or absence (PUVA) of 5 mM NAC. SA- β -gal positive as well as negative cells were counted and calculated in 10 randomly selected high power fields ($\times 100$ magnification) at 2 days (PUVA-2d), 4 days (PUVA-4d), 1 week (PUVA-1w), 2 weeks (PUVA-2w), 3 weeks (PUVA-3w) and 4 weeks (PUVA-4w) after PUVA treatment. $P > 0.6$ for each of the group indicating that there is no significant difference in the β -galactosidase expression of PUVA-treated fibroblasts with or without NAC (student t-test).

In summary, PUVA treatment leads to an enhanced ROS production which contributes to the senescent-like phenotypes, at least cell enlargement can be abrogated by antioxidants. Both mitochondrial dysfunction and NADPH oxidase activation are likely to be involved in the enhanced ROS production in PUVA-treated fibroblasts.

3.4. Molecular mechanisms of the decline in the overall life span in regrowing fibroblasts post PUVA treatment

As shown in Figure 9, regrowing fibroblasts revealed a reduced total life span as judged by the much lower CPD at which the replicative senescence stage was reached. Studies into the detailed mechanism are of potential interest not only for the understanding of replicative cellular senescence and stress-induced premature senescence, but also for premature skin aging, which is observed after repetitive long-term PUVA treatment of patients. As an increasing level of ROS production was observed during the growth arrest stage, the herein described study was focused on the question whether oxidative stress is involved and contributes to the early onset of cellular replicative senescence. In case ROS play a role, identifying the underlying molecular targets which finally lead to replicative senescence is of interest. In particular the following questions were addressed: In what fashion does oxidative stress interact, if at all, with other proposed determinants of cellular senescence such as telomere length? Is the premature senescence controlled by telomere erosion, by activation of telomere-independent mechanisms or a combination of both?

3.4.1. Fibroblasts regrowing post PUVA treatment reveal a decline in the overall life-span

The population doublings (CPDs) of regrowing fibroblasts post PUVA treatment was measured and compared with that of non-PUVA-treated control fibroblasts. As shown in Figure 9, starting from CPD 48, regrowing and mock-treated control fibroblasts showed a similar growth rate for the first 10 PDs. Afterwards, the growth rate of regrowing fibroblasts was slowed down and reached the replicative senescence stage after 150 days where the CPD increasing rate was lower than 0.02 PD/week with a final CPD of 62. By contrast, even at a CPD of 70 mock-treated control fibroblasts of the same strain did not show any sign of proliferation stop. Thus, even though PUVA-treated fibroblasts escape from the long-term growth arrest, they reveal a reduced life-span and reach the stage of replicative senescence much earlier after regrowth post PUVA treatment compared to mock-treated control fibroblasts.

3.4.2. Fibroblasts regrowing post PUVA treatment reveal enhanced reduction in telomere lengths

As telomere length is thought to serve as a “mitoclock” for replicative senescence, cells stop dividing when a critical telomere length is reached. In a first attempt to study whether the reduced life span of regrowing fibroblasts is due to a PUVA-induced telomere shortening, telomere length of regrowing fibroblasts post PUVA treatment was determined and compared with that of mock-treated control fibroblasts at the same CPD. For this purpose, fibroblasts of the same strain at an early passage (CPD = 18.6) were either PUVA-treated or frozen down for later use. After 13 weeks the PUVA-treated fibroblasts started to regrow. PUVA-treated fibroblasts in their repropagating stage as well as mock-treated control fibroblasts of the same strain at the same CPD were collected and cultured for further CPD determination. Genomic DNA was collected from regrowing and mock-treated control fibroblasts at comparable CPDs and subjected to telomere length measurement. Figure 29A shows the terminal restriction fragment (TRF) pattern. The mean telomere length was estimated by the size of the median of each band to the molecular weight markers. Lane 3, 5, 7, 9 represent the TRF patterns of regrowing fibroblasts at different CPDs (CPD 20.9, 28.4, 32.8 and 39.8, respectively), and Lane 2, 4, 6, 8 represent TRF patterns of mock-treated control fibroblasts with comparable CPDs (20.2, 29.4, 32.6, 41). Compared to mock-treated control fibroblasts at comparable CPDs, the mean TRF lengths in regrowing fibroblasts are significantly decreased with a 1 to 2 kb reduction. Since the CPD of regrowing fibroblasts before PUVA treatment was 18.6, and no CPD increase occurred during the growth arrest stage after PUVA treatment, the difference in telomere length between regrowing and mock-treated control fibroblasts happened either during the growth arrest stage or during the first 2.3 PDs of proliferation between initiation of regrowth and collection of genomic DNA. During their regrowing phase post PUVA treatment, regrowing fibroblasts showed a similar rate in telomere shortening compared to mock-treated control fibroblasts.

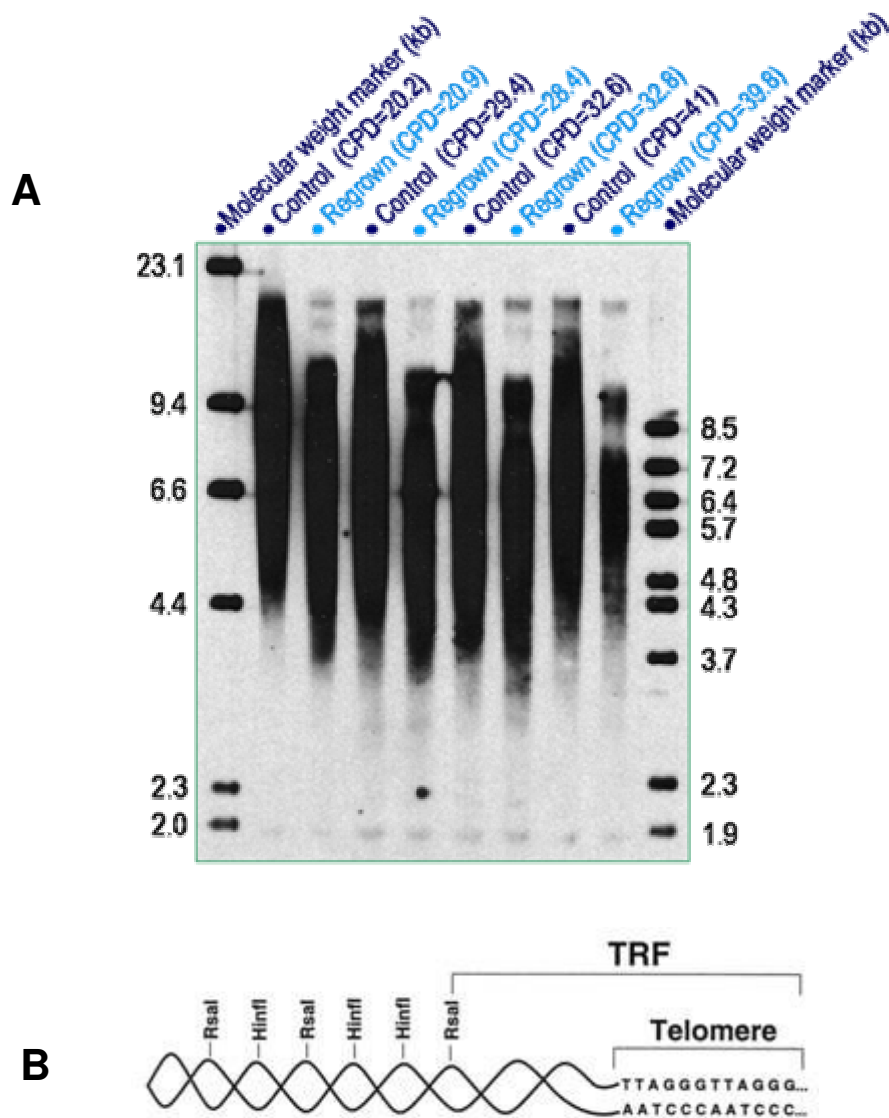


Figure 29 Regrowing fibroblasts post PUVA treatment showed a reduced telomere length compared to mock-treated fibroblasts at the same CPD. A, Terminal restriction fragment (TRF) analysis as an indication for telomere length was performed as indicated in Material and Methods. Briefly, genomic DNA was prepared from regrowing fibroblasts at different CPDs or from mock-treated fibroblasts and of the same strain at the same CPD. 1.5 μ g of HinfI/RsaI-digested DNA of each sample was subjected to electrophoresis on 0.6% agarose gels followed by Southern blot hybridization using a 51-mer biotinylated telomeric probe and visualized by chemiluminescence. **B** represents the principle for this analysis, as described in Materials and Methods.

3.4.3. Accumulation of single strand breaks in telomere regions

In an attempt to investigate why the telomere lengths of regrowing fibroblasts are substantially reduced compared to mock-treated control fibroblasts, telomere lengths of growth-arrested fibroblasts at different time points post PUVA treatment were determined. The strategy allows to study whether the long-term growth arrest itself could damage telomeres and, thus, led to telomere length reduction. As shown in Figure 30 lane 2 through lane 7, growth-arrested fibroblasts at different time points post PUVA treatment did not show any difference in telomere lengths when compared to each other. In addition no reduction was observed when compared to mock-treated control fibroblasts. However, PUVA-treated fibroblasts in their regrowing stage showed significantly shorter telomere lengths when compared to mock-treated control fibroblasts at comparable CPDs. Regarding these results, it should be noted that the above detected telomeres are double-stranded. The constant double-stranded telomere length does not necessarily mean that the telomere is intact and not damaged. Possibly, single strand breaks (SSBs) were generated in telomere region during growth arrest stage which, if not repaired, would result in telomere loss during DNA replication and cell division after fibroblasts start to regrow. To analyze whether single strand breaks are formed in the telomere region, the terminal restriction fragments (TRF) of the same batches used for double-stranded telomere length determination were denatured before being subjected to electrophoresis. As shown in Figure 30 Lane 10 to 14, a clear reduction in the lengths of single-stranded telomeres of growth-arrested fibroblasts at different time points post PUVA treatment was found with time after PUVA treatment. In fibroblasts at 11 weeks post PUVA treatment, single-stranded telomere length was comparable to that of regrowing fibroblasts at an early passage (CPD 20.9), while their double-stranded telomere lengths were significantly different (Lane 6 and 7). Thus, single strand DNA breaks did form in the telomere region and most likely are responsible for the significant telomere length reduction in regrowing fibroblasts post PUVA treatment. Notably in growth-arrested fibroblasts at 1 day post PUVA treatment, the mean of the single-stranded TRF length (Lane 10) is even increased when compared to that of mock-treated fibroblasts (Lane 9). This might suggest that psoralen-DNA interstrand cross-links were also formed in the telomere region.

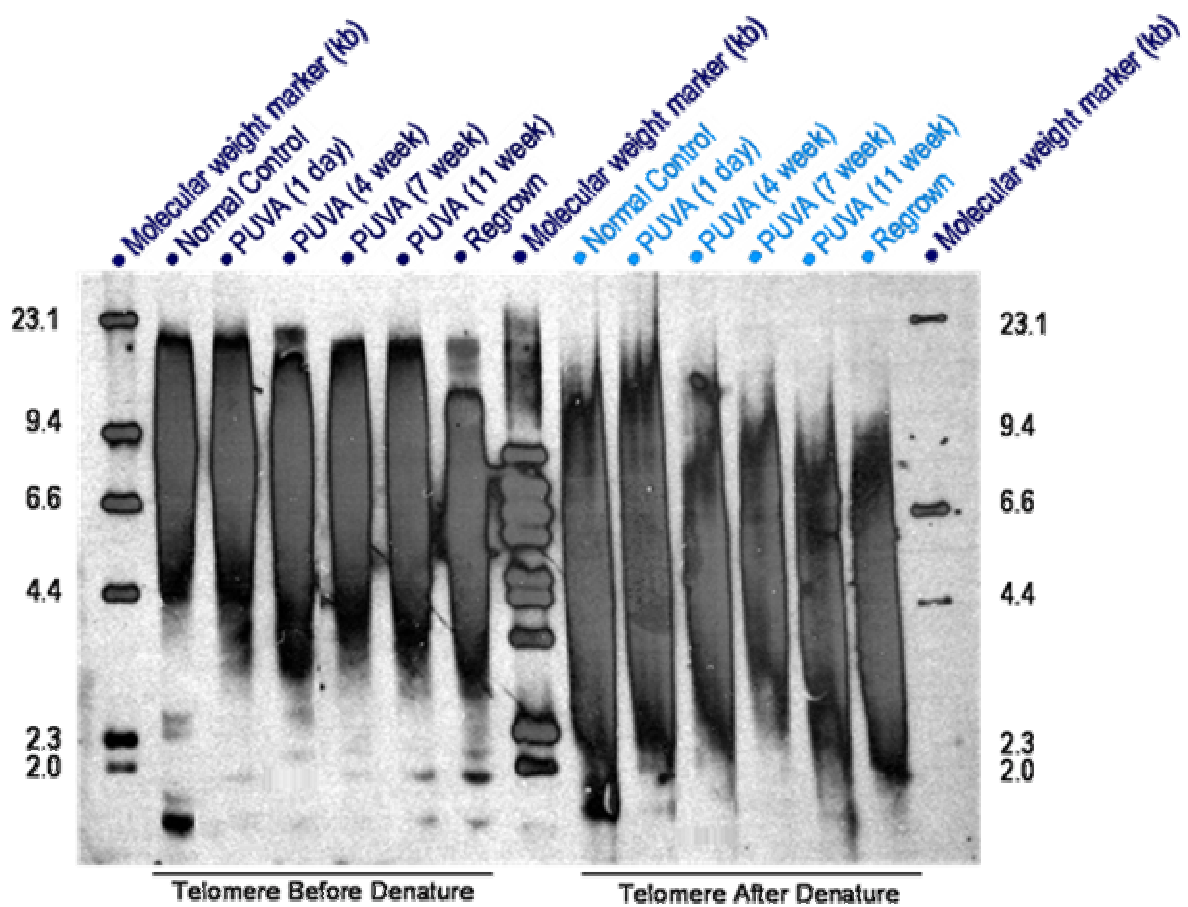


Figure 30. Double-stranded telomere lengths are constant throughout the growth arrest stage post PUVA treatment while single-stranded telomere lengths are clearly decreasing with time. The same strain of fibroblasts (FF95, P9, CPD=22) were PUVA-treated as indicated in Materials and Methods and genomic DNA was collected at different time points post PUVA treatment. Ten μg DNA of each sample was digested first with *HinfI/RsaI*. Half of the sample (20 μl , 5 μg DNA) was treated with alkaline buffer (0.4M NaOH, 4 mM EDTA) for 5-10 min to separate DNA double strands, and subjected to electrophoresis and Southern blot analysis as described in Materials and Methods. The other half of the samples which had not been denatured allowed to study telomere length of double-strand DNA.

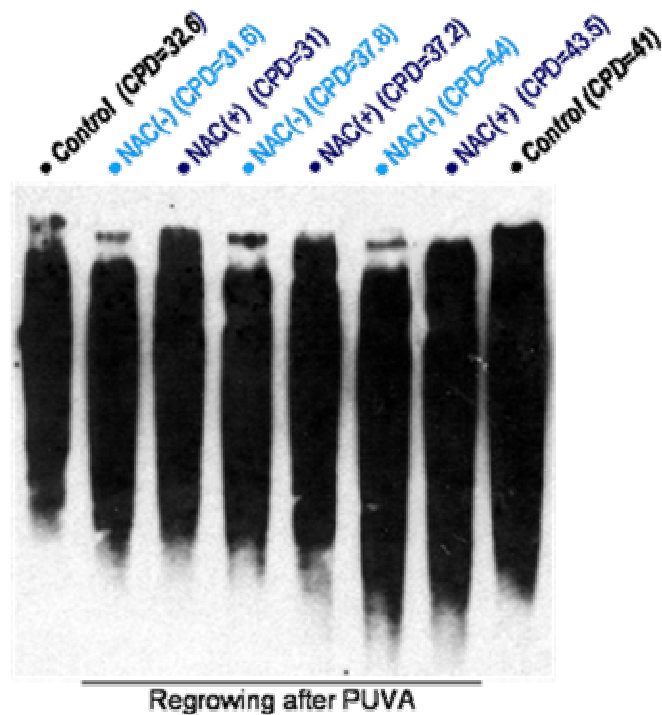


Figure 31. Supplementation with N-acetyl cystein (NAC) during the growth arrest stage after PUVA treatment protects telomeres from length reduction. NAC was supplemented during the growth arrest stage at a concentration of 5 mM and the medium was changed every three days to ensure an efficient antioxidant capacity. Thereafter genomic DNA of regrowing PUVA-treated fibroblasts with NAC supplementation (PUVA-NAC(+)) and without NAC supplementation (PUVA-NAC(-)) were collected at comparable CPD. Telomere lengths (TRF) were determined as described in Materials and Methods. Briefly, 5 μ g of *HinfI/RsaI*-digested DNA of each sample was subjected to electrophoresis with 0.6% agarose gels followed by Southern blot hybridisation using a 51-mer biotinylated telomeric probe and visualized by chemiluminescence.

3.4.4. Scavenging of reactive oxygen species by N-acetyl cystein rescues telomere length

Since ROS are produced in human dermal fibroblasts after PUVA treatment and increase with time, the question arises whether ROS are involved in and contribute to telomere length reduction. The causal role of ROS on telomere length reduction was investigated by scavenging ROS accumulation with N-acetyl-L-cysteine (NAC) in PUVA-treated fibroblasts during the growth arrest stage. Thereafter telomere length of fibroblasts in their regrowing phase was compared to that of identically PUVA-treated fibroblasts without exposure to NAC. NAC is a reduced glutathione (GSH) provider and a direct scavenger of ROS (Staal *et al.* 1990). As shown in Figure 26, with continuous supplementation of NAC, ROS levels in PUVA-treated fibroblasts were evidently decreased compared with mock-treated control fibroblasts. However, even with the decreased ROS level, PUVA-treated fibroblasts did not start to regrow at an earlier time point post PUVA treatment when compared to PUVA-treated fibroblasts without NAC. To explore whether ROS are involved in telomere reduction mediated by PUVA treatment, in their regrowing phase genomic DNA from regrowing PUVA-treated fibroblasts which had been cultivated in the presence of NAC (PUVA-NAC(+)) and in the absence of NAC (PUVA-NAC(-)) were collected at comparable CPDs and telomere lengths were determined. As shown in Figure 31, lane 3, 5 and 7 represent the TRF of PUVA-NAC(+) fibroblasts. Compared to the TRF lengths of PUVA-NAC(-) fibroblasts (lane 2, 4 and 6), the telomere lengths in PUVA-NAC(+) fibroblasts were visibly longer as judged by the median of the TRF lengths.

3.4.5. Partial restoration of the total life-span of PUVA-treated fibroblasts in the presence of N-acetyl cystein

Since telomere length in PUVA-NAC(+) fibroblasts was well protected compared to PUVA-NAC(-) fibroblasts, it was studied whether this would rescue the total life span, which had been shown to be substantially reduced in PUVA-treated fibroblasts in their regrowing phase (Figure 9). Therefore, total CPD of PUVA-NAC(+) fibroblasts in their regrowing phase were determined before reaching the replicative stage and compared with PUVA-NAC(-) fibroblasts as well as with mock-treated control fibroblasts. As shown in Figure 32, starting from CPD 21,

fibroblasts of the different experimental groups were cultured for over 300 days until reaching the replicative senescence stage where CPDs did not increase any more. Compared to PUVA-NAC(-) fibroblasts which reached replicative senescence at a CPD of 64.2, PUVA-NAC(+) fibroblasts showed 6 PDs more with a final CPD of 70. Compared to the total life-span of mock-treated fibroblasts with a total CPD of 73.9, the life-span of PUVA-NAC(+) fibroblasts was still not fully restored.

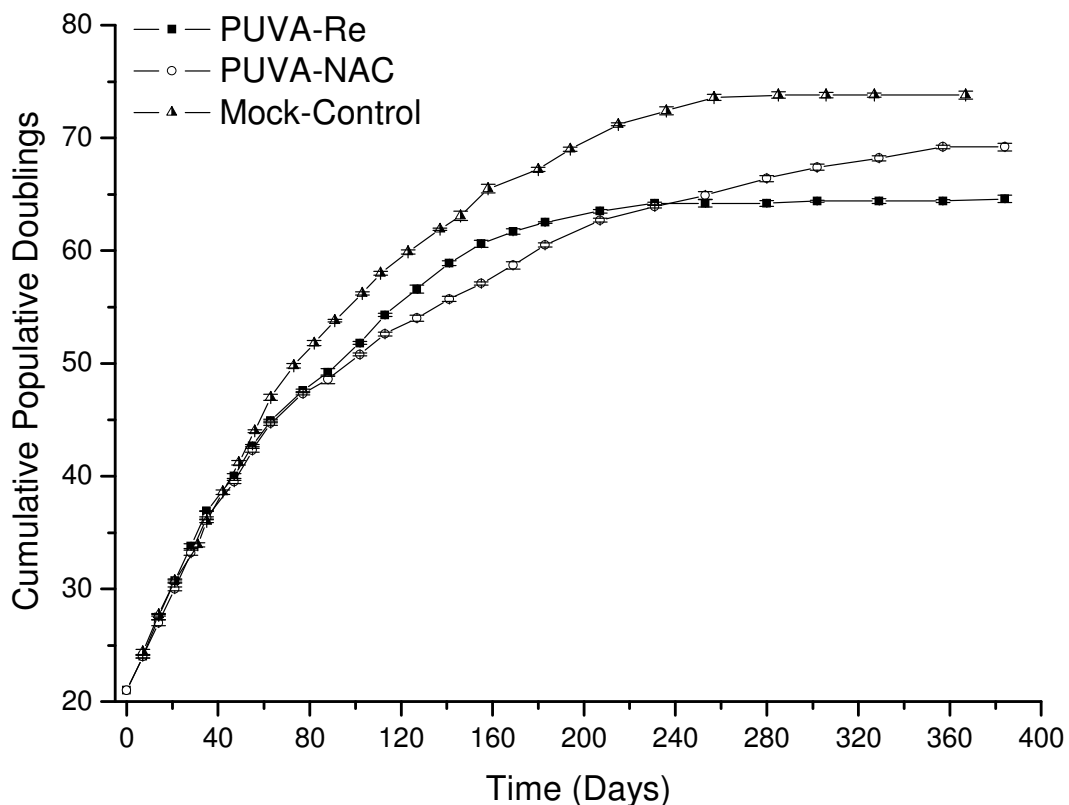


Figure 32. N-acetyl cystein (NAC) supplementation during the PUVA-induced growth arrest stage extended the life-span of PUVA-treated fibroblasts in their regrowing phase. Starting from the same CPD, mock-treated control fibroblasts (triangle), regrowing fibroblasts which had been treated with NAC (open circle) during the growth arrest stage and regrowing fibroblasts without NAC treatment (square), were passaged for more than 9 months until reaching the replicative senescent stage with no increases in population doubling. At each passage, cell numbers were determined in triplicates for each group and equal cell numbers (2×10^5) were transferred to a new tissue plate for further observation. Results were expressed as mean with standard deviation.

3.4.6. Up-regulated expression of p16^{INK4a} is maintained in regrowing fibroblasts post PUVA treatment

Beside telomere length reduction, an upregulated though low p16^{INK4a} expression, which might be involved and contribute to the early onset of replicative senescence of PUVA-treated fibroblasts in their regrowing phase was observed. As shown before in Figure 16 (see page 57), p16^{INK4a} expression was enhanced one week post PUVA treatment and maintained during the whole growth arrest stage. In contrast to p53 and p21^{Cip1}, which were initially also upregulated after PUVA treatment but completely returned to base levels of mock-treated control fibroblasts in regrowing fibroblasts (Figure 14 and Figure 15), p16^{INK4a} was still expressed at a higher level when compared to mock-treated control fibroblasts.

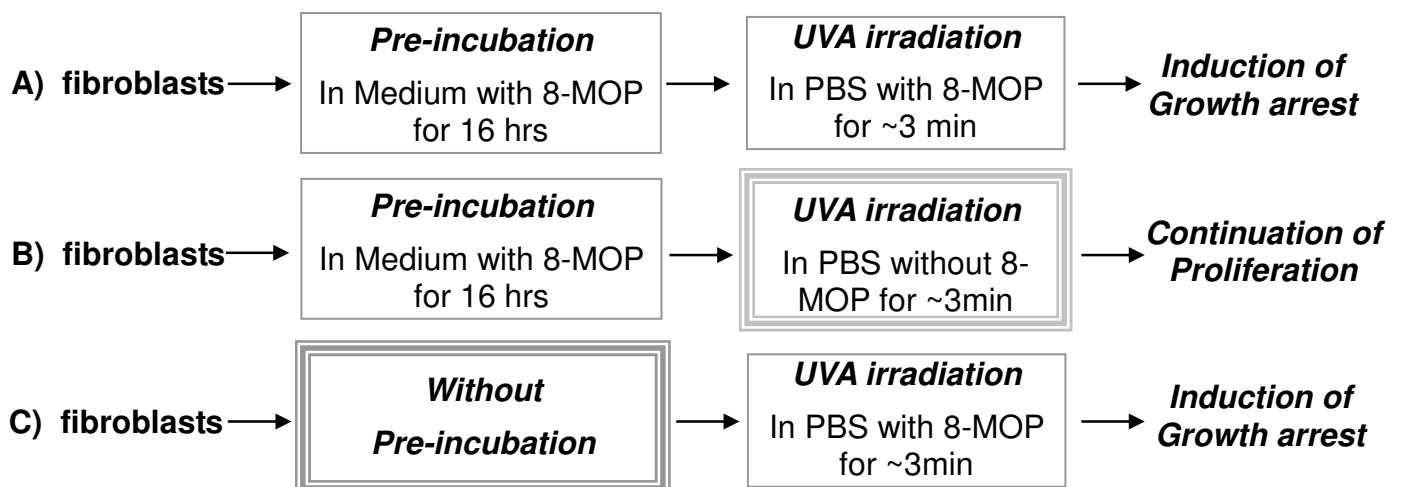
In summary, the results show that even though PUVA-treated fibroblasts could escape from long-term growth arrest after PUVA treatment, a recollection of the PUVA-damage contribute to the earlier occurring replicative senescence state when compared to control fibroblasts. The reduced total life-span in PUVA-treated fibroblasts is due to oxidative stress-induced telomere reduction as the abrogation of ROS production by the antioxidant NAC convincingly rescues telomere length reduction and partly restores total life-span of PUVA-treated fibroblasts in their regrowing phase comparable to that of mock-treated control fibroblasts.

3.5. Characterization of molecular mechanisms involved in the induction of growth arrest in PUVA-treated fibroblasts

3.5.1. Short-term incubation with 8-MOP during UVA-irradiation does result in growth arrest while long-term preincubation with 8-MOP does not

In accordance with the clinical PUVA regimen, where psoralen is ingested prior to UVA irradiation, the herein reported PUVA treatment of fibroblasts represents a two-step process as well. Fibroblasts are initially incubated with 8-MOP in the dark for 16 hours and thereafter cells were subjected to UVA irradiation in PBS containing the same concentration of 8-MOP. The irradiation time was 2-3 minutes depending on the UVA intensity. It was observed that the long pre-incubation of 8-MOP is not required for the induction of growth arrest. As shown in Table 4B, 16 hours pre-incubation with 8-MOP and subsequent UVA irradiation in PBS without 8-MOP (8-MOP-PRE) did not lead to growth arrest. By contrast, omitting the pre-incubation step, while fibroblasts were UVA irradiated for 3 minutes in PBS containing 8-MOP (8-MOP-UV) led to growth arrest. This result is intriguing since it was generally hypothesized that the proliferation inhibiting effect after PUVA treatment is due to psoralen-DNA interstrand crosslinks (ICLs). However, 3 minutes of 8-MOP incubation with fibroblasts during UVA irradiation may not be as sufficient to lead to the formation of interstrand DNA crosslinks as the long preincubation regimen with 8-MOP.

Table 4 Different regimens in PUVA treatment procedure lead to different results



3.5.2. The number of DNA interstrand crosslinks is not related to growth arrest

We first determined the numbers of ICLs in 8-MOP-Pre and 8-MOP-UV cells. For this purpose, genomic DNA isolated from differently treated fibroblasts was digested first with certain restriction enzymes and then subjected to alkaline gel electrophoresis. As described in Material and Methods, this technique was used to determine and compare crosslink numbers by the degree of retardation of DNA fragments after electrophoresis. DNA double strands cannot be separated by alkaline denaturation if psoralen-DNA ICLs are present, and this will result in a retarded DNA fragment pattern after electrophoresis compared to DNA without ICLs. Figure 33B reveals the electrophoresis pattern of DNA from differently treated fibroblasts after combined restriction digestion with Hae II and Nde I. Both restriction enzymes are 6-base pair frequency cutters recognizing sequences within which psoralen-DNA ICL could be potentially formed. All DNA was isolated immediately after treatment. Lane 2 of Figure 33B shows DNA isolated from mock-treated fibroblasts serving as control to show the standard DNA pattern after restriction and denaturation. Lane 3 represents the DNA pattern of fibroblasts when 8-MOP was present both during pre-incubation and UVA irradiation. Compared to mock-treated fibroblasts (Lane 2), more of the large DNA fragments were found in lane 3 indicating a high amount of ICLs formed after PUVA treatment. Lane 4 represents the DNA fragments distribution of fibroblasts which had been preincubated with 8-MOP and UVA-irradiated in the absence of 8-MOP (8-MOP-PRE). A similar pattern as PUVA-treated fibroblasts where 8-MOP was present both in preincubation and UVA-irradiation step (PUVA-1h) suggesting that ICL amounts under both conditions are similar. Lane 5 represents the DNA fragment pattern of fibroblasts which had been exposed to 8-MOP only during UVA irradiation (8-MOP-UV), large DNA fragments were substantially less than those in lane 3 and lane 4 suggesting reduced ICL formation under this condition. A similar DNA fragment pattern was found when using a single restriction enzyme for digestion as shown in Figure 33C. This experiment clearly shows that PUVA-treated fibroblasts when 8-MOP is present only during the preincubation step (8-MOP-PRE) resulted in the same amounts of ICLs as that in PUVA-treated fibroblasts when 8-MOP is present in both steps

(PUVA-1h), while fibroblasts with 8-MOP present only during the UVA irradiation step (8-MOP-UV) had a substantially lower amount of ICLs.

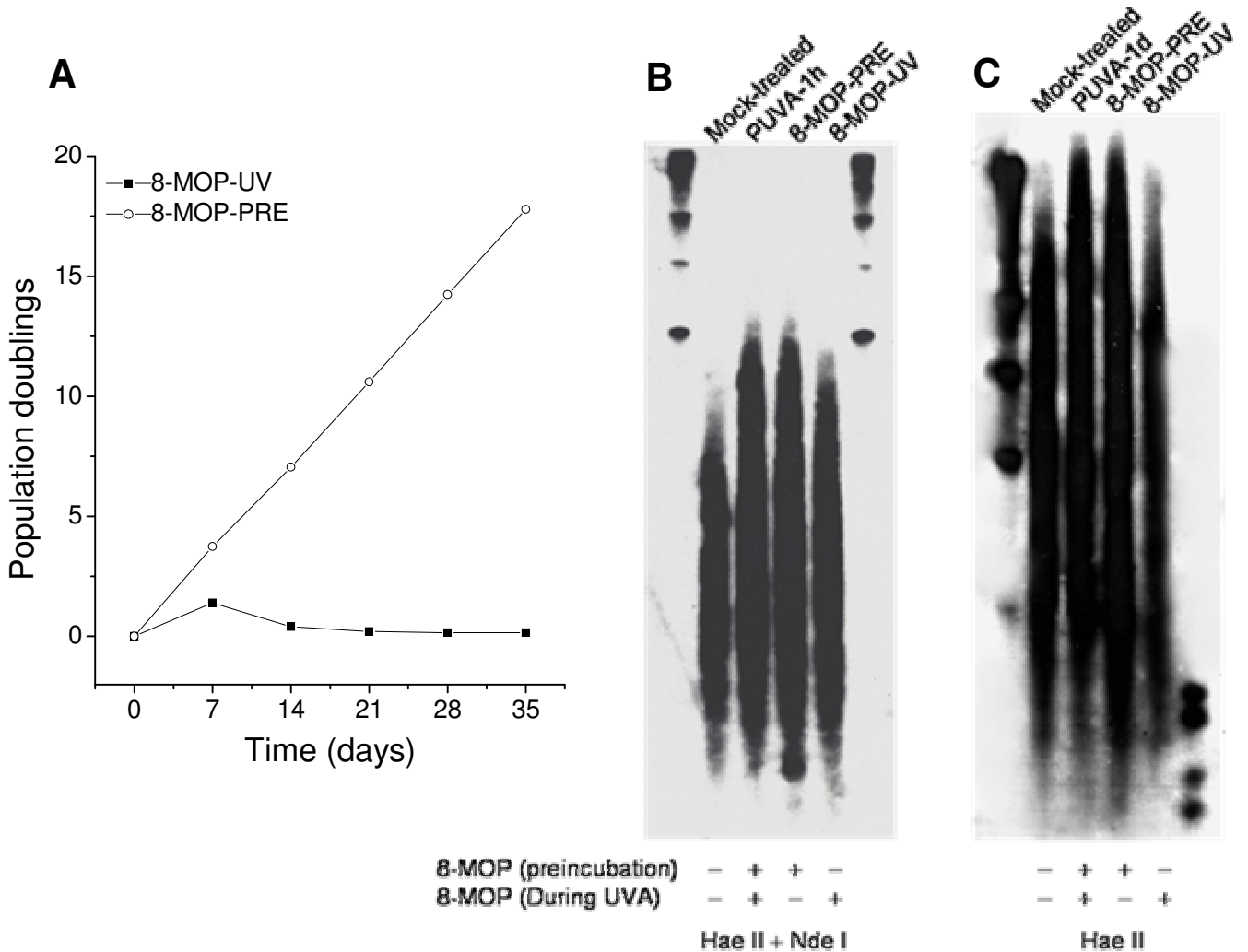


Figure 33. Determination of DNA interstrand crosslinks (ICL) and growth status of fibroblasts after different regimen of PUVA treatment. A, The growth curve of PUVA-treated fibroblasts with 8-MOP exclusively present during pre-incubation (8-MOP-PRE) or only during UVA irradiation (8-MOP-UV). B and C, ICL determination was performed by alkaline electrophoresis as described in Materials and Methods. Briefly, genomic DNA was isolated from mock-treated fibroblasts, PUVA-treated fibroblasts immediately after treatment (PUVA-1h), 8-MOP-PRE fibroblasts and 8-MOP-UV fibroblasts immediately after treatment. Thereafter DNA was digested with Hae II and Nde I, or Hae II only and subjected to alkaline gel electrophoresis.

Taken together, fibroblasts with 8-MOP present only during UVA irradiation step (8-MOP-UV) were growth-arrested, while fibroblasts with 8-MOP present only during preincubation step (MOP-PRE) were still proliferating (Figure 33A). This observation contradicts the traditional view that DNA interstrand cross-links are the exclusive reason responsible for proliferation inhibiting effects of PUVA.

3.5.3. Characterization of the contribution of changes in the karyoplast and the cytoplasm post PUVA treatment to PUVA-induced growth arrest

To further investigate what mechanism may initiate the long-term senescence-like growth arrest after PUVA treatment with particular interest on whether it was exclusively due to DNA damage in the nucleus or whether other targets located in the cytoplasm may be involved, cell fusion experiments were performed as follows: Cytoplasts (enucleated cells) of PUVA-treated fibroblasts were separated and fused with karyoplasts (minicells) of untreated primary fibroblasts. Vice versa the karyoplasts of PUVA-treated fibroblasts were fused to the cytoplasts of untreated primary fibroblasts. The behavior of these newly constructed fibroblasts should allow getting more insight in the targets of PUVA treatment (cytoplasm or nucleus or both) responsible for the long-term growth arrest.

3.5.3.1. Rationale for fusion of cytoplasts and karyoplasts

The development of efficient methods to enucleate mammalian cells in order to obtain cytoplasts and karyoplasts was the first step for cell fusion. Previous work of cytogeneticists had developed methods for enucleation of cells with cytochalasin B, an inhibitor of microfilament-assembly. The underlying mechanism is that the cytoskeleton of the cell can be altered with the formation of very soft cellular membranes. In addition cytochalasin B inhibits cytokinesis and, thus, the chromosomes are more compacted making it easier to remove the nucleus with only a minimal volume of cytoplasm (Shay 1987; Veomett 1982). High speed centrifugation with a Ficoll gradient was employed to facilitate enucleation and separation of different cellular components. Fusion of cytoplasts and karyoplasts was promoted by the addition of Polyethylene glycol (PEG) with a so far not fully clarified mechanism.

3.5.3.2. Experimental design for the identification of fused fibroblasts

The techniques for isolation of cytoplasts and karyoplasts yield fractions which are contaminated considerably with non-enucleated cells. The use of these contaminated fractions for fusion may give rise to difficulties in the interpretation of the results. Thus, the development of appropriate selection markers is a critical step to isolate and interpret specific fusion. Here four selection markers were used: neomycin resistance, GFP expression, Hoechst 33342 and latex beads. The experimental design is shown in Figure 34. Fibroblasts stably transfected with the nucleus-encoded neomycin resistance gene and the GFP-expression gene were PUVA-treated and used as supplier for PUVA-cytoplasts and PUVA-karyoplasts. Non-PUVA-treated fibroblasts were labeled with red-fluorescent latex beads which were located in the cytoplasm region. Two different hybrids were generated:

1. PUVA-cytoplasts fused with Mock-treated-karyoplasts
2. PUVA-karyoplasts fused with Mock-treated-cytoplasts

Although the separated karyoplasts were almost pure, the cytoplasm fraction was hardly free of contaminated non-enucleated fibroblasts. Thus, the following strategy was used as shown in Figure 34 and table 5. For fusion experiment 1: after enucleation, the PUVA-cytoplasm fraction was stained first with Hoechst 33342 before being fused with Mock-treated-karyoplasts. Hoechst 33342 is a cell membrane permeable DNA stain, which can be used for staining living cells in culture. This stain incorporates into DNA double strands and gives rise to blue fluorescence. After this procedure, all the contaminated non-enucleated fibroblasts were labeled, and could be identified by their blue-fluorescent nuclei. The intended fusions, thus, could be identified as non-fluorescent nuclei. The strategy for fusion experiment 2 is dependent on neomycin resistance, GFP expression, as well as the latex beads. Since PUVA-karyoplasts have the neomycin resistant gene, after fusing with Mock-treated-cytoplasts, fibroblasts are cultured in medium containing G418, thus all the contaminated non-enucleated normal fibroblasts will be killed while correctly fused fibroblasts will survive. The correct fusions are further identified by green fluorescence due to the expression of the GFP gene located in PUVA-karyoplasts and red fluorescence of latex beads in Mock-treated-cytoplasts.

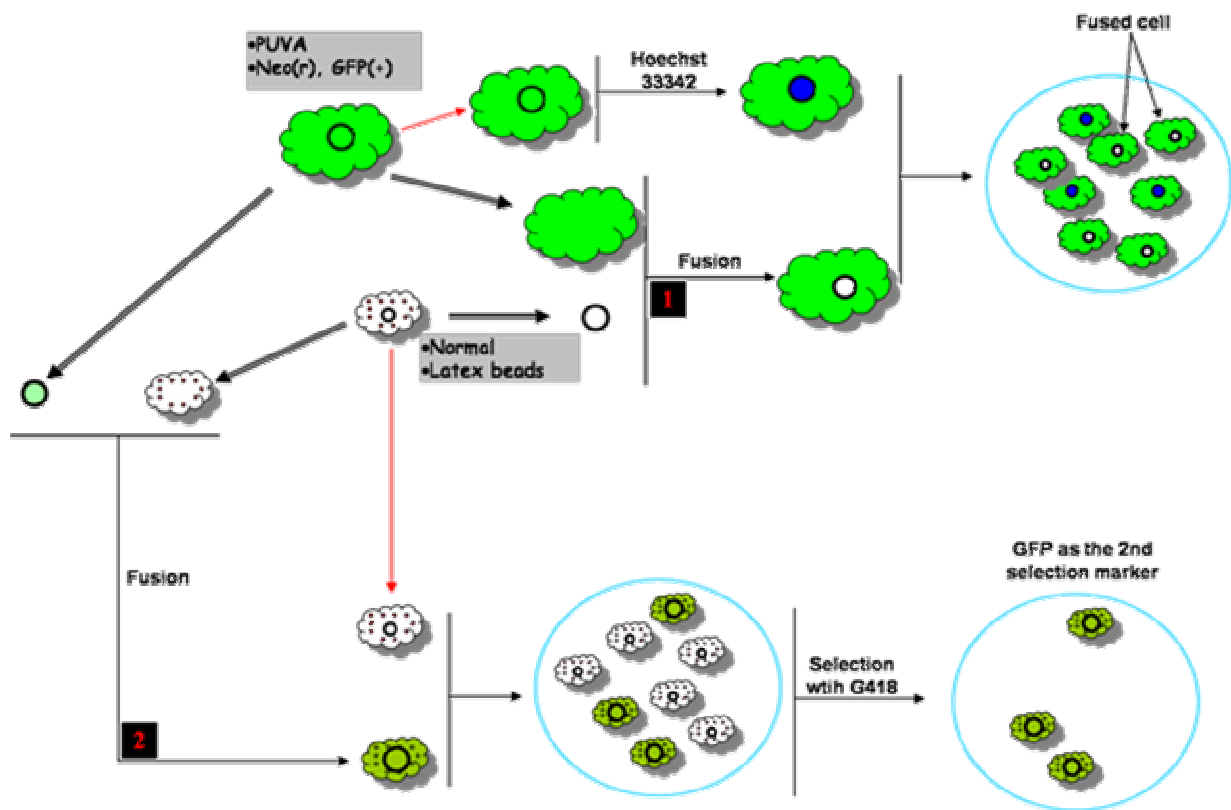


Figure 34. Scheme for selection and identification of fusions. Fibroblasts stably transfected with neomycin resistant gene (*Neo(r)*) and GFP (*GFP(+)*) gene were PUVA-treated. Non-PUVA-treated fibroblasts were labeled with red-fluorescent latex beads which are located in the cytoplasm region. Two different hybrids were generated: 1) PUVA-cytoplasts fused with Mock-treated-karyoplasts, 2) PUVA-karyoplasts fused with Mock-treated-cytoplasts. For the first hybrids, the PUVA-cytoplasm fraction was stained first with Hoechst 33342 after enucleation and before fusing with Mock-treated-karyoplasts to identify the contaminating non-enucleated PUVA-treated fibroblasts. The intended fusions could thus be identified as revealing non-fluorescent nuclei. For the second hybrid, separated PUVA-karyoplasts have *neo(r)* and *GFP (+)* genes. After fusing with Mock-treated-cytoplasts, fibroblasts are cultured in medium containing G418. Thus, all the contaminating non-enucleated normal fibroblasts will be killed, while fusions will be left. The correct fusions are further identified by green fluorescence due to the expression of GFP gene located in PUVA-karyoplasts and red fluorescence of latex beads in Mock-treated-cytoplasts.

Table 5 Selection and identification of fusions

| Fusion experiments | Cell types after fusion | GFP | Neo ^r | Latex beads | Hoechst |
|--------------------|--------------------------------|------------|------------------|-------------|---------|
| $K^p \times C^n$ | $K^p C^n$ (intended fusion) | + | + | + | n.u |
| | $K^n C^n$ (Contamination) | - | - | + | n.u |
| | K^p, C^n | Not stable | | | |
| $K^n \times C^p$ | $K^n C^p$ (intended fusion) | n.u | n.u | - | - |
| | $K^p C^p$ (Contamination) | n.u | n.u | - | + |
| | K^n, C^p | Not stable | | | |

K^p: PUVA-karyoplast; Kⁿ: Normal-karyoplast; C^p: PUVA-cytoplast; Cⁿ: Normal-cytoplast. K^pCⁿ and KⁿC^p represent fusions with cytoplasts and karyoplasts being from different sources, while KⁿCⁿ and K^pC^p represent non-enucleated whole cells contained in the cytoplast fraction. n.u: not used as a marker in this experiment.

3.5.3.3. Fusions of cytoplast/karyoplasts of fibroblasts immediately or at an early stage post PUVA with mock-treated karyoplasts/cytoplasts

We initially used fibroblasts immediately post PUVA treatment for the cell fusion experiments, as PUVA-induced damages will be repaired with time after PUVA treatment. After fusing with mock-treated karyoplasts or cytoplasts, a striking cell death was observed within the first 3 days with cells, including non-fused cytoplasts, being detached from bottom of culture dishes (data not shown). No fusions had been identified in fibroblasts which survived as detected by GFP fluorescence or Hoechst staining. A conclusive explanation might be that both cytoplasm and nuclear components are substantially damaged and can not survive the new stresses generated during fusion process. Based on these results, PUVA-treated fibroblasts at later time points after PUVA treatment were

used for fusion. Experiments with PUVA-treated fibroblasts taken within the first week after PUVA treatment (at day 1 or at 1 week after PUVA treatment) were studied without yielding stable fusions. Similar to the above results, substantial cell death occurred within the first 3 to 5 days after fusion. Thereafter, no cells could be positively recognized as intended fusions, neither by GFP fluorescence (for fusions of PUVA-karyoplasts and Mock-treated-cytoplasts) nor by Hoechst staining (for fusions of PUVA-cytoplasts and Mock-treated-karyoplasts). Fusions of PUVA-karyoplasts and Mock-treated-cytoplasts did not successfully occur as no cells were found to be green-fluorescent (GFP expression) even in the first three days after fusion when fibroblasts were still viable. For fusions of PUVA-cytoplasts with Mock-treated-karyoplasts, there were some cells that did not show Hoechst-stained nuclei at the first day after fusion which might represent the intended fusions. However, no intended fusions were observed after 3 days.

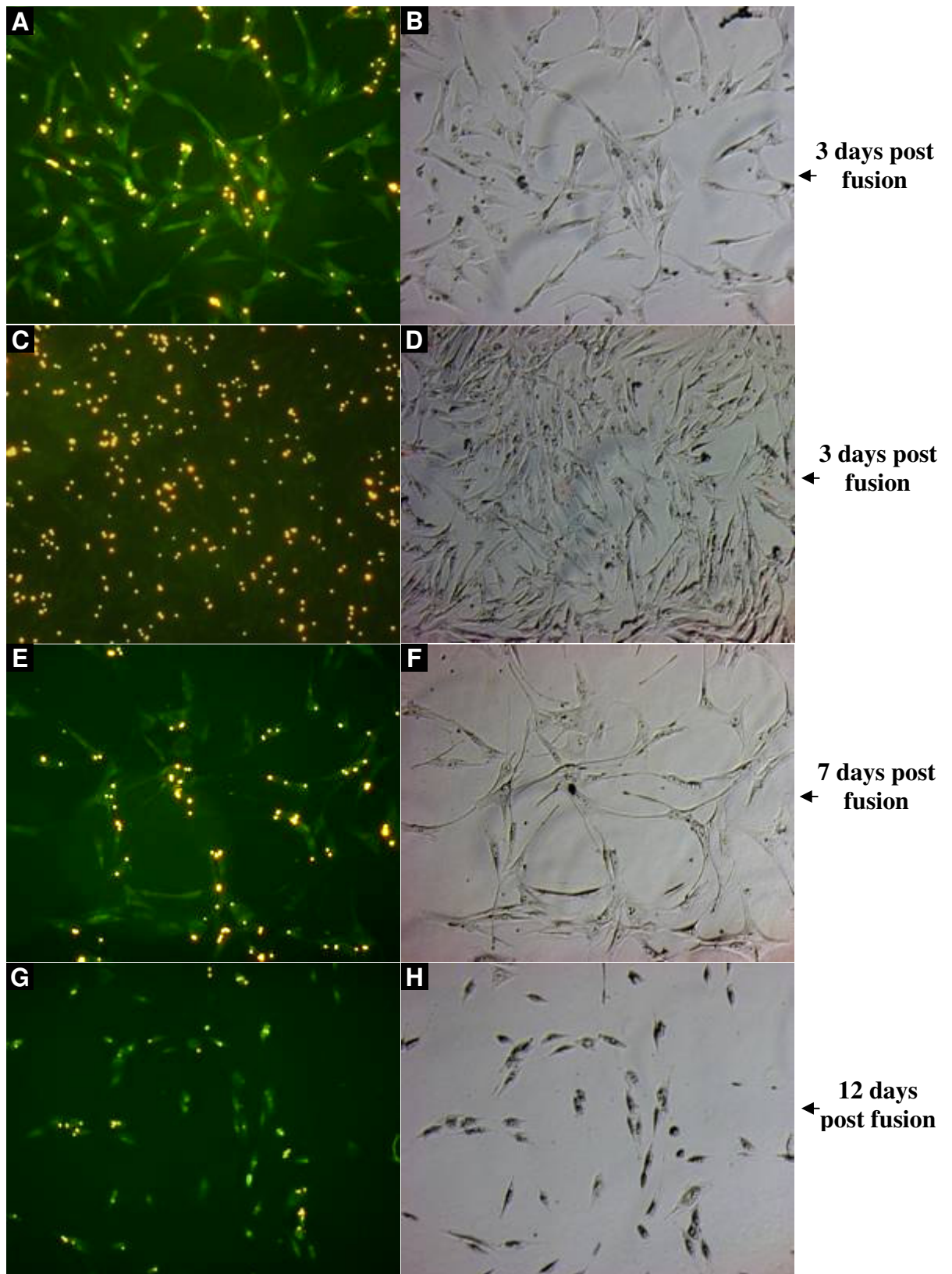
3.5.3.4. Fusions of cytoplast/karyoplasts of fibroblasts 2 weeks or 4 weeks post PUVA treatment with mock-treated karyoplasts/cytoplasts

Fibroblasts at 2 and 4 week post PUVA treatment were used for cell fusion experiments. The number of dead cells was reduced after fusion and stably fused cells were observed in fusions both between PUVA-karyoplasts and Mock-treated-cytoplasts as well as between PUVA-cytoplasts and Mock-treated-karyoplasts, respectively.

For fusions between PUVA-karyoplasts and Mock-treated-cytoplasts, the successfully fused cells were identified by latex beads and GFP expression. Figure 35 shows changes of fusions with time after fusion using PUVA-treated fibroblasts 2 weeks post PUVA treatment. As shown in Figure 35A, green-fluorescent cells with yellowish-red-fluorescent cytoplasmic latex beads, which represent intended fusions, could be observed 2-3 days after fusion. At the same time point, contaminated non-enucleated normal fibroblasts, which reveals cytoplasmic latex beads but had no green-fluorescence, were also observed in another region of the same dish (Figure 35C). These cells should be eliminated by G418 supplemented in medium due to lack of the neomycin resistance gene, though they may still be able to proliferate at the beginning. Fused cells appear morphologically to proliferate instead of being growth-arrested within the first

three days after fusion as green-fluorescent cells were cluster-like (Figure 35A and B). However, compared with those contaminated fibroblasts which revealed only red latex beads but no green fluorescence, the proliferation rate is lower as judged by the density of cell clusters (Figure 35B and D). Thereafter, numbers of dead cells increased with time, most probably due to the toxicity of G418 to the contaminating non-fused mock-treated fibroblasts. Fused fibroblasts are still stable at 7 days after fusion, and cell numbers didn't show any increase or decrease (Figure 35E and F). This might suggest that cell proliferation was stopped. Fusions of PUVA-treated karyoplasts with mock-treated cytoplasts were not stable for a longer time. These fused cells died off gradually after 12-14 days (Figure 35G and H). When using PUVA-treated fibroblasts 4 weeks post PUVA treatment for cell fusion, a similar cellular changing process was observed: fused fibroblasts with GFP green fluorescence and cytoplasmic red latex beads could be identified 3 days after fusion. However, fused fibroblasts were still not stable, and died off at around 15-17 days after fusion, though they apparently live longer compared to fusions with PUVA-2w cytoplasts (12-14 days).

Figure 35. Cell fusions between PUVA-karyoplasts from fibroblasts two weeks post PUVA treatment and Mock-treated-cytoplasts. A shows a power field of the Petri-dish with fused cells 3 days post fusion, where cells reveal green fluorescence and the yellowish-red fluorescence of latex beads indicating that a successful fusion between PUVA-karyoplasts and Mock-treated-cytoplasts has occurred. C shows another high power field of the same dish where cells reveal only latex beads without green fluorescence indicating that they are contaminating non-PUVA-treated fibroblasts. E represents cell hybrids 7 days post fusion which reveal green fluorescence and yellowish-red fluorescence of latex beads. G represents cell hybrids 12 days post fusion which reveal green fluorescence and the yellowish-red fluorescence of latex beads. B, D, F, H are the phase contrast photographs taken of the same power fields as in A, C, E, G, respectively. Photographs were taken at a magnification of $\times 100$.

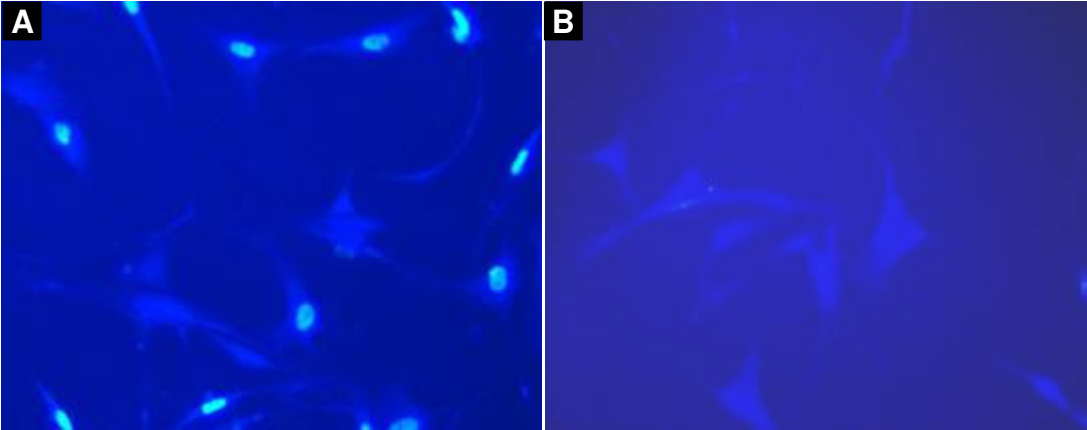


For fusions between PUVA-cytoplasts and Mock-treated-karyoplasts, fused cells did not show any proliferation at 1 week after fusion. Figure 36A and B represent fusions between PUVA-cytoplasts at 2 weeks post PUVA treatment and Mock-

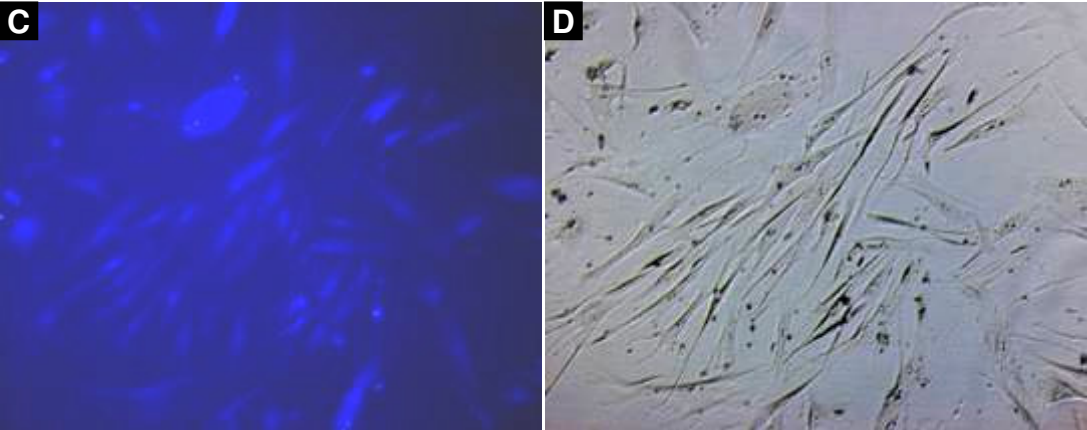
treated-karyoplasts. All non-enucleated contaminations in the PUVA-cytoplasm fraction are identified as pre-labeled with Hoechst 33342 before fusion as described above and, thus, reveal the bright blue nuclear fluorescence. The normal-karyoplast fraction was pure after separation. Figure 36A and B show cells 3 days post fusion. Part A represents an area where contaminated cells were found which reveal Hoechst-stained nuclei, and part B shows an area with mainly fused fibroblasts which do not reveal Hoechst-stained nuclei. Interestingly, the intended fusions of PUVA-cytoplasts with Mock-treated-karyoplasts did not reveal a growth arrest as long as found in PUVA-treated fibroblasts. When using PUVA-2w cytoplasts for fusions, re-proliferation of cells could be observed 26 days after fusion, as shown in Fig 17 C and D. Re-proliferation of cells could be observed even earlier when using PUVA-4w cytoplasts, which took only 12 days, as shown in Figure 36 E and F. These results indicate that cytoplasm changes could affect cell growth. However, PUVA-dependent cytoplasm changes were temporal and shorter-termed compared to PUVA-treated fibroblasts suggesting that apart from cytoplasmic damage other additional mechanisms are responsible for the long-term growth arrest.

Figure 36. Cell fusions between PUVA-cytoplasts and Mock-treated-karyoplasts. Panel 1) represent fusions between Mock-treated-karyoplasts and PUVA-cytoplasts derived from PUVA-treated fibroblasts two weeks post PUVA treatment. A and B represent fibroblasts 3 days post fusion. A shows an area with contamination of non-enucleated PUVA-treated fibroblasts as indicated by the Hoechst stained nuclei. B shows mainly successful fusions between PUVA-cytoplasts and Mock-treated-karyoplasts as only the cytoplasmic fluorescence is evident with no Hoechst stained nuclei. C and D represent the same cells 26 days post fusion, D was the phase contrast photograph of C. E and F were fusions using PUVA-cytoplasts from fibroblasts 4 weeks post PUVA; 12 days post fusion, many cells start to proliferate. Photographs were taken at a magnification of $\times 100$.

1) PUVA-cytoplasts (2 weeks post PUVA treatment) fused with Mock-treated-karyoplasts

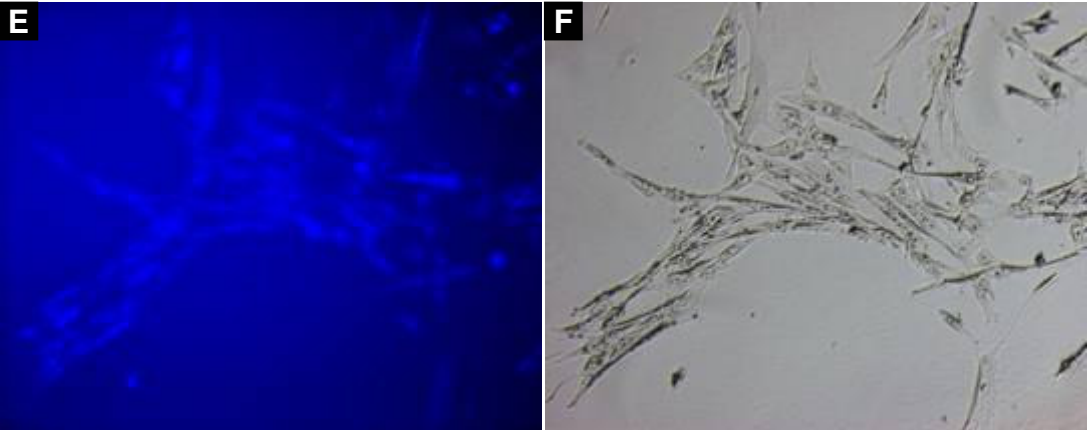


3 days post fusion



26 days post fusion

2) PUVA-cytoplasts (4 weeks post PUVA treatment) fused with Mock-treated-karyoplasts
12 days after fusion



In summary, herein it is shown that the number of psoralen-DNA interstrand crosslinks does not correlate with the long-term growth arrest. When reconstructing cells by fusing PUVA-cytoplasts with mock-treated karyoplasts, it is found that these cell hybrids start to regrow earlier after PUVA treatment. The reconstructed cells with PUVA-karyoplasts and non-PUVA-treated cytoplasts, however, can not survive for longer than 18 days, making it difficult to finally evaluate the overall effects of PUVA-induced nuclear damage for the maintenance of the growth arrest.

4 DISCUSSION

4.1. The escape of human dermal fibroblasts from PUVA-induced senescence-like growth arrest is not due to immortalization or transformation

The data shown in this thesis demonstrate that PUVA-induced long-term growth arrest, although with some functional and morphological changes reminiscent of cellular senescence, is reversible between day 90 to 120 post PUVA treatment. The capacity of PUVA-treated fibroblasts to regrow after long-term growth arrest is neither due to immortalization nor transformation. This finding further strengthens the view that PUVA-induced changes are indeed a transient phenocopy of senescence.

Immortalization and transformation have been reported to be critical for regrowth of senescent cells. At least, introduction of oncogenic Ras with subsequently enhanced intracellular ROS levels provokes premature senescence in murine and human fibroblasts (Lee *et al.* 1999; Serrano *et al.* 1997). Additional inactivation of either p53 or p16^{INK4a} in rodent cells and E1A in human cells reversed this Ras-induced growth arrest suggesting that prematurely enhanced senescence can be effectively reversed by disrupting important cell cycle regulating proteins. Regrowth of senescent cells has also been described in fibroblasts double-deficient for p53 and BRCA1, the latter being involved in the control of the G₂ phase of the cell cycle. These fibroblasts adopt a senescent phenotype upon γ -irradiation, however, following continued cultivation they form distinct proliferative foci, which according to the authors are most likely due to additional mutations (Shen *et al.* 1998). In this thesis several lines of evidence are provided that regrowth of long-term growth-arrested PUVA-treated human dermal fibroblasts is neither due to transformation nor immortalization.

First, four independently tested regrowing fibroblast strains did not show anchorage-independent growth in the soft agar assay. By contrast, the transformed cell lines HT1080 and HeLa, which served as positive controls, formed growing colonies in the soft agar assay. Second, telomerase activity which is mainly responsible for the maintenance of the telomere length in

immortalized and transformed fibroblasts (Bryan *et al.* 1995; Kim *et al.* 1994), was not detected in regrowing fibroblasts post PUVA treatment. In accordance with this, telomere length of regrowing fibroblasts continuously shortens with increasing CPD. Third, in contrast to the unlimited growth of immortalized or transformed cells, regrowing fibroblasts in their proliferative phase post PUVA treatment revealed a continuous decline in their proliferation rates with time. In addition, p53, p21^{cip1} and p16^{INK4a} genes, which were known to be the main players involved in both cellular senescence and other tumor suppressor mechanisms (e.g. apoptosis), did not show major mutations detectable by the applied PCR method in regrowing fibroblasts post PUVA. Thus, immortalization and transformation are not the reason for the resumed growth after PUVA-induced long-term senescence-like growth arrest.

Recently, the term stress-induced premature senescence (SIPS) has been introduced (Brack *et al.* 2000; Chen 2000; Toussaint *et al.* 2000b). Exposure of human fibroblasts to oxidative stress triggers a growth arrest state with appearance of several biomarkers for cellular senescence starting from 48 to 72 h after exposure to the respective stressors (Chen 2000; Toussaint *et al.* 2000b). Both chronic and acute oxidative stress protocols have been used to induce SIPS: continuous chronic stresses such as hyperoxia for several weeks, or short repeated discontinuous subcytotoxic stresses, with H₂O₂ or tert-butylhydroperoxide, followed by recovery periods of several days (Dumont *et al.* 2001).

Independent of the used protocols to induce oxidative stress, it was observed that there was no all-or-none response of cells, neither to chronic nor to acute oxidative stresses (Toussaint *et al.* 2000c). Under both protocols, senescent growth arrest occurred only in a certain fraction of cells though repeated stresses, with a stress every day or every two days, lead to an increased fraction of SIPS cells (Toussaint *et al.* 2000a). In the PUVA-treated fibroblasts, however, a more homogenous response of switching to a senescence-like long-term growth arrest was found. PUVA-treated fibroblasts without any exception revealed senescence-like features during the growth arrest stage, as evidenced by SA-β-gal expression with all fibroblasts being positive at 3-4 weeks post

PUVA treatment. No proliferating fibroblasts were found at least in the first 8 weeks post PUVA treatment as determined by BrdU incorporation. These data indicate that resumed growth was not due to the escape of rare non-senescence-like fibroblasts, which may have received no or less damage. However, the results do not necessarily mean that all treated fibroblasts recover from the growth-arrested stage at exactly the same time. Due to non-homogenous damages produced after PUVA in different fibroblasts and their expected different antioxidant and damage repair capacities, it is possible that some fibroblasts resumed growth earlier while others were still growth-arrested for an extended period. This prediction reflects exactly the data. The major finding, however, is that PUVA-induced senescence-like growth arrest is reversible and the earliest regrowth occurred at 90 days after PUVA treatment.

In summary, the herein reported data indicate that the long-term growth arrest following a single PUVA treatment, although sharing senescent markers currently used for the identification of replicative cellular senescence, is not identical to replicative senescence since the senescence-like growth arrest is still reversible. The regrowth post PUVA treatment is neither due to immortalization nor to transformation as a result of loss-of-function of tumor-suppressor genes involved in cellular senescence, such as p53, p21 and p16. The onset of regrowth is also not due to an escape mechanism of rare non-senescence-like fibroblasts which received no or less damage.

4.2. PUVA-induced growth arrest represents a phenocopy of senescence with ROS contributing to senescence-like phenotype changes

The observation that PUVA-treated fibroblasts were growth-arrested for longer than 90-120 days with biomarkers widely used for the identification of premature senescence with final regrowth makes it mandatory for re-evaluation of previously reported premature senescence models. In particular it is necessary to reconsider whether those models for stress-induced premature senescence are identical to replicative senescence in terms of irreversibility or whether they represent rather a “stress-induced mimic” of replicative cellular senescence. Thus, the important question is addressed whether senescence-like mechanisms

could be initiated in a non-senescence state and what mechanisms are involved and contribute to senescence-like features.

4.2.1. Senescence features in PUVA-induced long-term growth arrest are reversible

Established biomarkers of replicative cellular senescence also positive in SIPS and other premature senescence models include terminal growth arrest (Chen and Ames 1994; von Zglinicki *et al.* 1995), enlarged cell morphology (Chen and Ames 1994; Dumont *et al.* 2000), senescence associated β -galactosidase (Dumont *et al.* 2000), matrix metalloproteinase-1 (MMP-1) (reviewed in Campisi 2001b), accelerated shortening of telomere length (von Zglinicki *et al.* 1995), and lipofuscin accumulation (von Zglinicki *et al.* 1995). However, as these reported SIPS models have only been followed for several days or longest for a few weeks after the SIPS-inducing challenge, it is currently not clear whether the senescent-like growth arrest in these models is indeed irreversible as claimed by the authors.

Here it was found that fibroblasts, which escaped from growth arrest, had gone through phenotypic changes including senescent cell morphology and expression of SA- β -Gal. Interestingly, both senescent markers were reversible, and growth recovery after PUVA treatment was coupled with loss of all these senescence-like features. Besides morphological changes and SA- β -gal expression, another senescence-associated marker, matrix-metalloprotease-1(MMP-1), which was up-regulated for up to 90-110 days after PUVA treatment, also completely returned back to control levels in regrowing fibroblasts. The long-term induction of MMP-1, particularly if unbalanced by its inhibitor TIMP-1, will contribute to the degradation and disorganization of extracellular matrix proteins, like interstitial collagens and elastin, a hallmark in aging of the connective tissue (Kligman 1969; Scharffetter-Kochanek *et al.* 2000; Schwartz *et al.* 1993). The evident switch from the enlarged and SA- β -gal positive state to non-enlarged proliferating fibroblasts with loss of SA- β -gal as well as MMP-1 expression indicated that those currently accepted and used senescent markers, indeed, are not restricted to replicative cellular senescence.

4.2.2. Senescence controlling genes are up-regulated in PUVA-treated fibroblasts in a sequential and interrelated manner

To understand the mechanisms underlying PUVA-induced senescence-like growth arrest, the question is addressed whether it shares similar control pathways with mechanisms involved in replicative cellular senescence. Increasing evidence indicates that the molecular machinery that triggers and maintains the growth arrest of the senescent state is critically dependent on p53/p21^{Cip1} and Rb/p16^{INK4a} function (Shay *et al.* 1991b). Specifically, both p16^{INK4a} and p21^{Cip1} have been implicated in replicative cellular senescence (Brown *et al.* 1997; Noble *et al.* 1996). However, the manner in which it regulates the senescence machinery remains poorly understood. The data herein reveal that several cell cycle controlling proteins were upregulated in a sequential order. p53 and p21^{Cip1} seem to be involved in the initiation of the growth arrest, while p16^{INK4a} is most likely engaged in maintaining the long-term growth arrest.

p53 and p21^{Cip1} were concomitantly up-regulated after PUVA treatment. The tumor suppressor p53 is known to induce growth arrest or apoptosis in response to genotoxic stress. p53 levels transiently increase in oxidative stress or oncogenic Ras-induced premature senescence (Chen *et al.* 1998; Dimri *et al.* 2000; Serrano *et al.* 1997). Induction of p53 has been also observed in replicative senescence. p53 DNA binding and transcriptional activity were found to be increased several fold, although an increase in p53 protein or mRNA expression was not detected in replicative senescence (Atadja *et al.* 1995; Vaziri *et al.* 1997). In vivo, increased expression of p53 protein was observed in PUVA-treated skin sample (Hannuksela-Svahn *et al.* 1999; Zhao *et al.* 1999). One of the downstream target genes of p53 is p21^{Cip1}. p21^{Cip1} is an universal inhibitor of cyclin-dependent kinases, which can mediate both G1 and G2 arrest (Chen *et al.* 1995a; Harper *et al.* 1993; Macip *et al.* 2002). The importance of p21^{Cip1} and p53 in replicative senescence in vitro has been demonstrated in experiments blocking p21^{Cip1} and p53 expression in senescent cells (Bond *et al.* 1994; Gire and Wynford-Thomas 1998; Ma *et al.* 1999). As one of the major signal pathways characterized in replicative senescence, however, p53/p21^{Cip1} are unlikely to be the only pathway activated and responsible for the long-term senescence-like growth arrest induced by PUVA. This conclusion is related to the observation that

expression of p53 and p21^{Cip1} after initial up-regulation for 4 weeks returned to base levels. Thus, for maintaining the long-term growth arrest lasting for 3 months or even longer, other pathways have to be involved. One candidate could be p16^{INK4a}, which was induced 1 week after PUVA treatment and maintained a high expression level during the three months growth arrest stage. It has been postulated that high expression of p21^{Cip1} may be necessary for the entry into the arrest state, whereas p16^{INK4a} may be responsible for the maintenance of the senescent cell cycle arrest (Stein *et al.* 1999). The herein reported data are in good correlation to this model and the observations of other groups (Alcorta *et al.* 1996).

Although the expression of p16^{INK4a}, p21^{Cip1} and p53 has been investigated in different experimentally induced SIPS-models like 5-bromodeoxyuridine (Michishita *et al.* 1999), hydroxyurea (Yeo *et al.* 2000), hydrogen peroxide (Chen *et al.* 1998; Chien *et al.* 2000), histone deacetylase inhibitors (Ogryzko *et al.* 1996) or glucose-6-phosphate dehydrogenase deficiency (Ho *et al.* 2000), no uniform model for the role of these genes in the development of SIPS has been defined. Furthermore, the response pattern of these genes following PUVA treatment has not been addressed in detail although knowledge on its function is of great interest for PUVA therapy because of the high incidence of skin cancer limited to the histogenetic compartment of epidermal cells. Therefore, we were interested in the role of these tumor suppressor genes in the growth arrest following PUVA treatment in the non transforming compartment of the dermal fibroblasts. Unexpectedly, PUVA-treated fibroblasts with a null-mutation in either of the p53, p21^{Cip1} or p16^{INK4a} genes were still growth-arrested with enlarged cell morphology. Thus, the cell growth regulators p53, p21^{Cip1} and p16^{INK4a} are not exclusively required for the induction of PUVA-induced senescence-like growth arrest and may be replaced by each other and/or additional control genes. Recently, a similar response of p53, p21^{Cip1} and p16^{INK4a} deficient cell lines has been described for the induction of stress-induced replicative senescence by 5'-bromodeoxyuridine (Michishita *et al.* 1999).

In summary, the data show that several cell cycle control pathways are sequentially activated after PUVA treatment. Up-regulation of p53/p21^{Cip1}

occurred 1-2 day after PUVA and possibly played a pivotal role for initiating the growth arrest, while p16^{INK4a} might be involved in maintaining the long-term growth arrest. The exact pathways controlling PUVA-induced long-term growth arrest are far from being clear, and may involve several other pathways. As a study focusing on the senescence-like features in the long-term growth arrest, it was found that both of the two known pathways involved in cellular senescence, namely p53/p21^{Cip1} and pRb/p16^{INK4a}, are also up-regulated after PUVA treatment.

4.2.3. PUVA treatment leads to elevated ROS production which is related to mitochondria and NADPH oxidase

Many studies suggest that ROS may play a pivotal role in the induction of replicative cellular senescence. For example, examination of cells in culture suggests that “older” cells at higher CPD have higher levels of ROS than “younger” cells at lower CPD (Hagen *et al.* 1997). When cells were treated with antioxidants or grown in conditions of low oxygen, their life span is distinctly prolonged (Chen *et al.* 1995b; Yuan *et al.* 1995). Treatment of primary fibroblasts with a sublethal concentration of H₂O₂ was shown to induce a state resembling replicative senescence (Chen *et al.* 1998). Moreover, ROS were involved in the oncogenic Ras-induced senescence program (Lee *et al.* 1999). Based on the previous evidence linking oxidative stress to aging, in this thesis the possibility was explored whether PUVA treatment induces the senescence-like growth arrest as well as phenotypic changes by altering the intracellular levels of ROS. The results indicate that PUVA treatment leads to an increase in intracellular ROS, the source of which appears to be both mitochondria and the NADPH oxidase. This conclusion is based on the finding that only depletion of functional mitochondria in conjunction with inhibition of NADPH oxidase leads to the suppression of the enhanced ROS levels after PUVA treatment.

Under normal conditions the main source for ROS production are mitochondria. Mitochondria utilize over 90% of the oxygen consumed by mammalian cells, and up to 4% of this oxygen is transformed into ROS. It is generally accepted that defects in the respiratory-chain, which is located in the mitochondrial membrane, results in enhanced production of ROS and other free radicals. As an index for

mitochondrial membrane integrity, previous studies showed that reduced mitochondrial membrane potential ($\Delta\Psi$) led to increased generation of ROS (Zamzami *et al.* 1995). In line with this, our data show that $\Delta\Psi$ is significantly decreased 2 weeks after PUVA treatment and further decreased at later time points post PUVA treatment.

Since ATP production is driven by $\Delta\Psi$, lower $\Delta\Psi$ should lead to lower ATP production. However, this is not the case in PUVA-treated fibroblasts. With a decreasing $\Delta\Psi$ value, the ATP level of the PUVA-treated cells remained constant. Therefore, there must be an alternative mechanism to circumvent the energy loss. Interestingly, mitochondria still proliferate although cell proliferation is stopped after PUVA treatment. Thus the seemingly paradox results between constant ATP generation and a decrease in $\Delta\Psi_m$ may be explained by enhanced mitochondria proliferation. This means that proliferation of mitochondria may function as a compensatory response to restore an adequate mitochondrial function for ATP production. Since $\Delta\Psi$ decreased time-dependently after PUVA treatment, it is most likely though speculative that newly produced mitochondria at least in part still have defects in their electron chain, which would lead to more ROS production. In fact, an increase in intracellular ROS was observed time-dependently after PUVA treatment. Alternatively, the following scenario may be responsible for the enhanced ROS generation: initially enhanced ROS levels or mitochondrial DNA damage contributes to the further mitochondrial damage and ROS leakage. The mitochondrial biogenesis occurring in parallel may finally overcome the number of severely damaged ROS-overproducing fibroblasts. According to this explanation $\Delta\Psi$ should be restored gradually to normal or almost normal levels at the time point when cells start to regrow. However, this has not been observed, as the $\Delta\Psi$ of PUVA-treated fibroblasts was not increased at 11 weeks post PUVA treatment compared to PUVA-treated fibroblasts analyzed 16 days and 4 weeks after PUVA treatment. One explanation could be that PUVA-induced damages and the subsequent repair in fibroblasts are heterogeneous. Thus, the determination of $\Delta\Psi$ value might be overwhelmed by those heavily damaged fibroblasts, though a subpopulation of fibroblasts already gained a high ratio of healthy mitochondria to damaged mitochondria. At least

regrowing fibroblasts revealed the same $\Delta\Psi$ value as mock-treated control fibroblasts.

The molecular mechanisms involved in the control of mitochondria biogenesis are still poorly understood. It is a complex process that involves proliferation (increasing the number of mitochondria) and differentiation or maturation (increasing the activity of individual mitochondria) (Fernandez-Moreno *et al.* 2000). Mitochondria biogenesis is controlled both by the nucleus genome and the mitochondria genome (Attardi and Schatz 1988). Thus, the integrity of both mtDNA and the genomic DNA encoding mitochondrial components are critical for cellular energy generation and maintenance of functional mitochondria. Due to effects of PUVA in generating DNA monoadducts or interstrand crosslinks, both genomic DNA and mtDNA are preferred targets. In addition, mitochondria are not equipped with a similarly efficient repair system like that in the nucleus, and DNA interstrand crosslinks in mitochondria are most likely maintained and not repaired (Cullinane and Bohr 1998). Thus, even though fibroblasts contain hundreds of mitochondria and each mitochondrion contains several copies of mtDNA, this might not be enough to guarantee that all the newly replicated mtDNA is identical and has no mutations or deletions. If new mitochondria have defects in the mtDNA, the enhanced ROS production will be hardly prevented.

However, PUVA-induced ROS production was definitely not solely due to the uncontrolled ROS leakage from the defective mitochondria electron chain. In fact mitochondria depleted Rho0 fibroblasts still revealed enhanced ROS production after PUVA treatment, which may be related to NADPH oxidase. At least, Rho0 fibroblasts in conjunction with inhibition of the NADPH oxidase reveal a complete abrogation of enhanced ROS generation 3 and 6 weeks after PUVA treatment. It is currently not clarified why mitochondria depletion or NADPH oxidase inhibition alone does not show any decrease in ROS levels after PUVA treatment. The herein reported data would be compatible with a concept that NADPH oxidase compensates for a lack of mitochondrial ROS production in Rho0 fibroblasts. In fact, preliminary data suggest that the expression of the fibroblast-related NADPH oxidase is enhanced in Rho0 PUVA-treated fibroblasts (data not shown). Although NADPH oxidase is classically regarded as a key enzyme of neutrophils,

where it is involved in the production of reactive oxygen species in defense against infections, recent studies demonstrate that virtually all eukaryotic cell types have a similar oxidase system. NADPH oxidase is a membrane associated multisubunit enzyme consisting of a plasma membrane-associated flavohemoprotein complex which comprises two subunits, gp91phox and p22phox, and several cytosolic components including p40phox, p47phox, p67phox, and the small GTPase Rac. Since functional assembly of NADPH oxidase requires translocation of those cytosolic proteins into the membrane, ROS production via NADPH oxidase in PUVA-treated Rho0 fibroblasts suggests that it may play an important physiological role instead of acting only as damaging reagents.

The physiological role of NADPH oxidase related ROS production in non-phagocytic cells is currently unclear. Previous studies have established an important role for ROS in cell proliferation and activation of growth-related signaling pathways. For example, ROS have been implicated in the mitogenic response to platelet-derived growth factor (PDGF) (Sundaresan *et al.* 1995), phenylephrine (Nishio and Watanabe 1997), thrombin (Patterson *et al.* 1999) and epidermal growth factor (EGF) (Bae *et al.* 1997). Moreover, the addition of exogenous ROS to vascular smooth muscle cells was reported to induce cell proliferation, while suppression of ROS resulted in increased apoptosis (Baas and Berk 1995; Brown *et al.* 1999; Tsai *et al.* 1996). There is also growing evidence that increased ROS production is functionally associated with the regulation of gene expression and the activation of many transcription factors, such as NF κ B (Cominacini *et al.* 2000; Sulciner *et al.* 1996). Increased activation of NF κ B, in turn, has been reported to increase cell survival (Baichwal and Baeuerle 1997). Interestingly, it was lately found that increased ROS production induced by oncogenic H-Ras could enhance the DNA repair capacity via the Ras/PI3K/Rac1/NADPH oxidase-dependent pathway (Cho *et al.* 2002). This finding provides first evidence that ROS, which are generally accepted as DNA damaging reagents, on the other hand also facilitate DNA repair. As promoters of many DNA repair genes contain redox sensitive transcription factor-binding sites, involvement of ROS in the regulation of DNA repair activity might occur through the activation of redox-sensitive transcription factors (Cho *et al.* 2002). PUVA

treatment also leads to various DNA damages, however, so far it is not clear whether NADPH oxidase related ROS production also plays a role for facilitating DNA repair.

Two key studies demonstrated that overexpression of NADPH oxidase in NIH 3T3 cells leads to a proliferative phenotype (Irani *et al.* 1997; Suh *et al.* 1999). Interestingly, overexpression of Renox, an NADPH oxidase in kidney, in the same cell line was also found to lead to senescence (Geiszt *et al.* 2000). The latter finding may reflect a similar function of NADPH oxidase activation after exposure of fibroblasts to PUVA treatment. So far we have little knowledge on NADPH oxidase activation in PUVA-treated fibroblasts. It is unclear how the NADPH oxidase is activated. In addition, its exact role in PUVA-induced senescence-like growth arrest, and whether it drives cells at risk for tumorigenesis, remains poorly understood. To address these questions will be an interesting challenge for further studies.

4.2.4. Enhanced ROS concentration of reactive oxygen species is responsible for the enlarged morphology of fibroblasts but not for the enhanced expression of SA- β -galactosidase after PUVA treatment

Based on the previous evidence linking oxidants to cellular senescence and aging, the possibility was explored in this study of whether the PUVA-induced senescence-like phenotypic changes may be causally related to the enhanced ROS levels in fibroblasts after PUVA treatment. The herein reported results suggest that PUVA-induced high ROS level is essential for the senescence-like phenotypic changes after PUVA treatment. In fact, PUVA-treated fibroblasts grown in the presence of the ROS-scavenging antioxidant N-acetyl cystein (NAC) are rescued from the PUVA-induced cytoplasmic enlargement. However, the long-term growth arrest after PUVA treatment was not affected. Reduced ROS level in the presence of NAC did not result in earlier regrowth after PUVA treatment. So far little is known which signal pathways ROS are engaged to change cell morphology. Possibly, it is due to its active role on cell proliferation and activation of growth-related signaling pathways such as mitogen-activated protein kinase (MAPK) and AKT pathways. In this regard, cell enlargement might also be related to the increasing number in mitochondria found after PUVA

treatment, as mitochondria proliferate in response to new metabolic requirements by the regulation of ATP levels or lipid metabolism. In fact, mitochondrial DNA depleted Rho0 fibroblasts show an elongated small phenotype and not the flattened, enlarged cell morphology post PUVA treatment (data not shown). In contrast to the active role of ROS in morphological changes of fibroblasts, scavenging ROS by NAC did not lead to any effect on the senescence-associated β -galactosidase. This either suggests that SA- β -galactosidase is not downstream of ROS, or alternatively, that low levels of ROS maintained in NAC-treated PUVA-fibroblasts are already sufficient to up-regulate SA- β -galactosidase.

The PUVA-induced changes are a model particularly suited to study mechanisms of stress-induced premature senescence. Further investigations into the downstream signaling molecules following PUVA-induced ROS production and its linkage to the senescent phenotypic changes might provide important insights for senescence as well as new therapeutic strategies to combat aging.

4.3. PUVA treatment of human dermal fibroblasts leads to an early onset of replicative senescence related to oxidative telomere shortening

PUVA-treated fibroblasts, although escaping from the long-term growth arrest, seem to retain memory of the damaging PUVA effects. PUVA-treated fibroblasts cultured in their regrowing state reach the stationary phase at a much lower overall cumulative population doubling compared to mock-treated control fibroblasts. These data support the view that preceding damage affects a counting mechanism contributing to the overall limited proliferation potential of PUVA-treated fibroblasts.

Telomere shortening is thought to serve as a “replicometer” (counting the finite number of cell divisions) and as a trigger of replicative senescence (Harley *et al.* 1990; Harley and Villeponteau 1995). In the absence of telomerase, human telomeres shorten by 30-200 bp per population doubling (PD) (Harley *et al.* 1990). After 50-100 PD, this process depletes the telomere reserve of primary human cells and results in replicative senescence. Therefore, in this thesis it was studied whether the reduced life-span is related to telomere length, which in addition to the end-replication problem is eroded by PUVA-induced telomere

damage. Onset of replicative senescence in vitro is mainly dependent on telomere length. Therefore, it is predicted that telomere shortening occurring in addition to the regular DNA replication will drive fibroblasts into senescence at a lower CPD. The results, indeed, indicate that ROS-induced telomere shortening represents the alternative mechanism responsible for the additional telomere shortening in PUVA-treated fibroblasts. Although the telomere length in PUVA-treated fibroblasts seems to be constant during the growth arrest stage, a significant reduction in telomere length (~1-1.5 kb) is found in regrowing fibroblasts post PUVA treatment compared to mock-treated fibroblasts at exactly the same CPD. Clearly, this substantial difference is generated at the very beginning of regrowth, while thereafter regrowing fibroblasts showed a similar shortening rate in telomere length comparable to mock-treated control fibroblasts. After 2 weeks from the emergence of growth foci until newly growing fibroblasts reached confluence, and thereafter at different CPDs, genomic DNA for telomere length determination was collected. The question of how a more than 1-1.5 kb telomere reduction could occur within 1-2 weeks after regrowth of PUVA-treated fibroblasts was addressed. Under standard culture conditions, human dermal fibroblasts could divide at most 7-9 PD in 2 weeks, and the telomere reduction, thus, should be less than 500 bp. This is shown in Figure 29, where regrowing fibroblasts from CPD 20.9 to CPD 28.4 results in a small telomere decrease of <500 bp. Accordingly, the end-replication problem is apparently not sufficient to fully explain this reduction. No telomere length changes occurred during the growth arrest stage of fibroblasts after PUVA treatment, but definitely are observed after regrowth of fibroblasts within the first cycles of DNA replication. Thus, it is possible that single strand breaks were generated in the telomere region during the growth arrest stage which, if not repaired, might lead to telomere loss during DNA replication when separation of DNA double-strands occurred, as has previously been suggested in an other SIPS model (von Zglinicki *et al.* 2000). In addition, telomeres have long single-stranded 3' overhangs at both ends with an average of 130-210 bases being essential for the stabilization of the "telomeric t-loop" (Blackburn 2000; Campisi *et al.* 2001). It was suggested to be generated due to the end replication problem and possibly to the action of a C-strand-specific exonuclease, with a 5' – 3' exonuclease, which specifically trims back the completely synthesized telomere

ends to form a 3' overhangs for the T-loop formation (Makarov *et al.* 1997). Single strand breaks in this overhang and subsequent loss during DNA double strand separation and replication most likely drive telomere length reduction. Here it is reported that single strand breaks are formed and accumulate in the telomere region with time after PUVA treatment as determined by denaturing gel electrophoresis (Figure 30). A clear pattern of telomere reduction could be observed in denatured telomeres which gave strong support for the hypothesis that single strand breaks contribute to telomere reduction. Although the length of double-stranded telomeres is constant during the whole growth arrest period after PUVA treatment, the length of single stranded telomeres at 11 weeks post PUVA treatment is nearly identical to that of regrowing fibroblasts. This finding may indicate that separation of telomere double strands of growth-arrested fibroblasts results in telomere fragment loss. Thus, the two steps leading to telomere shortening, such as single strand breaks and telomere fragments loss, occur at different time post PUVA treatment. Single strand breaks are generated during the growth arrest stage, while telomere fragment loss most likely occurs during DNA replication and cell proliferation. Increased shortening of single-stranded telomere during the growth arrest stage, in addition, indicates that single strand breaks in this region are not efficiently repaired. The reason and underlying mechanism of a potential telomeric DNA repair deficiency is not understood. Nevertheless, this finding might have far-reaching consequences. Accumulation of DNA damage and the inability of efficient DNA repair have been suggested as a causal factor in aging (Chen *et al.* 1995b; de Boer *et al.* 2002). As telomeres serve as a biological clock for cellular senescence, the herein reported data that single strand breaks of telomere are not repaired not only provide a reasonable explanation for accelerated telomeres shortening after PUVA treatment, but also imply a rationale for understanding DNA damage related cellular senescence and aging processes.

There is increasing evidence suggesting that oxidative stress is causally involved in telomere erosion (Proctor and Kirkwood 2002; von Zglinicki 2000, 2002). Reduction in telomere length occurs five to ten times faster in fibroblasts subjected to chronic hyperoxia, a rather mild oxidative stress compared to mock-treated fibroblasts (Vaziri *et al.* 1997; von Zglinicki *et al.* 1995). On the other

hand, the rate of telomere loss decreases by half if human dermal fibroblasts are treated with the spin trap α -phenyl-t-butyl-nitrone (PBN), a potent free radical scavenger (von Zglinicki *et al.* 2000). These data indicate that telomere shortening could be the result of oxidative stress. However, it has also been suggested that the accelerated telomere shortening under oxidative stress observed in the above reports might be an artifact resulting from the increased replicative demand on a subpopulation when a significant proportion of the cells are forced to drop out of the cell cycle by stress (Dumont *et al.* 2001; von Zglinicki 2002). In other words, if only a subpopulation of cells starts to regrow after PUVA treatment, while a significant proportion of the cells are still growth-arrested, the small population of regrowing fibroblasts will have to divide many times until confluences with subsequent accelerated telomere shortening (Dumont *et al.* 2001). So far, there is no agreement on whether telomere shortening occurs due to oxidative damage or to proliferation of a small subpopulation after stress-induced premature senescence. PUVA treatment leads to a dramatic increase in ROS production during the growth arrest stage, as well as a significant telomere reduction in regrowing fibroblasts thereafter. In addition, scavenging ROS by N-acetyl cystein (NAC) could prevent telomere erosion and replicative senescence occurs at a later CPD in fibroblasts after PUVA treatment compared to simply PUVA-treated fibroblasts. In addition, compared to other SIPS-models with low concentrations of peroxide and its derivatives, where growth arrest was investigated only for several days or at most weeks, our long-term growth arrest model induced by PUVA has the definite advantage that its long-lasting oxidative stress results in a subsequent clearly visible loss of telomere length.

Several lines of evidence support the notion that oxidative stress plays an important role in the accelerated decrease of telomere length in PUVA-treated fibroblasts. First, based on a simple mathematical analysis of the data, it can be shown that the significant telomere reduction following PUVA treatment can not be solely be explained by the fact that it is due to the repetitive division of a subpopulation of fibroblasts as has been explained above (Name it S-hypothesis for brief; "S" stands for subpopulation). Second, treatment with NAC, an

antioxidant, during the growth arrest period protected fibroblasts from telomere reduction as mentioned above.

In the PUVA-induced growth arrest and regrowth model, the S-hypothesis could be mathematically described as follows. In the CPD calculation, it is proposed that regrowing fibroblasts derive from the total fibroblast population (2×10^5 cells) of growth-arrested fibroblasts instead of a subpopulation:

2×10^5 fibroblasts ----- divide N times ($N = PD$) ----- 10^6 fibroblasts (confluence in dish)

N could be calculated by the equation: $(2 \times 10^5) \times 2^N = 10^6$

$N = \text{Log} [10^6 / (2 \times 10^5)] / \text{Log} 2 \approx 2.3$ (PD)

C_r : CPD of growth resuming fibroblasts when reaching confluence in the dish.

C_0 : CPD of fibroblasts before PUVA treatment.

However, the CPD calculated here might be not the real CPD of regrowing fibroblasts, since it may be that only a subpopulation of fibroblasts starts to proliferate, while others are still growth-arrested.

To obtain the real CPD, it is mandatory to know the exact number of fibroblasts, which escaped from the growth arrest. However, this is difficult to determine. When considering the extreme case that only one fibroblast out of the 2×10^5 growth-arrested fibroblasts escapes from growth arrest and finally divides multiple times so that it is responsible for the occurring confluence ($\sim 10^6$ cells), the following equation would result:

1 fibroblast - ----- divide N times ($N = PD$) ----- 10^6 fibroblasts (confluence in dish)

N could be calculated by the equation: $1 \times 2^N = 10^6$

$N = \text{Log} 10^6 / \text{Log} 2 \approx 20$ (PD)

Thus, $C_r = C_0 + 20$ (PD)

As shown by the BrdU incorporation experiments the number of regrowing fibroblasts is definitely more than one and less than the total seeded fibroblast number within the dish. Accordingly, the real CPD of regrowing fibroblasts should fit into the following equation:

$$C_0 + 2.3 \leq C_r \leq C_0 + 20$$

Based on the assumption that no other factors than CPD contribute to telomere length, then the telomere length of regrowing fibroblasts should be:

$$T_n (C_0 + 20) \leq T_r (C_r) \leq T_n (C_0 + 2.3)$$

$T_r (C_r)$: telomere length of regrowing fibroblasts, CPD = C_r .

$T_n (C_0 + x)$: telomere length of mock-treated control fibroblasts, CPD = $(C_0 + x)$.

According to the above equation, in any case the telomere length of regrowing fibroblasts at a certain CPD should be at least higher than that of mock-treated control fibroblasts at a CPD of 20 more in numerical value ($T_n (C_0 + 20) \leq T_r (C_r)$). By contrast, as shown in Figure 29, the telomere length of regrowing fibroblasts with a CPD of 20.9 is still shorter than that of mock-treated control fibroblasts with a CPD of 41. Thus, the observed increase in telomere shortening rates after PUVA treatment is too large to be explained by the S-Hypothesis, suggesting other factors contributing to telomere reduction.

In this thesis ROS have been identified as a major factor responsible for telomere shortening. NAC incubation during the growth arrest stage significantly protects PUVA-treated fibroblasts from telomere reduction (Figure 31). Thus, it is clear that the significant reduced telomere length of fibroblasts after PUVA treatment is at least in part related to the high level of ROS production. These data are in line with previous findings from the von Zglinicki's group and confirm the idea that oxidative stress is an important determinant for telomere length (Saretzki and von Zglinicki 2002; von Zglinicki 2002). In addition, it is of clinical importance to know whether PUVA leads to significant ROS production and has profound effects on telomere length, since PUVA therapy is widely used for many skin disorders.

However, the data stem from *in vitro* experiments. Therefore, it has to be proven that the *in vitro* data hold true for the *in vivo* situations as well. Thus, increasing the antioxidative defense capacity in patients during and after PUVA treatment by antioxidants or other means possibly could be of advantage for patients to prevent premature aging, a major side effect of long-term PUVA treatment.

So far it is hard to say whether the reduced total life span of PUVA-treated fibroblasts is exclusively controlled by oxidative telomere reduction. Although NAC treatment evidently reversed telomere reduction in PUVA-treated fibroblasts, the total life span is only in part restored (Figure 32). Nevertheless, the fact that NAC-treated fibroblasts with a longer telomere length partly recovered their total life-span implies that oxidative telomere erosion plays a central role for the reduced life-span of PUVA-treated fibroblasts.

Recently, it has been demonstrated that replicative cellular senescence in culture is not only induced by an intrinsic cell division counter mechanism (replicative senescence), but can also be induced by extrinsic factors such as culture conditions (premature senescence). Epithelial cells, for instance, seem to experience a telomere length-independent senescent cell cycle block via the pRb pathway (Kiyono *et al.* 1998). In this context the question was addressed whether an alternative pathway – in addition to telomere shortening – is activated and contributes to the early onset of senescence in regrowing fibroblasts after PUVA treatment.

p53/p21^{Cip1} and/or p16^{INK4A}/Rb are the two main pathways known to be involved in replicative senescence. Replicative senescence of human cells can be abrogated by suppression of both pathways. For instance, suppression of these pathways by SV40 large T antigen or the human papillomavirus E6 and E7 oncogenes can fully suppress replicative senescence, leading to a cell population with an extended lifespan (Counter *et al.* 1992; Shay *et al.* 1991a).

Herein it is shown that during PUVA-induced growth arrest, both p53/p21^{Cip1} and p16^{INK4A}/pRb are up-regulated. Although p53 and p21^{Cip1} expression returned to the control level after fibroblasts regrow, p16^{INK4a} is still expressed at a low while

up-regulated level. However, it is not clear whether p16^{INK4a} is induced in response to short telomeres or rather serves as an alternative mechanism contributing to the early onset of senescence. Although it is widely assumed that critically shortened telomere ends can initiate a signaling cascade that eventually results in the upregulation of p21^{Cip1} and/or p16^{INK4a}, it has also been shown that aging-related p16^{INK4a} up-regulation could be induced under suboptimal culture conditions independent of telomere dynamics (Dickson *et al.* 2000; Kiyono *et al.* 1998; Munro *et al.* 2001). In addition, introduction of hTERT into pre-senescent fibroblasts blocked the upregulation of p21^{Cip1} (Modestou *et al.* 2001) but the high level of p16^{INK4a} was not reduced. Although a study from the Wright and Shay laboratory (Ramirez *et al.* 2001) found that p16^{INK4a} was not induced and telomerase-mediated telomere maintenance is sufficient to generate cells with infinite replicative potential under optimal cell culture conditions. Nevertheless, these results suggest that p16^{INK4a} can be induced both by certain culture conditions or other kinds of stresses as well as telomere shortening. Maintenance of up-regulated p16^{INK4a} levels in regrowing fibroblasts after PUVA treatment definitely is not due to insufficient culture conditions since mock-treated control fibroblasts under the same conditions do not reveal enhanced p16^{INK4a} expression. Thus, enhanced p16^{INK4a} expression might be due to PUVA-induced damage or the high ROS production. However, it is unclear why p16^{INK4a} level is maintained in the regrowing phase.

In summary, replicative senescence *in vitro* is a complex and heterogeneous process. It may be dependent on the telomeric 'clock', the chronic exposure to various types of stresses, or a combination of both. The molecular pathways of senescence have begun to be unraveled, and their further characterization will undoubtedly provide a more complete picture. Using the PUVA-induced premature senescence as a model for stress-induced premature senescence, in this thesis the underlying mechanisms of the early onset of replicative senescence have been studied. Our data support the idea that telomere length is not only dependent on cell proliferation, but also on oxidative stress from endogenous origin which is undoubtedly involved and contributes to accelerated telomere reduction. In addition, maintenance of up-regulated p16^{INK4a} expression might be an additional mechanism contributing to early onset of senescence.

However, a causal relationship cannot be concluded from the present data. The data might have profound clinical implications. They are the first data showing that PUVA treatment leads to early onset of senescence, which is related to oxidative telomere reduction and possibly to p16^{INK4a} activation. In the clinical situation, senescence appears to be a relevant factor in determining treatment outcome and warrants further investigation, especially for PUVA and other kinds of chemotherapies, which induce DNA or other cellular damages. It is extremely important to investigate the cellular response after treatment, i.e., apoptosis or senescence. Such information could be of great value in choosing an appropriate photo-chemotherapeutic strategy and may explain some of the controversy concerning the clinical use of chemotherapies.

4.4. Initiation of the long-term growth arrest

The efficacy of PUVA treatment on many skin diseases is believed to be related to its proliferation inhibiting effects. However, the mechanism of how PUVA treatment initiates growth arrest in many different cell types is not completely understood. Since psoralens are known to intercalate within DNA in a dark reaction and form mono- and bifunctional adducts with pyrimidine bases following UVA irradiation (Song and Tapley 1979), it has been proposed that psoralen-DNA interstrand crosslinks are responsible for the proliferation inhibition as it blocks DNA replication (Tokura *et al.* 1991). However, this is still rather speculative and lacks substantial evidence that, apart from crosslink formation other mechanisms are not involved. The results here indicate that PUVA-induced long-term growth arrest is unlikely to be due to psoralen-DNA interstrand crosslinks, at least under the conditions, which have been used for PUVA treatment. It is herein found that fibroblasts with more interstrand crosslinks (ICLs) were not necessarily growth-arrested as is the case for PUVA-treated fibroblasts where 8-MOP was present only during the pre-incubation step (8-MOP-PRE), while cells with less ICLs could be growth-arrested as is the case for PUVA-treated fibroblasts without the 8-MOP pre-incubation step (8-MOP-UV).

Herein it was therefore studied which additional factors are responsible for the long-term growth arrest. We first proposed that it might be due to PUVA-induced damage of cellular membrane or other cytoplasmic components. In fact, different

cellular components including DNA, proteins and lipids have been shown to be photo-modified by 8-MOP (Schmitt *et al.* 1995). Fractionated cellular components of the rat epidermis after treatment with 8-MOP and UVA showed that only 17% of the 8-MOP was bound to DNA, while 57% was bound to protein and 26% to lipids (Beijersbergen van Henegouwen *et al.* 1989). In addition, it was reported that a cell membrane receptor represent also a major target for psoralens (Laskin and Lee 1991; Yurkow and Laskin 1987). In this thesis by separation of the nuclei and cytoplasts of PUVA-treated fibroblasts and reconstructing new cell-hybrids, which have either undamaged cytoplasts or undamaged nuclei, it was studied whether PUVA-induced changes in the cytoplasm and/or nucleus play a key role for the initiation of the growth arrest. The results suggest that combined 8-MOP and UVA irradiation leads to changes both in cytoplasts and nuclei. Reconstructed cells with PUVA-cytoplasts, although initially growth-arrested, revealed an overall shorter growth arrest. Compared to simply PUVA-treated fibroblasts with a growth arrest stage longer than three months, fusions of PUVA-cytoplasts with mock-treated nuclei reveal growth arrest for only 20-26 days (PUVA-2w) and 8-12 days (PUVA-4w) after fusion, respectively. These data indicate that the damages or changes in cytoplasts induced by PUVA treatment could be repaired in a relatively short phase of 5-6 weeks. Unfortunately, fusions of PUVA-treated nuclei with mock-treated control cytoplasts reveal growth arrest for two weeks and thereafter all hybrids die. Thus, the experiments do not allow to fully estimating the overall contribution of PUVA-induced damages in karyoplasts. However, it is nevertheless highly interesting that PUVA-induced damages in the cytoplasts are able to initiate and maintain the growth arrest for 26 days. The underlying mechanism is unknown.

As discussed above, psoralen-DNA crosslinks, although formed after PUVA treatment, do not appear to be the key player responsible for the long-term growth arrest. However, this does not necessarily mean that other kinds of DNA damages were not involved and responsible for the growth arrest. Psoralens are multifunctional agents, forming two types of monoadducts and a diadduct (or crosslink) (Song and Tapley 1979). Although the number of interstrand crosslinks is obviously lower in PUVA-treated fibroblasts without pre-incubation of 8-MOP (8-MOP-UV) compared to PUVA-treated fibroblasts with pre-incubation where 8-

MOP was not present during UVA irradiation (8-MOP-PRE), there is no evidence that DNA monoadducts were also lower in 8-MOP-UV fibroblasts. As to the two different procedures of PUVA treatment which generate different numbers of interstrand crosslinks, it is possible that 8-MOP-UV induces more psoralen-DNA monoadducts although treatment with 8-MOP is transitory compared with 8-MOP-PRE. ICL formation is a three-step process (Figure 37) with 1) intercalation between DNA base pairs and formation of weak bands with the pyrimidine bases, 2) the first four-center photocycloaddition reaction to form either of two cyclobutyltype monoadducts, 3,4-monoadduct or 4',5'-monoadduct, 3) with absorption of a second UVA photon by the 4',5'-monoadduct leads to a second four-center photocycloaddition at the pyrone end of the molecule and subsequent formation of a crosslink (Gasparro 1988). Although photoreaction is a fast step, intercalating into DNA double strand at sites suitable for crosslink formation (with adjacent pyrimidines in opposite strands) may not be as fast. Therefore, it is highly questionable whether within three minutes 8-MOP-UV could have enough time for intercalating into the right DNA sites. On the other hand, as can be seen from Figure 37, weak bonds formed between DNA and psoralen after intercalation occur in a dark reaction. Once psoralen has intercalated into a DNA double strand, it may not be easy to be washed out. For 8-MOP-PRE fibroblasts, although free 8-MOP was likely to be washed away shortly before/during the 3-minute irradiation, intercalated 8-MOP is unlikely to be washed away, and these 8-MOPs may be responsible for the total ICL formation.

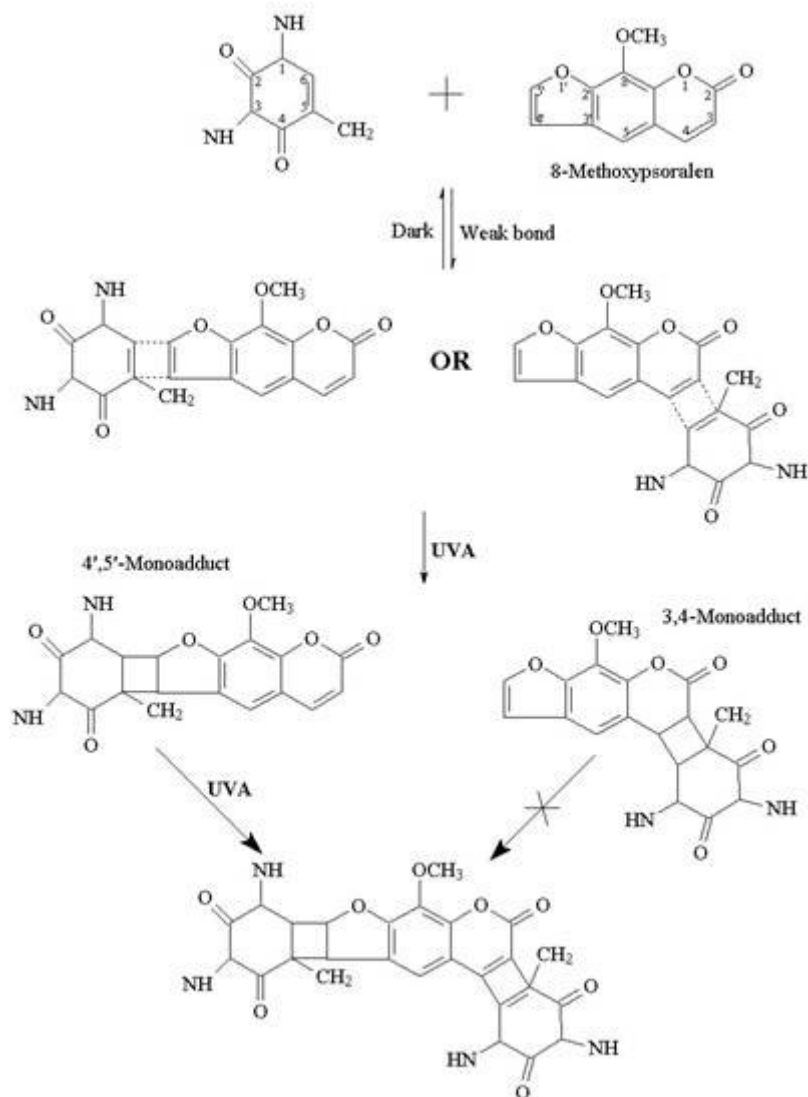


Figure 37. Psoralen-DNA mono- or bi-adduct formation. Psoralens react with DNA in three steps. First the psoralen intercalates into the DNA double strand in the absence of UV radiation and form weak bonds with pyrimidine bases. Upon UV irradiation, cyclobutane monoadducts with a pyrimidine base are formed. If the initial photoreaction occurs at a 5'-TpA site, the 4'5'-monoadducts can absorb a second photon and undergo another cyclobutyl reaction with the adjacent thymine at the opposite strand resulting in the formation of a bi-adduct (psoralen-DNA crosslink).

In fact, the question of which adduct(s) is (are) responsible for various biological effects of PUVA is an active field of investigation. Cross-link formation appears to be a relatively low yield reaction compared to monoadducts. Hyodo et al. showed that mouse FM3A cells treated with 8-MOP and UVA contained ~ 2 cross-links per 1 million base pairs (Hyodo *et al.* 1982). Under similar conditions, however, human lymphocytes were shown to contain 120 adducts per 1 million base pairs (Gasparro *et al.* 1985). Thus, only a small fraction of all adducts appears to be crosslinks. We have no direct evidence that more monoadducts were formed in 8-MOP-UV cells. However, the total photoadducts could be calculated according to previously published data. It has been determined previously that photoadduct formation in 8-MOP/UVA-treated cells (human and murine) is independent of cell type. The number of photoadducts formed can be directly related to the combined dose of 8-MOP and UVA (Gasparro *et al.* 1997), which is a linear correlation between photoadduct number and the product of 8-MOP concentration in ng/ml and the UVA dose in J/cm² (8-MOP concentrations over the range 10 – 20000 ng/ml and UVA dose over the range 1-10 J/cm²). There are about 4 adducts per million base pairs when the product of 8-MOP and UVA is 100. Therefore, the photoadducts formed in the herein PUVA-treated fibroblasts system are about 18 adducts per million base pairs.

In summary, our data suggest that PUVA-induced long-term growth arrest was not mainly related to psoralen-DNA interstrand crosslinks. While nuclei seem still the primary target, PUVA also induces changes in the cytoplasmic region, repair of which need about 5-6 weeks, which finally contribute to the initiation and initial maintenance of growth arrest.

5 Perspectives

The herein presented data indicate that PUVA-induced senescence-like growth arrest is reversible in a large proportion of cells. The finally returning growth capacity is not due to immortalization, transformation or loss of function of the senescence controlling genes p53, p21 and p16. These findings strengthen the view that PUVA-induced changes do not fully reflect replicative senescence, but rather represent a long-term transient phenocopy of senescence. PUVA treatment leads to enhanced ROS production which contributes to the

senescent-like phenotypes. Elevated ROS production seems related to both mitochondrial dysfunction and NADPH oxidase activation. PUVA-treated fibroblasts cultured in their regrowing state reach the stationary phase at a much lower overall cumulative population doubling compared to mock-treated control fibroblasts. The reduced total life-span in PUVA-treated fibroblasts is due to oxidative stress-induced telomere reduction as the abrogation of ROS production by the antioxidant NAC rescues telomere length reduction and partly restored total life-span of PUVA-treated fibroblasts. These data support the view that preceding damage affects a counting mechanism contributing to the overall limited proliferation potential of PUVA-treated fibroblasts.

The model reported here is particularly suited to elucidate mechanisms underlying long-term senescence-like growth arrest, the related functional changes, and the release of cells thereof. In general, the following directions might be of interest for further studies:

- The characterization of the molecular mechanisms of enhanced ROS production as well as their active role involved in the long-term growth arrest which is largely unknown. The activation of NADPH oxidase after PUVA treatment might provide a hint on the signal pathways involved and should be further studied.
- As a main source of ROS production, the role of mitochondria deserves further investigation. It has already been shown that the number of mitochondria increased after PUVA treatment. Thus, it would be interesting to know what mechanisms are underlying the biogenesis of mitochondria, the role of mitochondria in PUVA-induced growth arrest, as well as the relationship between mitochondria and the senescent phenotype.
- As to the mechanism on how PUVA treatment leads the long-term growth arrest, the herein reported data suggest that the formation of psoralen DNA interstrand crosslinks seems not to be the main reason. However, whether it is due to psoralen-DNA monoadducts or damages of other cellular components is so far unknown, and might be of interest for further investigation.

Answers to these questions will provide further insight into molecular mechanisms of stress-induced premature senescence and replicative senescence of fibroblasts in vitro which may have relevance for fibroblasts within the dermis in vivo. Definition of distinct molecular pathways may allow specific targeting for novel preventive and therapeutic strategies.

6 References

- Alcorta, D. A., Xiong, Y., Phelps, D., Hannon, G., Beach, D. and Barrett, J. C. (1996). Involvement of the cyclin-dependent kinase inhibitor p16 (INK4a) in replicative senescence of normal human fibroblasts. *Proc Natl Acad Sci U S A* **93**(24): 13742-7.
- Amin, A. R., Attur, M. and Abramson, S. B. (1999). Nitric oxide synthase and cyclooxygenases: distribution, regulation, and intervention in arthritis. *Curr Opin Rheumatol* **11**(3): 202-9.
- Atadja, P., Wong, H., Garkavtsev, I., Veillette, C. and Riabowol, K. (1995). Increased activity of p53 in senescing fibroblasts. *Proc Natl Acad Sci U S A* **92**(18): 8348-52.
- Attardi, G. and Schatz, G. (1988). Biogenesis of mitochondria. *Annu Rev Cell Biol* **4**: 289-333.
- Averbeck, D. (1989). Recent advances in psoralen phototoxicity mechanism. *Photochem Photobiol* **50**(6): 859-82.
- Avilion, A. A., Piatyszek, M. A., Gupta, J., Shay, J. W., Bacchetti, S. and Greider, C. W. (1996). Human telomerase RNA and telomerase activity in immortal cell lines and tumor tissues. *Cancer Res* **56**(3): 645-50.
- Baas, A. S. and Berk, B. C. (1995). Differential activation of mitogen-activated protein kinases by H₂O₂ and O₂⁻ in vascular smooth muscle cells. *Circ Res* **77**(1): 29-36.
- Bae, Y. S., Kang, S. W., Seo, M. S., Baines, I. C., Tekle, E., Chock, P. B. and Rhee, S. G. (1997). Epidermal growth factor (EGF)-induced generation of hydrogen peroxide. Role in EGF receptor-mediated tyrosine phosphorylation. *J Biol Chem* **272**(1): 217-21.
- Baichwal, V. R. and Baeuerle, P. A. (1997). Activate NF-kappa B or die? *Curr Biol* **7**(2): R94-6.
- Balin, A. K., Fisher, A. J. and Carter, D. M. (1984). Oxygen modulates growth of human cells at physiologic partial pressures. *J Exp Med* **160**(1): 152-66.
- Bayreuther, K., Rodemann, H. P., Hommel, R., Dittmann, K., Albiez, M. and Francz, P. I. (1988). Human skin fibroblasts in vitro differentiate along a terminal cell lineage. *Proc Natl Acad Sci U S A* **85**(14): 5112-6.
- Beijersbergen van Henegouwen, G. M., Wijn, E. T., Schoonderwoerd, S. A. and Dall'Acqua, F. (1989). A method for the determination of PUVA-induced in vivo irreversible binding of 8-methoxypsoralen (8-MOP) to epidermal lipids, proteins and DNA/RNA. *J Photochem Photobiol B* **3**(4): 631-5.
- Blackburn, E. H. (1991). Structure and function of telomeres. *Nature* **350**(6319): 569-73.

- Blackburn, E. H. (2000). Telomere states and cell fates. *Nature* **408**(6808): 53-6.
- Bodnar, A. G., Ouellette, M., Frolkis, M., Holt, S. E., Chiu, C. P., Morin, G. B., Harley, C. B., Shay, J. W., Lichtsteiner, S. and Wright, W. E. (1998). Extension of life-span by introduction of telomerase into normal human cells. *Science* **279**(5349): 349-52.
- Bond, J. A., Wyllie, F. S. and Wynford-Thomas, D. (1994). Escape from senescence in human diploid fibroblasts induced directly by mutant p53. *Oncogene* **9**(7): 1885-9.
- Brack, C., Lithgow, G., Osiewacz, H. and Toussaint, O. (2000). EMBO WORKSHOP REPORT: Molecular and cellular gerontology Serpiano, Switzerland, September 18-22, 1999. *Embo J* **19**(9): 1929-34.
- Bringold, F. and Serrano, M. (2000). Tumor suppressors and oncogenes in cellular senescence. *Exp Gerontol* **35**(3): 317-29.
- Broccoli, D., Smogorzewska, A., Chong, L. and de Lange, T. (1997). Human telomeres contain two distinct Myb-related proteins, TRF1 and TRF2. *Nat Genet* **17**(2): 231-5.
- Brown, J. P., Wei, W. and Sedivy, J. M. (1997). Bypass of senescence after disruption of p21^{CIP1}/WAF1 gene in normal diploid human fibroblasts. *Science* **277**(5327): 831-4.
- Brown, M. R., Miller, F. J., Jr., Li, W. G., Ellingson, A. N., Mozena, J. D., Chatterjee, P., Engelhardt, J. F., Zwacka, R. M., Oberley, L. W., Fang, X., Spector, A. A. and Weintraub, N. L. (1999). Overexpression of human catalase inhibits proliferation and promotes apoptosis in vascular smooth muscle cells. *Circ Res* **85**(6): 524-33.
- Bryan, T. M., Englezou, A., Dalla-Pozza, L., Dunham, M. A. and Reddel, R. R. (1997). Evidence for an alternative mechanism for maintaining telomere length in human tumors and tumor-derived cell lines. *Nat Med* **3**(11): 1271-4.
- Bryan, T. M., Englezou, A., Gupta, J., Bacchetti, S. and Reddel, R. R. (1995). Telomere elongation in immortal human cells without detectable telomerase activity. *Embo J* **14**(17): 4240-8.
- Campisi, J. (1996). Replicative senescence: an old lives' tale? *Cell* **84**(4): 497-500.
- Campisi, J. (1997). The biology of replicative senescence. *Eur J Cancer* **33**(5): 703-9.
- Campisi, J. (1998). The role of cellular senescence in skin aging. *J Investig Dermatol Symp Proc* **3**(1): 1-5.
- Campisi, J. (2000). Cancer, aging and cellular senescence. *In Vivo* **14**(1): 183-8.

- Campisi, J. (2001a). Cellular senescence as a tumor-suppressor mechanism. *Trends Cell Biol* **11**(11): S27-31.
- Campisi, J. (2001b). From cells to organisms: can we learn about aging from cells in culture? *Exp Gerontol* **36**(4-6): 607-18.
- Campisi, J., Dimri, G. P. and Hara, E. (1996). Control of replicative senescence. *Handbook of the biology of aging*. E. Schneider and J. Rowe. New York, Academic Press: 121-49.
- Campisi, J., Kim, S. H., Lim, C. S. and Rubio, M. (2001). Cellular senescence, cancer and aging: the telomere connection. *Exp Gerontol* **36**(10): 1619-37.
- Chen, J., Jackson, P. K., Kirschner, M. W. and Dutta, A. (1995a). Separate domains of p21 involved in the inhibition of Cdk kinase and PCNA. *Nature* **374**(6520): 386-8.
- Chen, Q. M. (2000). Replicative senescence and oxidant-induced premature senescence. Beyond the control of cell cycle checkpoints. *Ann N Y Acad Sci* **908**: 111-25.
- Chen, Q. M. and Ames, B. N. (1994). Senescence-like growth arrest induced by hydrogen peroxide in human diploid fibroblast F65 cells. *Proc Natl Acad Sci U S A* **91**(10): 4130-4.
- Chen, Q. M., Bartholomew, J. C., Campisi, J., Acosta, M., Reagan, J. D. and Ames, B. N. (1998). Molecular analysis of H₂O₂-induced senescent-like growth arrest in normal human fibroblasts: p53 and Rb control G1 arrest but not cell replication. *Biochem J* **332** (Pt 1): 43-50.
- Chen, Q. M., Fischer, A., Reagan, J. D., Yan, L. J. and Ames, B. N. (1995b). Oxidative DNA damage and senescence of human diploid fibroblast cells. *Proc Natl Acad Sci U S A* **92**(10): 4337-41.
- Chien, M., Rinker-Schaeffer, C. and Stadler, W. M. (2000). A G2/M growth arrest response to low-dose intermittent H₂O₂ in normal uroepithelial cells. *Int J Oncol* **17**(3): 425-32.
- Chiu, C. P. and Harley, C. B. (1997). Replicative senescence and cell immortality: the role of telomeres and telomerase. *Proc Soc Exp Biol Med* **214**(2): 99-106.
- Cho, H. J., Jeong, H. G., Lee, J. S., Woo, E. R., Hyun, J. W., Chung, M. H. and You, H. J. (2002). Oncogenic H-Ras enhances DNA repair through the Ras/phosphatidylinositol 3-kinase/Rac1 pathway in NIH3T3 cells. Evidence for association with reactive oxygen species. *J Biol Chem* **277**(22): 19358-66.
- Chong, L., van Steensel, B., Broccoli, D., Erdjument-Bromage, H., Hanish, J., Tempst, P. and de Lange, T. (1995). A human telomeric protein. *Science* **270**(5242): 1663-7.
- Cominacini, L., Pasini, A. F., Garbin, U., Davoli, A., Tosetti, M. L., Campagnola, M., Rigoni, A., Pastorino, A. M., Lo Cascio, V. and Sawamura, T. (2000).

- Oxidized low density lipoprotein (ox-LDL) binding to ox-LDL receptor-1 in endothelial cells induces the activation of NF-kappaB through an increased production of intracellular reactive oxygen species. *J Biol Chem* **275**(17): 12633-8.
- Cong, Y. S., Wright, W. E. and Shay, J. W. (2002). Human telomerase and its regulation. *Microbiol Mol Biol Rev* **66**(3): 407-25, table of contents.
- Counter, C. M., Avilion, A. A., LeFeuvre, C. E., Stewart, N. G., Greider, C. W., Harley, C. B. and Bacchetti, S. (1992). Telomere shortening associated with chromosome instability is arrested in immortal cells which express telomerase activity. *Embo J* **11**(5): 1921-9.
- Cristofalo, V. J., Allen, R. G., Pignolo, R. J., Martin, B. G. and Beck, J. C. (1998). Relationship between donor age and the replicative lifespan of human cells in culture: a reevaluation. *Proc Natl Acad Sci U S A* **95**(18): 10614-9.
- Cullinane, C. and Bohr, V. A. (1998). DNA interstrand cross-links induced by psoralen are not repaired in mammalian mitochondria. *Cancer Res* **58**(7): 1400-4.
- de Boer, J., Andressoo, J. O., de Wit, J., Huijmans, J., Beems, R. B., van Steeg, H., Weeda, G., van der Horst, G. T., van Leeuwen, W., Themmen, A. P., Meradji, M. and Hoeijmakers, J. H. (2002). Premature aging in mice deficient in DNA repair and transcription. *Science* **296**(5571): 1276-9.
- Di Leonardo, A., Linke, S. P., Clarkin, K. and Wahl, G. M. (1994). DNA damage triggers a prolonged p53-dependent G1 arrest and long-term induction of Cip1 in normal human fibroblasts. *Genes Dev* **8**(21): 2540-51.
- Dickson, M. A., Hahn, W. C., Ino, Y., Ronfard, V., Wu, J. Y., Weinberg, R. A., Louis, D. N., Li, F. P. and Rheinwald, J. G. (2000). Human keratinocytes that express hTERT and also bypass a p16(INK4a)-enforced mechanism that limits life span become immortal yet retain normal growth and differentiation characteristics. *Mol Cell Biol* **20**(4): 1436-47.
- Dimri, G. P., Itahana, K., Acosta, M. and Campisi, J. (2000). Regulation of a senescence checkpoint response by the E2F1 transcription factor and p14(ARF) tumor suppressor. *Mol Cell Biol* **20**(1): 273-85.
- Dimri, G. P., Lee, X., Basile, G., Acosta, M., Scott, G., Roskelley, C., Medrano, E. E., Linskens, M., Rubelj, I., Pereira-Smith, O. and et al. (1995). A biomarker that identifies senescent human cells in culture and in aging skin in vivo. *Proc Natl Acad Sci U S A* **92**(20): 9363-7.
- Dubrana, K., Perrod, S. and Gasser, S. M. (2001). Turning telomeres off and on. *Curr Opin Cell Biol* **13**(3): 281-9.
- Dumont, P., Burton, M., Chen, Q. M., Gonos, E. S., Fripiat, C., Mazarati, J. B., Eliaers, F., Remacle, J. and Toussaint, O. (2000). Induction of replicative senescence biomarkers by sublethal oxidative stresses in normal human fibroblast. *Free Radic Biol Med* **28**(3): 361-73.

- Dumont, P., Royer, V., Pascal, T., Dierick, J. F., Chainiaux, F., Fripiat, C., de Magalhaes, J. P., Eliaers, F., Remacle, J. and Toussaint, O. (2001). Growth kinetics rather than stress accelerate telomere shortening in cultures of human diploid fibroblasts in oxidative stress-induced premature senescence. *FEBS Lett* **502**(3): 109-12.
- Edelson, R., Berger, C., Gasparro, F., Jegasothy, B., Heald, P., Wintroub, B., Vonderheid, E., Knobler, R., Wolff, K., Plewig, G. and et al. (1987). Treatment of cutaneous T-cell lymphoma by extracorporeal photochemotherapy. Preliminary results. *N Engl J Med* **316**(6): 297-303.
- Feng, J., Funk, W. D., Wang, S. S., Weinrich, S. L., Avilion, A. A., Chiu, C. P., Adams, R. R., Chang, E., Allsopp, R. C., Yu, J. and et al. (1995). The RNA component of human telomerase. *Science* **269**(5228): 1236-41.
- Ferbeyre, G., de Stanchina, E., Querido, E., Baptiste, N., Prives, C. and Lowe, S. W. (2000). PML is induced by oncogenic ras and promotes premature senescence. *Genes Dev* **14**(16): 2015-27.
- Fernandez-Moreno, M. A., Bornstein, B., Campos, Y., Arenas, J. and Garesse, R. (2000). The pathogenic role of point mutations affecting the translational initiation codon of mitochondrial genes. *Mol Genet Metab* **70**(3): 238-40.
- Finkel, T. (1999). Signal transduction by reactive oxygen species in non-phagocytic cells. *J Leukoc Biol* **65**(3): 337-40.
- Fleischmajer, R., Perlish, J. S., Krieg, T. and Timpl, R. (1981). Variability in collagen and fibronectin synthesis by scleroderma fibroblasts in primary culture. *J Invest Dermatol* **76**(5): 400-3.
- Frenkel, K. and Gleichauf, C. (1991). Hydrogen peroxide formation by cells treated with a tumor promoter. *Free Radic Res Commun* **12-13 Pt 2**: 783-94.
- Gasparro, F. P. (1988). Psoralen DNA interactions: Thermodynamics and photochemistry. *Psoralen DNA photobiology*. F. P. Gasparro, CRC Press, Inc.: 5-36.
- Gasparro, F. P., Chan, G. and Edelson, R. L. (1985). Phototherapy and photopharmacology. *Yale J Biol Med* **58**(6): 519-34.
- Gasparro, F. P., Felli, A. and Schmitt, I. M. (1997). Psoralen photobiology: the relationship between DNA damage, chromatin structure, transcription, and immunogenic effects. *Recent Results Cancer Res* **143**: 101-27.
- Gasparro, F. P., Liao, B., Foley, P. J., Wang, X. M. and McNiff, J. M. (1998). Psoralen photochemotherapy, clinical efficacy, and photomutagenicity: the role of molecular epidemiology in minimizing risks. *Environ Mol Mutagen* **31**(2): 105-12.
- Geiszt, M., Kopp, J. B., Varnai, P. and Leto, T. L. (2000). Identification of renox, an NAD(P)H oxidase in kidney. *Proc Natl Acad Sci U S A* **97**(14): 8010-4.

- Gire, V. and Wynford-Thomas, D. (1998). Reinitiation of DNA synthesis and cell division in senescent human fibroblasts by microinjection of anti-p53 antibodies. *Mol Cell Biol* **18**(3): 1611-21.
- Goldstein, S. (1990). Replicative senescence: the human fibroblast comes of age. *Science* **249**(4973): 1129-33.
- Goytisolo, F. A., Samper, E., Edmonson, S., Taccioli, G. E. and Blasco, M. A. (2001). The absence of the dna-dependent protein kinase catalytic subunit in mice results in anaphase bridges and in increased telomeric fusions with normal telomere length and G-strand overhang. *Mol Cell Biol* **21**(11): 3642-51.
- Greider, C. W. and Blackburn, E. H. (1985). Identification of a specific telomere terminal transferase activity in Tetrahymena extracts. *Cell* **43**(2 Pt 1): 405-13.
- Hagen, T. M., Yowe, D. L., Bartholomew, J. C., Wehr, C. M., Do, K. L., Park, J. Y. and Ames, B. N. (1997). Mitochondrial decay in hepatocytes from old rats: membrane potential declines, heterogeneity and oxidants increase. *Proc Natl Acad Sci U S A* **94**(7): 3064-9.
- Hanahan, D. and Weinberg, R. A. (2000). The hallmarks of cancer. *Cell* **100**(1): 57-70.
- Hannuksela-Svahn, A., Paakko, P., Autio, P., Reunala, T., Karvonen, J. and Vahakangas, K. (1999). Expression of p53 protein before and after PUVA treatment in psoriasis. *Acta Derm Venereol* **79**(3): 195-9.
- Harley, C. B., Futcher, A. B. and Greider, C. W. (1990). Telomeres shorten during ageing of human fibroblasts. *Nature* **345**(6274): 458-60.
- Harley, C. B., Vaziri, H., Counter, C. M. and Allsopp, R. C. (1992). The telomere hypothesis of cellular aging. *Exp Gerontol* **27**(4): 375-82.
- Harley, C. B. and Villeponteau, B. (1995). Telomeres and telomerase in aging and cancer. *Curr Opin Genet Dev* **5**(2): 249-55.
- Harper, J. W., Adami, G. R., Wei, N., Keyomarsi, K. and Elledge, S. J. (1993). The p21 Cdk-interacting protein Cip1 is a potent inhibitor of G1 cyclin-dependent kinases. *Cell* **75**(4): 805-16.
- Harrington, L., Zhou, W., McPhail, T., Oulton, R., Yeung, D. S., Mar, V., Bass, M. B. and Robinson, M. O. (1997). Human telomerase contains evolutionarily conserved catalytic and structural subunits. *Genes Dev* **11**(23): 3109-15.
- Hart, R. W. and Setlow, R. B. (1974). Correlation between deoxyribonucleic acid excision-repair and life-span in a number of mammalian species. *Proc Natl Acad Sci U S A* **71**(6): 2169-73.
- Hayflick, L. (1965). The limited in vitro life-time of human diploid cell strains. *Exp Cell Res* **37**: 614-36.

- Hayflick, L. (1998). How and why we age. *Exp Gerontol* **33**(7-8): 639-53.
- Hayflick, L. and Moorhead, P. S. (1961). The serial cultivation of human diploid cell strains. *Exp Cell Res* **25**: 585-621.
- Herrmann, G., Brenneisen, P., Wlaschek, M., Wenk, J., Faisst, K., Quel, G., Hommel, C., Goerz, G., Ruzicka, T., Krieg, T., Sies, H. and Scharffetter-Kochanek, K. (1998). Psoralen photoactivation promotes morphological and functional changes in fibroblasts in vitro reminiscent of cellular senescence. *J Cell Sci* **111** (Pt 6): 759-67.
- Ho, H. Y., Cheng, M. L., Lu, F. J., Chou, Y. H., Stern, A., Liang, C. M. and Chiu, D. T. (2000). Enhanced oxidative stress and accelerated cellular senescence in glucose-6-phosphate dehydrogenase (G6PD)-deficient human fibroblasts. *Free Radic Biol Med* **29**(2): 156-69.
- Hoeijmakers, J. H. (2001). Genome maintenance mechanisms for preventing cancer. *Nature* **411**(6835): 366-74.
- Honig, B., Morison, W. L. and Karp, D. (1994). Photochemotherapy beyond psoriasis. *J Am Acad Dermatol* **31**(5 Pt 1): 775-90.
- Honigsmann, H. (1986). Psoralen photochemotherapy--mechanisms, drugs, toxicity. *Curr Probl Dermatol* **15**: 52-66.
- Honigsmann, H. (2001). Phototherapy for psoriasis. *Clin Exp Dermatol* **26**(4): 343-50.
- Hsu, H. L., Gilley, D., Blackburn, E. H. and Chen, D. J. (1999). Ku is associated with the telomere in mammals. *Proc Natl Acad Sci U S A* **96**(22): 12454-8.
- Hyodo, M., Zanma, T., Hori, T., Yoshino, K. and Suzuki, K. (1982). DNA crosslinks and DNA replication in mouse FM3A cells after treatment with 8-methoxypsoralen plus near-ultraviolet radiation. *Biochim Biophys Acta* **699**(2): 164-9.
- Irani, K., Xia, Y., Zweier, J. L., Sollott, S. J., Der, C. J., Fearon, E. R., Sundaresan, M., Finkel, T. and Goldschmidt-Clermont, P. J. (1997). Mitogenic signaling mediated by oxidants in Ras-transformed fibroblasts. *Science* **275**(5306): 1649-52.
- Jacobson-Kram, D., Roe, J. L., Williams, J. R., Gange, R. W. and Parrish, J. A. (1982). Decreased in-vitro lifespan of fibroblasts derived from skin exposed to photochemotherapy in vivo. *Lancet* **2**(8312): 1399-400.
- Johnson, F. B., Sinclair, D. A. and Guarente, L. (1999). Molecular biology of aging. *Cell* **96**(2): 291-302.
- Kapahi, P., Boulton, M. E. and Kirkwood, T. B. (1999). Positive correlation between mammalian life span and cellular resistance to stress. *Free Radic Biol Med* **26**(5-6): 495-500.

- Karlseder, J., Broccoli, D., Dai, Y., Hardy, S. and de Lange, T. (1999). p53- and ATM-dependent apoptosis induced by telomeres lacking TRF2. *Science* **283**(5406): 1321-5.
- Kass-Eisler, A. and Greider, C. W. (2000). Recombination in telomere-length maintenance. *Trends Biochem Sci* **25**(4): 200-4.
- Kim, N. W., Piatyszek, M. A., Prowse, K. R., Harley, C. B., West, M. D., Ho, P. L., Coviello, G. M., Wright, W. E., Weinrich, S. L. and Shay, J. W. (1994). Specific association of human telomerase activity with immortal cells and cancer. *Science* **266**(5193): 2011-5.
- Kim, S. H., Kaminker, P. and Campisi, J. (2002). Telomeres, aging and cancer: in search of a happy ending. *Oncogene* **21**(4): 503-11.
- King, M. P. and Attardi, G. (1989). Human cells lacking mtDNA: repopulation with exogenous mitochondria by complementation. *Science* **246**(4929): 500-3.
- Kiyono, T., Foster, S. A., Koop, J. I., McDougall, J. K., Galloway, D. A. and Klingelutz, A. J. (1998). Both Rb/p16INK4a inactivation and telomerase activity are required to immortalize human epithelial cells. *Nature* **396**(6706): 84-8.
- Klapper, W., Parwaresch, R. and Krupp, G. (2001). Telomere biology in human aging and aging syndromes. *Mech Ageing Dev* **122**(7): 695-712.
- Kligman, A. M. (1969). Early destructive effect of sunlight on human skin. *Jama* **210**(13): 2377-80.
- Kricka, L. J. (1988). Clinical and biochemical applications of luciferases and luciferins. *Anal Biochem* **175**(1): 14-21.
- Laskin, J. D. and Lee, E. (1991). Psoralen binding and inhibition of epidermal growth factor binding by psoralen/ultraviolet light (PUVA) in human epithelial cells. *Biochem Pharmacol* **41**(1): 125-32.
- LeBel, C. P., Ischiropoulos, H. and Bondy, S. C. (1992). Evaluation of the probe 2',7'-dichlorofluorescein as an indicator of reactive oxygen species formation and oxidative stress. *Chem Res Toxicol* **5**(2): 227-31.
- Lee, A. C., Fenster, B. E., Ito, H., Takeda, K., Bae, N. S., Hirai, T., Yu, Z. X., Ferrans, V. J., Howard, B. H. and Finkel, T. (1999). Ras proteins induce senescence by altering the intracellular levels of reactive oxygen species. *J Biol Chem* **274**(12): 7936-40.
- Lerner, A. B. (1988). Comments on the history of the psoralens. *Psoralen DNA photobiology*. F. P. Gasparro, CRC Press, Inc.: 5-36.
- Lingner, J., Hughes, T. R., Shevchenko, A., Mann, M., Lundblad, V. and Cech, T. R. (1997). Reverse transcriptase motifs in the catalytic subunit of telomerase. *Science* **276**(5312): 561-7.

- Liu, X. H., Yao, S., Kirschenbaum, A. and Levine, A. C. (1998). NS398, a selective cyclooxygenase-2 inhibitor, induces apoptosis and down-regulates bcl-2 expression in LNCaP cells. *Cancer Res* **58**(19): 4245-9.
- Lloyd, A. C. (2002). Limits to lifespan. *Nat Cell Biol* **4**(2): E25-7.
- Lundberg, A. S., Hahn, W. C., Gupta, P. and Weinberg, R. A. (2000). Genes involved in senescence and immortalization. *Curr Opin Cell Biol* **12**(6): 705-9.
- Ma, Y., Prigent, S. A., Born, T. L., Monell, C. R., Feramisco, J. R. and Bertolaet, B. L. (1999). Microinjection of anti-p21 antibodies induces senescent Hs68 human fibroblasts to synthesize DNA but not to divide. *Cancer Res* **59**(20): 5341-8.
- Macip, S., Igarashi, M., Fang, L., Chen, A., Pan, Z. Q., Lee, S. W. and Aaronson, S. A. (2002). Inhibition of p21-mediated ROS accumulation can rescue p21-induced senescence. *Embo J* **21**(9): 2180-8.
- Makarov, V. L., Hirose, Y. and Langmore, J. P. (1997). Long G tails at both ends of human chromosomes suggest a C strand degradation mechanism for telomere shortening. *Cell* **88**(5): 657-66.
- Martin, J. B. (1970). Commissioner on aging stresses complexity of problems of elderly. *Geriatrics* **25**(11): 41 passim.
- Maser, R. S. and DePinho, R. A. (2002). Connecting chromosomes, crisis, and cancer. *Science* **297**(5581): 565-9.
- Mathon, N. F. and Lloyd, A. C. (2001). Cell senescence and cancer. *Nat Rev Cancer* **1**(3): 203-13.
- Michishita, E., Nakabayashi, K., Suzuki, T., Kaul, S. C., Ogino, H., Fujii, M., Mitsui, Y. and Ayusawa, D. (1999). 5-Bromodeoxyuridine induces senescence-like phenomena in mammalian cells regardless of cell type or species. *J Biochem (Tokyo)* **126**(6): 1052-9.
- Modestou, M., Puig-Antich, V., Korgaonkar, C., Eapen, A. and Quelle, D. E. (2001). The alternative reading frame tumor suppressor inhibits growth through p21-dependent and p21-independent pathways. *Cancer Res* **61**(7): 3145-50.
- Munro, J., Steeghs, K., Morrison, V., Ireland, H. and Parkinson, E. K. (2001). Human fibroblast replicative senescence can occur in the absence of extensive cell division and short telomeres. *Oncogene* **20**(27): 3541-52.
- Nishio, E. and Watanabe, Y. (1997). The involvement of reactive oxygen species and arachidonic acid in alpha 1-adrenoceptor-induced smooth muscle cell proliferation and migration. *Br J Pharmacol* **121**(4): 665-70.
- Noble, J. R., Rogan, E. M., Neumann, A. A., Maclean, K., Bryan, T. M. and Reddel, R. R. (1996). Association of extended in vitro proliferative potential with loss of p16INK4 expression. *Oncogene* **13**(6): 1259-68.

- Ogryzko, V. V., Hirai, T. H., Russanova, V. R., Barbie, D. A. and Howard, B. H. (1996). Human fibroblast commitment to a senescence-like state in response to histone deacetylase inhibitors is cell cycle dependent. *Mol Cell Biol* **16**(9): 5210-8.
- Ohtani, N., Zebedee, Z., Huot, T. J., Stinson, J. A., Sugimoto, M., Ohashi, Y., Sharrocks, A. D., Peters, G. and Hara, E. (2001). Opposing effects of Ets and Id proteins on p16INK4a expression during cellular senescence. *Nature* **409**(6823): 1067-70.
- Patterson, C., Ruef, J., Madamanchi, N. R., Barry-Lane, P., Hu, Z., Horaist, C., Ballinger, C. A., Brasier, A. R., Bode, C. and Runge, M. S. (1999). Stimulation of a vascular smooth muscle cell NAD(P)H oxidase by thrombin. Evidence that p47(phox) may participate in forming this oxidase in vitro and in vivo. *J Biol Chem* **274**(28): 19814-22.
- Pearson, M., Carbone, R., Sebastiani, C., Cioce, M., Fagioli, M., Saito, S., Higashimoto, Y., Appella, E., Minucci, S., Pandolfi, P. P. and Pelicci, P. G. (2000). PML regulates p53 acetylation and premature senescence induced by oncogenic Ras. *Nature* **406**(6792): 207-10.
- Proctor, C. J. and Kirkwood, T. B. (2002). Modelling telomere shortening and the role of oxidative stress. *Mech Ageing Dev* **123**(4): 351-63.
- Ramirez, R. D., Morales, C. P., Herbert, B. S., Rohde, J. M., Passons, C., Shay, J. W. and Wright, W. E. (2001). Putative telomere-independent mechanisms of replicative aging reflect inadequate growth conditions. *Genes Dev* **15**(4): 398-403.
- Rasheed, S., Nelson-Rees, W. A., Toth, E. M., Arnstein, P. and Gardner, M. B. (1974). Characterization of a newly derived human sarcoma cell line (HT-1080). *Cancer* **33**(4): 1027-33.
- Reers, M., Smiley, S. T., Mottola-Hartshorn, C., Chen, A., Lin, M. and Chen, L. B. (1995). Mitochondrial membrane potential monitored by JC-1 dye. *Methods Enzymol* **260**: 406-17.
- Reers, M., Smith, T. W. and Chen, L. B. (1991). J-aggregate formation of a carbocyanine as a quantitative fluorescent indicator of membrane potential. *Biochemistry* **30**(18): 4480-6.
- Rohme, D. (1981). Evidence for a relationship between longevity of mammalian species and life spans of normal fibroblasts in vitro and erythrocytes in vivo. *Proc Natl Acad Sci U S A* **78**(8): 5009-13.
- Saito, H., Hammond, A. T. and Moses, R. E. (1995). The effect of low oxygen tension on the in vitro-replicative life span of human diploid fibroblast cells and their transformed derivatives. *Exp Cell Res* **217**(2): 272-9.
- Saitoh, Y., Goto, T., Pudukall, V. K., Murakami, M., Kochi, M., Levin, V. A., Kyritsis, A. P. and Ushio, Y. (1999). Induction of apoptosis by N-(4-hydroxyphenyl)retinamide in glioma cells. *Int J Oncol* **15**(3): 499-504.

- Salvioli, S., Ardizzoni, A., Franceschi, C. and Cossarizza, A. (1997). JC-1, but not DiOC6(3) or rhodamine 123, is a reliable fluorescent probe to assess delta psi changes in intact cells: implications for studies on mitochondrial functionality during apoptosis. *FEBS Lett* **411**(1): 77-82.
- Samper, E., Goytisolo, F. A., Slijepcevic, P., van Buul, P. P. and Blasco, M. A. (2000). Mammalian Ku86 protein prevents telomeric fusions independently of the length of TTAGGG repeats and the G-strand overhang. *EMBO Rep* **1**(3): 244-52.
- Saretzki, G. and von Zglinicki, T. (2002). Replicative aging, telomeres, and oxidative stress. *Ann N Y Acad Sci* **959**: 24-9.
- Scharffetter-Kochanek, K., Brenneisen, P., Wenk, J., Herrmann, G., Ma, W., Kuhr, L., Meewes, C. and Wlaschek, M. (2000). Photoaging of the skin from phenotype to mechanisms. *Exp Gerontol* **35**(3): 307-16.
- Schmitt, I. M., Chimenti, S. and Gasparro, F. P. (1995). Psoralen-protein photochemistry--a forgotten field. *J Photochem Photobiol B* **27**(2): 101-7.
- Schulz, V. P., Zakian, V. A., Ogburn, C. E., McKay, J., Jarzebowicz, A. A., Edland, S. D. and Martin, G. M. (1996). Accelerated loss of telomeric repeats may not explain accelerated replicative decline of Werner syndrome cells. *Hum Genet* **97**(6): 750-4.
- Schwartz, E., Cruickshank, F. A., Christensen, C. C., Perlish, J. S. and Lebwohl, M. (1993). Collagen alterations in chronically sun-damaged human skin. *Photochem Photobiol* **58**(6): 841-4.
- Serrano, M. and Blasco, M. A. (2001). Putting the stress on senescence. *Curr Opin Cell Biol* **13**(6): 748-53.
- Serrano, M., Lin, A. W., McCurrach, M. E., Beach, D. and Lowe, S. W. (1997). Oncogenic ras provokes premature cell senescence associated with accumulation of p53 and p16INK4a. *Cell* **88**(5): 593-602.
- Shay, J. W. (1987). Cell enucleation, cybrids, reconstituted cells, and nuclear hybrids. *Methods Enzymol* **151**: 221-37.
- Shay, J. W., Pereira-Smith, O. M. and Wright, W. E. (1991a). A role for both RB and p53 in the regulation of human cellular senescence. *Exp Cell Res* **196**(1): 33-9.
- Shay, J. W. and Wright, W. E. (2000). Hayflick, his limit, and cellular ageing. *Nat Rev Mol Cell Biol* **1**(1): 72-6.
- Shay, J. W., Wright, W. E. and Werbin, H. (1991b). Defining the molecular mechanisms of human cell immortalization. *Biochim Biophys Acta* **1072**(1): 1-7.
- Shay, M., Braester, A. and Cohen, I. (1991c). Dermatomyositis as presenting symptom of Hodgkin's disease. *Ann Hematol* **63**(2): 116-8.

- Shelton, D. N., Chang, E., Whittier, P. S., Choi, D. and Funk, W. D. (1999). Microarray analysis of replicative senescence. *Curr Biol* **9**(17): 939-45.
- Shen, E. L. and Bogenhagen, D. F. (2001). Developmentally-regulated packaging of mitochondrial DNA by the HMG-box protein mtTFA during *Xenopus* oogenesis. *Nucleic Acids Res* **29**(13): 2822-8.
- Shen, S. X., Weaver, Z., Xu, X., Li, C., Weinstein, M., Chen, L., Guan, X. Y., Ried, T. and Deng, C. X. (1998). A targeted disruption of the murine *Brca1* gene causes gamma-irradiation hypersensitivity and genetic instability. *Oncogene* **17**(24): 3115-24.
- Shiloh, Y., Tabor, E. and Becker, Y. (1985). In vitro phenotype of ataxia-telangiectasia (AT) fibroblast strains: clues to the nature of the "AT DNA lesion" and the molecular defect in AT. *Kroc Found Ser* **19**: 111-21.
- Smiley, S. T., Reers, M., Mottola-Hartshorn, C., Lin, M., Chen, A., Smith, T. W., Steele, G. D., Jr. and Chen, L. B. (1991). Intracellular heterogeneity in mitochondrial membrane potentials revealed by a J-aggregate-forming lipophilic cation JC-1. *Proc Natl Acad Sci U S A* **88**(9): 3671-5.
- Smith, J. R. and Pereira-Smith, O. M. (1996). Replicative senescence: implications for in vivo aging and tumor suppression. *Science* **273**(5271): 63-7.
- Song, K., Jung, D., Jung, Y., Lee, S. G. and Lee, I. (2000). Interaction of human Ku70 with TRF2. *FEBS Lett* **481**(1): 81-5.
- Song, P. S. and Tapley, K. J., Jr. (1979). Photochemistry and photobiology of psoralens. *Photochem Photobiol* **29**(6): 1177-97.
- Staal, F. J., Roederer, M. and Herzenberg, L. A. (1990). Intracellular thiols regulate activation of nuclear factor kappa B and transcription of human immunodeficiency virus. *Proc Natl Acad Sci U S A* **87**(24): 9943-7.
- Stanulis-Praeger, B. M. (1987). Cellular senescence revisited: a review. *Mech Ageing Dev* **38**(1): 1-48.
- Stein, G. H., Drullinger, L. F., Soulard, A. and Dulic, V. (1999). Differential roles for cyclin-dependent kinase inhibitors p21 and p16 in the mechanisms of senescence and differentiation in human fibroblasts. *Mol Cell Biol* **19**(3): 2109-17.
- Stern, R. S. and Laird, N. (1994). The carcinogenic risk of treatments for severe psoriasis. Photochemotherapy Follow-up Study. *Cancer* **73**(11): 2759-64.
- Suh, Y. A., Arnold, R. S., Lassegue, B., Shi, J., Xu, X., Sorescu, D., Chung, A. B., Griendling, K. K. and Lambeth, J. D. (1999). Cell transformation by the superoxide-generating oxidase Mox1. *Nature* **401**(6748): 79-82.

- Sulciner, D. J., Irani, K., Yu, Z. X., Ferrans, V. J., Goldschmidt-Clermont, P. and Finkel, T. (1996). *rac1* regulates a cytokine-stimulated, redox-dependent pathway necessary for NF-kappaB activation. *Mol Cell Biol* **16**(12): 7115-21.
- Sundaresan, M., Yu, Z. X., Ferrans, V. J., Irani, K. and Finkel, T. (1995). Requirement for generation of H₂O₂ for platelet-derived growth factor signal transduction. *Science* **270**(5234): 296-9.
- Tokura, Y., Edelson, R. L. and Gasparro, F. P. (1991). Formation and removal of 8-MOP-DNA photoadducts in keratinocytes: effects of calcium concentration and retinoids. *J Invest Dermatol* **96**(6): 942-9.
- Toussaint, O., Dumont, P., Dierick, J. F., Pascal, T., Fripiat, C., Chainiaux, F., Magalhaes, J. P., Eliaers, F. and Remacle, J. (2000a). Stress-induced premature senescence as alternative toxicological method for testing the long-term effects of molecules under development in the industry. *Biogerontology* **1**(2): 179-83.
- Toussaint, O., Dumont, P., Dierick, J. F., Pascal, T., Fripiat, C., Chainiaux, F., Sluse, F., Eliaers, F. and Remacle, J. (2000b). Stress-induced premature senescence. Essence of life, evolution, stress, and aging. *Ann N Y Acad Sci* **908**: 85-98.
- Toussaint, O., Medrano, E. E. and von Zglinicki, T. (2000c). Cellular and molecular mechanisms of stress-induced premature senescence (SIPS) of human diploid fibroblasts and melanocytes. *Exp Gerontol* **35**(8): 927-45.
- Tsai, J. C., Jain, M., Hsieh, C. M., Lee, W. S., Yoshizumi, M., Patterson, C., Perrella, M. A., Cooke, C., Wang, H., Haber, E., Schlegel, R. and Lee, M. E. (1996). Induction of apoptosis by pyrrolidinedithiocarbamate and N-acetylcysteine in vascular smooth muscle cells. *J Biol Chem* **271**(7): 3667-70.
- van Steensel, B., Smogorzewska, A. and de Lange, T. (1998). TRF2 protects human telomeres from end-to-end fusions. *Cell* **92**(3): 401-13.
- Vaziri, H. and Benchimol, S. (1998). Reconstitution of telomerase activity in normal human cells leads to elongation of telomeres and extended replicative life span. *Curr Biol* **8**(5): 279-82.
- Vaziri, H., West, M. D., Allsopp, R. C., Davison, T. S., Wu, Y. S., Arrowsmith, C. H., Poirier, G. G. and Benchimol, S. (1997). ATM-dependent telomere loss in aging human diploid fibroblasts and DNA damage lead to the post-translational activation of p53 protein involving poly(ADP-ribose) polymerase. *Embo J* **16**(19): 6018-33.
- Veomett, G. E. (1982). *Techniques in Somatic Cell Genetics*. J. W. Shay. New York, Plenum: 67.
- von Zglinicki, T. (2000). Role of oxidative stress in telomere length regulation and replicative senescence. *Ann N Y Acad Sci* **908**: 99-110.

- von Zglinicki, T. (2002). Oxidative stress shortens telomeres. *Trends Biochem Sci* **27**(7): 339-44.
- von Zglinicki, T., Pilger, R. and Sitte, N. (2000). Accumulation of single-strand breaks is the major cause of telomere shortening in human fibroblasts. *Free Radic Biol Med* **28**(1): 64-74.
- von Zglinicki, T., Saretzki, G., Docke, W. and Lotze, C. (1995). Mild hyperoxia shortens telomeres and inhibits proliferation of fibroblasts: a model for senescence? *Exp Cell Res* **220**(1): 186-93.
- Weinberg, R. A. (1989). Oncogenes, antioncogenes, and the molecular bases of multistep carcinogenesis. *Cancer Res* **49**(14): 3713-21.
- West, M. D., Pereira-Smith, O. M. and Smith, J. R. (1989). Replicative senescence of human skin fibroblasts correlates with a loss of regulation and overexpression of collagenase activity. *Exp Cell Res* **184**(1): 138-47.
- Wright, W. E. and Shay, J. W. (1992). The two-stage mechanism controlling cellular senescence and immortalization. *Exp Gerontol* **27**(4): 383-9.
- Wright, W. E. and Shay, J. W. (2001). Cellular senescence as a tumor-protection mechanism: the essential role of counting. *Curr Opin Genet Dev* **11**(1): 98-103.
- Yeo, E. J., Hwang, Y. C., Kang, C. M., Kim, I. H., Kim, D. I., Parka, J. S., Choy, H. E., Park, W. Y. and Park, S. C. (2000). Senescence-like changes induced by hydroxyurea in human diploid fibroblasts. *Exp Gerontol* **35**(5): 553-71.
- Yuan, H., Kaneko, T. and Matsuo, M. (1995). Relevance of oxidative stress to the limited replicative capacity of cultured human diploid cells: the limit of cumulative population doublings increases under low concentrations of oxygen and decreases in response to aminotriazole. *Mech Ageing Dev* **81**(2-3): 159-68.
- Yurkow, E. J. and Laskin, J. D. (1987). Characterization of a photoalkylated psoralen receptor in HeLa cells. *J Biol Chem* **262**(18): 8439-42.
- Zakian, V. A. (1995). Telomeres: beginning to understand the end. *Science* **270**(5242): 1601-7.
- Zamzami, N., Marchetti, P., Castedo, M., Decaudin, D., Macho, A., Hirsch, T., Susin, S. A., Petit, P. X., Mignotte, B. and Kroemer, G. (1995). Sequential reduction of mitochondrial transmembrane potential and generation of reactive oxygen species in early programmed cell death. *J Exp Med* **182**(2): 367-77.
- Zhao, J. F., Zhang, Y. J., Kubilus, J., Jin, X. H., Santella, R. M., Athar, M., Wang, Z. Y. and Bickers, D. R. (1999). Reconstituted 3-dimensional human skin as a novel in vitro model for studies of carcinogenesis. *Biochem Biophys Res Commun* **254**(1): 49-53.

Abbreviations

| | |
|---------------------------|---|
| AEBSF | 4-(2-aminoethyl)-benzenesulfonyl fluoride |
| ATP | adenosine triphosphate |
| bp | base pairs |
| BSA | Bovine Serum Albumin |
| cDNA | Complementary deoxyribonucleic acid |
| CPD | cumulative population doubling |
| DCF | dichlorodihydrofluorescein |
| DPI | diphenylene iodonium |
| dsDNA | double-stranded deoxyribonucleic acid |
| EDTA | ethylene diamine tetraacetic acid |
| EtBr | ethidium bromide |
| GFP | green fluorescent protein |
| H₂DCFDA | 2'-7' dichlorodihydrofluorescein diacetate |
| HEPES | 4-(2-hydroxyethyl)-1-piperazinethanesulfonic acid |
| HRP | horseradish peroxidase |
| ICL | interstrand crosslink |
| Kb | kilo base |
| kDa | kilo Dalton |
| mRNA | messenger ribonucleic acid |
| NAC | N-acetyl cystein |
| ROS | reactive oxygen species |
| rpm | revolutions per minute |
| PCR | polymerase chain reaction |
| PD | population doubling |
| PEG | polyethylene glycol |
| PUVA | psoralen plus UVA irradiation |
| TRF | terminal restriction fragments |
| SDS | sodium dodecyl sulfate |
| SDS-PAGE | sodium dodecyl sulfate polyacrylamide gel electrophoresis |
| SIPS | stress-induced premature senescence |
| ssDNA | single-stranded deoxyribonucleic acid |
| wt | wild type |

Summary

Following psoralen photoactivation (PUVA) human dermal fibroblasts undergo long-term growth arrest as well as morphological and functional changes reminiscent of cellular senescence. In the absence of molecular data what constitutes normal senescence, it has been difficult to decide whether these PUVA-induced changes reflect cellular senescence or rather a mimic thereof. By contrast to replicative senescence, PUVA-induced growth arrest was reversible. Ninety to 120 days post PUVA treatment, cells start to regrow. As cellular senescence has been proposed to serve as a barrier for tumorigenesis, the escape from senescence was studied in regard to immortalization and transformation. Regrowing fibroblasts did not show telomerase activity which is a main way to ensure immortalization. Anchorage-independent growth, a hallmark of transformation, was not detected. In addition, the senescence control genes p53, p16 and p21 did not show obvious mutations. Together with the observation that regrowing fibroblasts underwent replicative senescence, these results indicate that regrowing fibroblasts were neither immortalized nor transformed.

PUVA-induced senescence features were reversible. Enlarged cell morphology, expression of senescence-associated (SA) β -galactosidase and matrix-metalloprotease-1 were lost when fibroblasts resumed growth. Senescence control genes p53 and p21 were maintained for 1 month, whereas upregulation of p16 was maintained during the whole growth arrest. ROS levels were elevated increasingly after PUVA treatment with a maximum of 20-fold at six weeks post PUVA, which is both due to mitochondria and NADPH oxidase. Scavenging of ROS by the antioxidant N-acetyl cystein (NAC) prevented PUVA-treated fibroblasts from cytoplasmic enlargement but not from SA- β -galactosidase expression suggesting a role of ROS in the induction of phenotypical but not of functional senescent changes.

Interestingly, PUVA-treated fibroblasts cultured in their regrowing state reach the stationary phase at a much lower cumulative population doubling than control fibroblasts. The reduced total life-span was due to oxidative stress induced telomere erosion as scavenging of ROS by NAC rescued cell from telomere erosion and partly restored the life-span. These data support the view that the

preceding damage affects a counting mechanism contributing to the overall proliferation potential.

The initiation of the growth arrest was studied, and the amount of interstrand cross-links was not correlative. To further study whether damaged cytoplasts or damaged nuclear DNA are responsible for the growth arrest, nuclei and cytoplasts of PUVA-treated fibroblasts were fused with control cytoplasts or nuclei to reconstruct hybrids with either undamaged cytoplasts or undamaged nuclei. Fused cells with PUVA-cytoplasts, although growth arrested, start to regrow earlier post-PUVA at about day 40. Fused cells with PUVA-karyoplasts did not adopt a flattened phenotype and die after 2 weeks. These data indicate that PUVA-induced changes in the cytoplasts contribute to growth arrest, but may not be exclusively, while the contribution of the nuclear damage after PUVA cannot be fully evaluated by these experiments.

Collectively, these data suggest that PUVA-induced changes do not fully reflect replicative senescence but rather represent a long-term transient phenocopy. The model reported here is particularly suited to elucidating mechanisms underlying long-term senescence-like growth arrest and related functional changes.

Zusammenfassung

Replikative Seneszenz bezeichnet das irreversible Ende der Teilungsfähigkeit somatischer Zellen. In der Dermatologie werden hyperproliferative Hauterkrankungen mit der Kombination aus oraler Aufnahme des Photosensibilisators 8-Methoxypsoralen (P) und Ultraviolett-A (UVA) Bestrahlung als PUVA-Therapie behandelt. Humane dermale Fibroblasten reagierten auf PUVA mit Verlust der Teilungsfähigkeit und morphologischen und funktionalen Kennzeichen einer seneszenten Zelle. Im Gegensatz zur unumkehrbaren replikativen Seneszenz wurde nach drei Monaten eine Wiederaufnahme der Proliferation beobachtet. Die vorliegende Arbeit beschäftigt sich mit den molekularen Mechanismen des PUVA-induzierten Arrestes und der Wiederaufnahme des Wachstums im Vergleich zur replikativen Seneszenz als Folge erschöpfter Teilungsfähigkeit.

Ein Zusammenhang zwischen direkten und indirekten DNA-Schäden nach Psoralen-Photoaktivierung und dem Wachstumsarrest konnte experimentell nicht gezeigt werden. Zellhybride aus Zytoplasten PUVA-behandelter und Karyoplasten un behandelter Fibroblasten arretierten nach wenigen Tagen für ein bis zwei Monate. Diese Ergebnisse weisen auf die Bedeutung von Schäden des Zytoplasmas und der Membranen hin. Vergrößertes Zellvolumen, Expression von Matrixmetalloproteinase-1, SA-beta-Galaktosidase und von p16, p21 und p53 als Zeichen der replikativen Seneszenz waren innerhalb der Arrestphase, nach der Wiederaufnahme der Proliferation jedoch nicht mehr nachweisbar. Wachstumsarretierte Fibroblasten steigerten die Produktion reaktiver Sauerstoffintermediate in den Mitochondrien oder durch NADPH-Oxidasen bis auf das 20-fache. Nach Reproliferation zeigten die Fibroblasten eine "molekulare Narbe" in Form einer verminderten Lebensspanne. Ursächlich war die Sauerstoffradikal-abhängige Telomeren-Erosion. N-Acetylcystein schützte als Antioxidans vor den morphologischen Veränderungen und zumindest teilweise vor der Reduktion der Lebensspanne. Da reprodzierende Fibroblasten weder Adhäsions-unabhängig wuchsen noch de novo Telomeraseaktivität zeigten, wurden Immortalisierung und neoplastische Transformation als Ursachen der Reproliferation ausgeschlossen.

Eine PUVA-"Therapie" von Fibroblasten führt zu einem deutlich von der replikationsabhängigen zellulären Seneszenz unterscheidbaren Alterungsphänotyp. Diese Phänokopie der replikativen Seneszenz scheint geeignet, die Ursachen und Mechanismen der zellulären Seneszenz im molekularen Detail zu untersuchen.

Acknowledgement

I would like to thank Prof. Krieg who gave me the opportunity to work in his Department.

It is beyond the power of expression for my esteemed advisor, Prof. Karin Scharffetter-Kochanek. Without her support and supervision, it would have been impossible to bring this work to this stage. Her valuable guidance, creative suggestions, constructive criticism and constant encouragement during the course of my investigations are not only praiseworthy but also memorable. My deepest gratitude goes to her for all kinds of support she has provided during my stay in Germany.

I am grateful to PD. Dr. Roswitha Nischt for being my official supervisor and for many valuable advices, guidance and kind encouragement throughout my study.

I am deeply indebted to Dr. Meinhard Wlaschek for his supervision of the whole research project and for the critical reading of my thesis. It has been great fun to work with him. He tried to teach me how to be a good and careful scientist as well as clarifying my thoughts in scientific discussion and presentations. I hope I have learnt this lesson!

Moreover, I would like to express my gratitude toward to PD. Dr. Peter Brenneisen for his valuable suggestions and discussions during the early period of my present investigations.

I would like to thank Professor Krämer and Professor Langer who accepted a membership in my thesis committee.

My sincere thanks also go to old and new members of the Scharffetter-Kochanek's lab. Especially Tina and Edith for teaching me cell culture and molecular techniques. Lars, Daniel, Thorsten, Lale, Ziba, Ralf, Jan, Jutta, Maria and Heidi for the generous help they offered in many different ways.

This list would not be complete without the appreciation to my wife and my parents for their continued support and encouragement.

Erklärung

Ich versichere, daß ich die von mir vorgelegte Dissertation selbständig angefertigt, die benutzten Quellen und Hilfsmittel vollständig angegeben und die Stellen der Arbeit - einschließlich Tabellen, Karten und Abbildungen -, die anderen Werken im Wortlaut oder dem Sinn nach entnommen sind, in jedem Einzelfall als Entlehnung kenntlich gemacht habe; daß diese Dissertation noch keiner anderen Fakultät oder Universität zur Prüfung vorgelegen hat; daß sie - abgesehen von unten angegebenen Teilpublikationen - noch nicht veröffentlicht worden ist sowie, daß ich eine solche Veröffentlichung vor Abschluß des Promotionsverfahrens nicht vornehmen werde.

Die Bestimmungen dieser Promotionsordnung sind mir bekannt. Die von mir vorgelegte Dissertation ist von Frau PD Dr. rer. nat. Roswitha Nischt betreut worden.

Köln, den 31. 01. 2003

Parts of this thesis has been published:

1. **Ma W.**, Hommel C., Brenneisen P., Peters T., Smit N., Sedivy J., Scharffetter-Kochanek K., Wlaschek M. (2003) Longterm growth arrest of PUVA-treated fibroblasts in G2/M is independent of the tumor suppressor genes p16^{INK4a}, p21^{Cip1} or p53. *Exp. Dermatol.* 12: 1-9
2. **Ma W**, Wlaschek M, Brenneisen P, Schneider LA, Hommel C, Hellweg C, Sauer H, Wartenberg M, Herrmann G, Meewes C, Boukamp P, Scharffetter-Kochanek K. (2002) Human dermal fibroblasts escape from the long-term phenocopy of senescence induced by psoralen photoactivation. *Exp Cell Res.* 274(2):299-309

Curriculum Vitae

Name: Wenjian Ma
Data of Birth: March 19, 1970
Place of Birth: Shandong, China

Education:

July 1986 – July 1989 Senior high School, The first high school of Linqu, Shandong
Sept. 1989 – July 1993 B.S. in Biochemistry
Department of Biochemistry, Shandong University, China
Sept. 1994 – July 1997 Thesis: *Chymotrypsin: extraction and characterization*
M.S. in Cell Biophysics
Institute of Biophysics, The Chinese Academy of Sciences, China, Professor En-Hua Cao.
Thesis: *Studies on DNA-related chemiluminescence and its application in antioxidant evaluation*
June 1999 to present Ph.D student in the department of Dermatology, University of Cologne, PD. Dr. Nischt.
Thesis: *Long-term growth arrest and regrowth of human dermal fibroblasts after 8-MOP plus UVA treatment – Implications for stress-induced premature senescence and replicative cellular senescence*

Awards:

1996

1997

Chairman Prize of Institute of Biophysics, Chinese Academy of Sciences.

Di-Ao prize, Chinese Academy of Sciences.

Appointments:

1993 – 1994

1997-1999

Staff scientist, Chinese Environment Protection Bureau Linqu Branch.

Institute of Biophysics, Chinese Academy of Sciences, China. Professor En-Hua Cao
Project: *Oxidative DNA damage and natural antioxidants evaluation*